DEVELOPMENT OF COPPER BASED ANTI-INFLAMMATORY DRUGS: HISTIDINE DERIVATIVES

A thesis submitted to the

UNIVERSITY OF CAPE TOWN

In fulfillment of the requirements for the degree of

MASTER OF SCIENCE

By

'MAMOHALE MOHAJANE

BSc (National University of Lesotho)

DEPARTMENT OF CHEMISTRY

UNIVERSITY OF CAPE TOWN

RONDEBOSCH 7701

CAPE TOWN

SOUTH AFRICA

FEBRUARY 2010

DECLARATION

I, ’Mamohale Mohajane, declare that **Development of Copper based anti-inflammatory Drugs: Histidine Derivatives** is my own unaided work, and that all sources that I have used and quoted have been indicated and acknowledged by means of complete and clear references. This thesis is submitted for the Master of Science (MSc) degree, to the Department of Chemistry, Faculty of Science, University of Cape Town, it has not been submitted before for any degree or any examination at the University of Cape Town or any other university.

’Mamohale Mohajane Signed by candidate

February 2010

ACKNOWLEDGEMENTS

- My supervisor Professor Graham Jackson for guidance and support throughout the research,
- My colleagues in the research group for their contribution and discussion,
- Members of staff and fellow students in the Department of Chemistry UCT for the contributions, seminars, symposia and conferences,
- Dr. Sophie Rees-Jones and the Professors Roger Hunter and Dave Gammon for their guidance in the synthesis experiments,
- Mr. Dave Woolley from the Division of Chemical Pathology, Clinical Laboratory Sciences, Faculty of Health Sciences, UCT for guidance in the ITC experiments,
- Mr. Hesselink Gerald and Mr. Achleitner Klaus for technical support,
- Mr. Hendricks Noel and Peter Roberts for running the NMR experiments,
- My family and the Government of Lesotho for financial support

CONFERENCES AND PROCEEDINGS

Results were presented in the following conferences and symposia;

- Inorganic Symposium; October 2008 at Business School, University of Cape Town; *Design and synthesis of the ligand; protonation and complexation of glycine with Cu(II)*
- South African Chemical Institute Conference; November/December 2008 at main Campus Stellenbosch University; *Protonation of glycyl-L-histidine, complexes of glycyl-L-histidine with Cu(II), Ni(II) and Zn(II)*
- Inorganic 2009 Conference; September 2009 at University of the Free State; *Development of copper based anti-inflammatory drugs, histidine derivatives.*

ABSTRACT

Methyliminodiacetylhistidine dimethyl ester could not be synthesised. However the other two ligands, glycine and glycyl-L-histidine were purchased and used for this study. The equilibrium constants of the ligand (glycyl-L-histidine) and the ligand complexes with Cu(II), Ni(II) and Zn(II) were investigated with glass electrode potentiometry and isothermal titration calorimetry at 25±0.01^{o}C at an ionic strength 0.15M with NaCl. Potentiometric studies show that glycyl-L-histidine has three dissociable protons, and the neutral form of the ligand forms around pH 6.60. Potentiometric results of copper(II) complexes with glycyl-L-histidine were compared to the potentiometric titration of the ligand with Ni(II) and Zn(II). Copper(II) complexes of glycyl-L-histidine were more stable than Ni(II) and Zn(II) complexes of glycyl-L-histidine. The potentiometric results for these systems were in good agreement with the literature results.

From the potentiometric studies, the LH form of glycine was more stable than the LH form of glycyl-L-histidine by 1.19 log units. The second protonation of glycyl-L-histidine is on the imidazole ring and hence there is so comparable protonation site for glycine. Instead the third protonation step of glycyl-L-histidine is comparable to the second protonation step of glycine. The ML form of Cu(II)-glycyl-L-histidine complexes was more stable than that of Cu(II)-glycine complexes by 1.07 log units. ML was the only common species for the two systems.

The interaction between copper(II) and glycyl-L-histidine was also studied with isothermal titration calorimetry (ITC) from pH 5 to pH 8. This was compared to a simpler system of glycine. The change in speciation for this method was characterized by the N value. The speciation from ITC results followed that of potentiometric results. The ML species of Cu(II) and glycine formed in acidic solutions, and the ML_2 formed in basic solutions. In this pH range, the ML species of Cu(II) and glycyl-L-histidine were the most predominant species in solution.

The ITC results agreed with the potentiometric results. At pH 5 where ML was the most predominate species in both the Cu(II)-glycine system and the Cu(II)-glycyl-L-histidine

system (N ≈ 1) Log K of the glycyl-L-histidine system was greater than that of the glycine system.

The structures of the complexes were predicted with ultraviolet-visible (UV-Vis) spectrophotometry. The visible spectra obtained for the different Cu(II)/Glycyl-L-histidine species in solution were typical of Cu(II) complexes in a tetragonally distorted, octahedral environment. The molar extinction coefficients are also typical of Cu(II) complexes and reflect the distortion of the metal-ion environment.

The sequence of protonation/deprotonation of the ligand was studied with ^{1}H NMR spectroscopy. The first deprotonation of glycyl-L-histidine occurred at very acidic environments, and this was the deprotonation of the carboxylate proton. The second deprotonation occurred at one of the imidazole nitrogens and the last one occurred in highly basic environments. This was the deprotonation of the NH_2 terminal. The structure of complexes of Cu(II) with glycyl-L-histidine were also studied by ^{1}H NMR. Form ^{1}H NMR results, the active binding sites for glycyl-L-histidine are the imidazole nitrogens, the amide nitrogen and the terminal NH_2 group. The imidazole nitrogen involved in coordination first, followed by the amide nitrogen, followed by the terminal NH_2 group

The capacity with which the ligand can increase the low molecular weight Cu(II) complexes in blood plasma was studied using a computer model of blood plasma. At reasonable concentrations, the ligand was not able to mobilise endogenous copper. Most of the ligand existed as LH and LH_2 in blood plasma. Moreover, glycyl-L-histidine increased the low molecular weight complexes of Zn(II) more than of Cu(II).

LIST OF SYMBOLS

[L]	-concentration of the free ligand
[H]	-concentration of the free hydrogen ion
[M]	-concentration of the free metal ion
{X}	-activity of the species X (X = ligand, metal ion, protonated ligand or complex)
Υ_X	-activity coefficient of species X
K_L	-protonation/deprotonation constant of the ligand
K_{ML}	-stability constant of the complex
β_L	-overall protonation/deprotonation constant of the ligand
β_{ML}	-overall stability constant of the complex
$\Delta H^{\ominus}$	-standard enthalpy change of the reaction
ΔH	-enthalpy change of the reaction
ΔS	-entropy change of the reaction
ΔG	-Gibb's free energy change
$\Delta G^{\ominus}$	-standard Gibb's free energy change
Q	-heat absorbed or evolved by the reaction
T	-temperature
R	-gas constant
$T_{k,L}$	-total concentration of the free ligand
$T_{k,M}$	-total concentration of the free metal ion
$T_{k,H}$	-total concentration of the free hydrogen ion
E_{cell}	-potential of the cell
E_{ref}	-potential of the reference electrode
E_j	-liquid junction potential
$E^{\ominus}_g$	-standard potential of the glass electrode
$E^{\ominus}$	-potential of the glass electrode
F	-Faraday's constant
a_i	-activity
Υ_i	-activity coefficient of species i

C_i	-free concentration of species i
I	-ionic strength
z_i	-charge on species i
U_{obj}	-objective function
N	-is the total number of experimental titration points
N	-number of binding sites of the ligand
n_p	-total number of points
R^H	-Hamilton R-factor
R^H_{lim}	-Hamilton R-factor limit
σ	-standard deviation
K_b	-binding constant
K_d	-dissociation constant
A	-absorbance
ε	-molar extinction coefficients
b	-path length of the curvet
P_o	-initial radiation power
P	-final radiation power
%T	-percentage transmittance
λ_{max}	-maximum wavelength
n_i	- the number of equatorial donor group
ν_i	-the ligand field of the complex.

LIST OF ABBREVIATIONS

RA	-Rheumatoid arthritis
RF	-Rheumatoid factor
SLE	-Systematic lupus erythematosus
Anti-CCP	-Anticitrullinated cyclic protein
NSAIDs	-non-steroidal anti-inflammatory drugs
COX	-cyclooxygenase
DMARDs	-Disease modifying anti-rheumatic drugs
SOD	-Superoxide dismutase
HAS	-Human serum albumin
DCC	-dicyclohexylcarbodiimide
DIC	-diisopropylcarbodiimide
HOBt	-1-hydroxybenzotriazole
HOAt	-1-hydroxy-7-azabenzotriazole
THF	-tetrahydrofuran
DMF	-dimethylformamide
(Et_3N)	- triethylamine
ESTA	- Equilibrium Simulations for Titration Analysis
ITC	-Iothermal titration calorimetry
EDTA	- ethylenediaminetetraacetic acid
NH_4 Ac/Acetic acid	-ammonium acetate/acetic acid buffer
MES.TMAH	-(2-[N-morpholino] ethanesulfonic acid)
MPOS.TMAH	-(3-[N-morpholinino] propanesulfonic acid)
EPPS.TMAH	-(3-[4,(2-hydroxyethyl)-1-piperazinyl] propanesulfonic acid)
UV-Vis	- Ultraviolet-Visible
NMR	- nuclear magnetic resonance
ECCLES	- Evaluation of Constituent Concentrations in Large Equilibrium Systems
p.m.i	- plasma mobilizing indices
GlyHis	-Glycyl-L-histidine

TABLE OF CONTENTS

1. INTRODUCTION

1.1 RHEUMATIOD ARTHRITIS

Rheumatoid arthritis, RA is an autoimmune disease that causes chronic inflammation of the joints [1, 2]. The body produces an antibody which is active against part of other antibodies, resulting in some changes in the synovial membranes [1, 3]. The cause of RA is not yet known, but the symptoms include morning stiffness, non specific joint pains, swelling and tenderness around inflamed joints, and loss of functioning and mobility of joints [1, 4].

Rheumatoid arthritis progresses in three stages [4, 5]. The first stage is the swelling of the synovial membrane, causing pain, warmth, stiffness, redness and swelling around the joint. Second is the rapid growth and division of pannus, which causes the synovium fluid to thicken. In the final stage, the inflamed cells release enzymes that may erode cartilage and bone, often causing the joint to lose its shape and alignment, resulting in more pain and loss of movement [5, 6].

Figure 1.1a and figure 1.1b show the cross-sectional structure of an affected joint and that of a normal joint respectively.

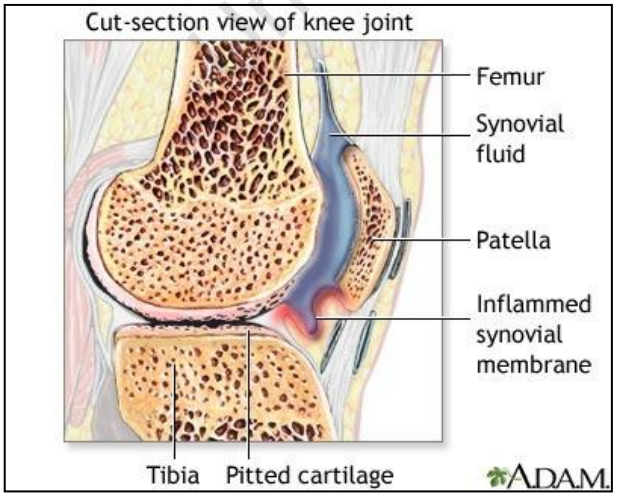

Figure 1.1a: cross-sectional view of a joint affected by RA

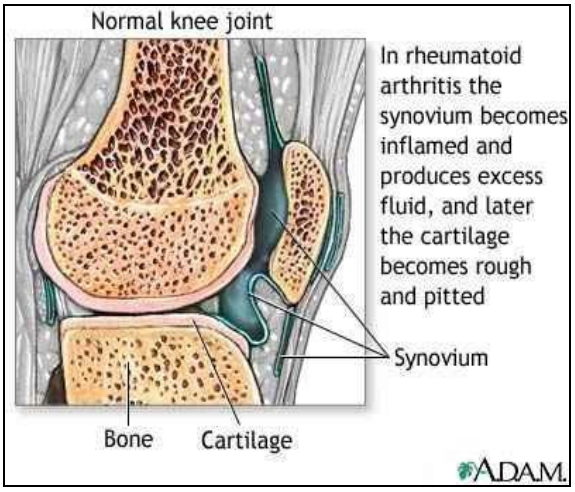

Figure 1.1b: cross-sectional view of a normal healthy joint

Unlike in a normal healthy joint, the cartilage of a joint affected by RA gets eroded; the synovial membrane gets swollen and reddens [7].

In addition, Rheumatoid arthritis is said to be systemic because it can also cause inflammation of the tissue around the joints, as well as in other organs in the body such as eyes [8]. RA is common and it affects about 2% of the world population. About 2.4 million cases have been reported in USA [9, 10]. RA is more common in females. The female/male ratio is 3:1, with the age group 35-55 being more prone to the condition. Everyone can have RA [11]. However, it is rare in rural black patients in South Africa, but the numbers increases with urbanization [12-14].

RA can be diagnosed by blood test for Rheumatoid factor, RF. Rheumatoid factor is a group of auto-antibodies which may be present in the blood of people with Rheumatoid arthritis [15, 16]. The amount of Rheumatoid factor in the blood can be measured in two major methods [16-18].

i. Agglutination test: in this method, blood samples are mixed with tiny rubber (latex) beads that are covered with human antibodies. If Rheumatoid factor is present the latex beads agglutinate together. This method is best used as a first-time screening test for Rheumatoid arthritis. Another agglutination test mixes blood samples with a sheep's red blood cells that have been covered with rabbit antibodies. If the RF is present, the red blood cells clump together. This method is often used to confirm the presence of RF [19].

ii. Nephelometry test: in this method, blood samples are mixed with antibodies that cause the blood to clump if RF is present. A laser light is shone on the tube containing the mixture and the amount of light blocked by the blood samples is measured. As the levels of RF increases, more clumping occurs, causing a cloudier sample and less light to pass through the tube [19, 20].

Rheumatoid factor is not only present in patients with Rheumatoid arthritis [21, 22]. It can also occur in patients with other autoimmune conditions such as systematic lupus

erythematosus (SLE). Other conditions that may cause a positive RF test results include chronic hepatitis, sarcoidosis, chronic inflammation, various cancers, syphilis, infectious mononucleosis, parasites, liver disease and tuberculosis [23, 24].

Not all patients of Rheumatoid arthritis have a detectable Rheumatoid factor. A more specific test is needed for such patients [24]. Anticitrullinated cyclic protein (anti-CCP) test measures the presence of an antibody associated with Rheumatoid arthritis. The anti CCP test is gradually becoming more common. Anti CCP test can reliably help to diagnose Rheumatoid arthritis in three different people [25].

i. Those with early-stage disease for whom uncertainty remains about diagnosis.
ii. Those with mild conditions who test negative for RF, and
iii. Those with critical conditions.

1.2 THERAPY FOR RHEUMATOID ARTHRITIS

There is no cure for the disease. However for centuries the inflammation associated with this condition has been treated with copper rich diets such as crayfish, chocolates and peanuts [26]. Copper bracelets were also worn with a conviction that sweat will transport copper from the bracelets to the binding sites where it is needed [27]. Pharmacological evidence suggests the use of copper complexes to be beneficial in alleviation and treatment of RA, and that these compounds have disease remitting qualities [27-29].

Medication for the treatment of RA is used to

1. Relieve or reduce pain,
2. Improve daily joint function,
3. Reduce joint inflammation,
4. Prevent or delay significant joint damage,
5. Prevent permanent joint damage, and
6. Improve quality of life.

Advanced means have been developed and these include the use of anti-inflammatory drugs, analgesia and steroids [30]. Surgical treatment in rheumatoid arthritis is used to relieve severe pain and improve function of severely deformed joints that do not respond to medication and physical therapy. Total joint replacement (arthroplasty) can be done for many different joints in the body. Its success varies depending on which joint is replaced [31].

1.2.1 Non-steroidal Anti-inflammatory drugs

The non-steroidal anti-inflammatory drugs (NSAIDs) are used to relieve pain. The mechanism through which they work NSAIDs reduce pain is by blocking cyclooxygenase (COX) [31-35]. This enzyme exists in two isoenzymatic forms, cyclooxygenase-1 (COX-1) and cyclooxygenase-2 (COX-2). Cyclooxygenase-1 induces the production of prostaglandins by the cells of the body and has several important functions. They encourage inflammation, pain, and fever; support the blood clotting function of platelets; and protect the lining of the stomach from the damaging effects of acid [35, 36]. Cyclooxygenase-2 activity is stimulated by proinflammatory cytokines and produces prostaglandins that arbitrate the inflammatory response and pain signaling transmission [36, 37].

However, NSAIDs can only be used for mild to moderate conditions and they are associated with some serious side effects [38]. The frequency of the side effects varies among NSAIDs [38, 39]. Nausea, decreased appetite, vomiting, diarrhea, constipation, rash, dizziness, drowsiness and headache are the most common side effects. Prolonged and excessive use of NSAIDs may lead to even more serious side effects like gastrointesinal bleeding, renal impairment and toxicity due to inhibition of prostaglandin production, kidney failure and liver failure [40].

Examples of nonsteroidal anti-inflammatory are aspirin, ibuprofen, indomethacin, ketoprofen and naproxen [41].

1.2.2 Disease modifying anti-rheumatic drugs (DMARDs)

These are used to reduce the progression of the disease and sometimes to prevent joint damage [42]. The mechanism through which they work is not fully understood but it is believed that DMARDs work to "suppress the body's overactive immune and/or inflammatory systems." [43] The DMARDs can be used at an earlier stage of the disease. Examples of DMARDs are azathioprine, hydroxychloroquine, methotrexate, sulfasazine, etanercept, infliximab, leflunomide and gold salts [44, 45].

Disease modifying anti-rheumatic drugs also have side effects. They can cause myelosuppression, renal or liver toxicity, skin rash or gastrointestinal disturbances [46].

1.2.3 Corticosteroids (Glucocorticoids)

Corticosteroids reduce inflammation, attendant swelling and pain. This is achieved by suppressing the immune system. [47, 48] Corticosteroids have a higher potency than the NSAIDs and DMARDs but they have terrible side effects too. Examples of corticosteroids are predonisone and metgylprenisolone [49].

Since they are strong medicines, the corticosteroids can lower the resistance of the immune system to infections [50]. Moreover, if taken for prolonged periods of time, the corticosteroids can cause glaucoma, gastrointestinal bleeding, diabetic metabolism, edemas, pancreatitis, aseptic bone necrosis, osteoporosis, myopathies, obesity, hypertension, sleep disturbances, psychiatric syndromes, delayed wound healing, atrophy, potassium loss, cataracts, peptic ulcers, and fragility of the skin [50, 51].

1.3 COPPER(II) AND RHEUMATOID ARTHRITIS

Several reports show that copper(II) salts and organic complexes can increase anti-inflammatory activity *in vivo* or they can strengthen the body's natural inflammatory processes [52-56]. The exact mechanism by which this is achieved is not fully understood but there are several possibilities:

1. Cu(II) may modify the production of prostaglandins by the body cells. Reduced amounts of prostaglandins may reduce inflammation since they(prostaglandins) encourage inflammation and pain,

2. It may stimulate the production of lysyl oxidase or it may modify the activity of lysyl oxidase which is a copper-containing enzyme liable for the protection of collagen and elastin in tissues. Increased amounts of lysyl oxidase may reduce the destruction of tissues, especially the cartilage tissue inpatients with rheumatoid arthritis.

3. It may enhance the activity of histamine. Histamine regulates the inflammation response.

4. It may induce the production of superoxide dismutase or activity of superoxide dismutase. Superoxide Dismutase (SOD) is an enzyme that repairs cells and reduces the destruction done to them by superoxide radicals ($^{\bullet}O_2$).

5. Cu(II) may improve lysosomal membranes. The lysosomes are acidic enzymes that may destroy the synovial membrane. Improved lysosomal membrane may reduce the destruction of the synovial membrane.

1.4 AIM

The main aim of this study was to develop a novel copper based anti-inflammatory drug that will reduce inflammation associated with rheumatoid arthritis. The drug (ligand) should have the following features;

i. It should be more selective to Cu(II) than most bivalent cations especially Ca(II) and Zn(II) which are found in large concentrations in blood plasma.

ii. It must form strong and kinetically labile complexes with Cu(II) in order to transport and release Cu(II) at the biological sites where it is needed.

iii. It should form bioavailable copper(II) complexes. This means that the complex should be lipophilic and hence neutral (uncharged) and form thermodynamically stable complexes with Cu(II).

iv. The ligand that promotes dermal absorption of Cu(II) is desired so that it will permit transportation across the skin (or the cell membrane).

1.5 OBJECTIVES

1. Design of the new ligand which meets the criteria above.
2. Synthesis and characterization of the ligand
3. Measure thermodynamic data for the complexes using;
    a) Glass electrode potentiometry,
    b) Isothermal titration calorimetry,
4. investigating the structure using;
    a) UV-Vis spectrophotometry, and
    b) ^{1}H NMR
5. Use the results to evaluate the ligand *in silica* using a blood plasma model.

REFERENCES

1. Clair, W. E.,Pisetsky, D. S. and Haynes B. F. (2004) *Rheumatoid Arthritis*. Wolters Kluwer Health. 26-27
2. Cush, J. J. and Arthur, K. (2005) Rheumatoid *Arthritis: Early Diagnosis and Treatment.* Wolters Kluwer Health. 1-5
3. Aeschlinmann, A., Munzinger, U., Simmen, B. R. (1995) *Rheumatoid Arthritis.* Thieme Medical Publishers
4. Catherine A. O. (2008) *Rheumatoid arthritis: A chronic inflammation* (7) 42 - 51
5. Aeschlinmann, A. et al. (1995) *Rheumatiod Arthritis*. Thieme Medicinal publishers, Inc. New York
6. Fischbach, M. (1991) *Rheumatoid arthritis*. Churchill Livingstone, New York
7. Baeten, D. et al. (2004) *Infiltration of the synovial membrane with macrophage subsets and polymorphonuclear cells reflects global disease activity in spondyloarthropathy*.(7) 361-363
8. Wolfe, F., Mitchell, D. M, Sibley, J. T. (1994). *The mortality of rheumatoid arthritis.*37 (4): 481–494.
9. Simone, A. K., Monique, A. M. Gignac, Elizabeth M. Badley. (2009) *Rheumatoid Arthritis.* 61(5)**:** 605 - 613
10. Hootman, J. M., Sniezek, J. E, Helmick CG. (2002) *Journal of Women's Health Gender-Based Medicine.* (11) 407-16
11. Talamo, J,. Frater, A., Gallivan S, Young A. (1997) arthritis. *British Journal Rheumatology.* 36(4): 463-9.
12. Edwards, C. J. and Cooper, C. (2005) *Early environmental factors and rheumatoid arthritis*. 143(1): 1–5.

13. Solomon, L. Robin, G. Valkenburg H. A. (1975) *Rheumatoid arthritis in an urban South African Negro population*. 34(2):128-35

14. Chou, . T., Pei, L., Chang, D.M., Lee, C.F., Schumacher, H.R., Liang, M. H. (1994) *Prevalence of rheumatic diseases in Taiwan: a population study of urban, suburban, rural differences*. 21(2):302-6

15. Goodyear, C. S, Tighe, H., McInnes, I B., (2008) *Kelley's Textbook of Rheumatology*. 8th ed. Philadelphia, Pa: W.B. Saunders Company. Chapter 51.

16. Tyssen, P. (1085) *The Immobilization of Immunoreactions on solid phases*. 297-314

17. Kjetil, A at el. (1987) *Rheumatoid Factor in Psioratic scale, serum and circulating Immune complexes detected by an Isotype-specific ELISA*. 161-166

18. Teitsson et al (1984) *J. Immunological Methods*. 71 (4): 149-161

19. Pope, R. M. et al (1981) *Journal of Laboratory and Clinical Medicine* 97(6): 842-853

20. Philadelphia, P. A., T. Palosuo et al. (1982) *Immunoglobulin G rheumatoid factor: Detection by enzyme immunoassay in rheumatoid arthritis and normal subjects* 73(9): 6363

21. Peen, E., O. J. Mellbye and H. J. Haga (2009) *Scandinavian Journal of Rheumatology*. 38 (1) : 46 - 49

22. Franklin, E. C., M. D., H. G. Kunkel, M. D., J. R. Ward, M. D. (2005) *Arthritis and Rheumatism: Clinical studies of seven patients with rheumatoid arthritis and uniquely large amounts of rheumatoid factor*. 5(1): 400-409

23. Ghosh, A. K. (2008) *Mayo Clinic Internal Medicine Review*. 972-97 Mayo Scientific Press, Florence, USA .8Ed

24. Lee, A. N, Beck, C. E., Hall, M. (2008) *Rheumatoid factor and anti-CCP autoantibodies in rheumatoid arthritis: a review*. 21(1); 15-28

25. Luca, Q. et al (2008) *Rheumatoid factor positivity rather than anti-CCP positivity, a lower disability and a low number of anti-TNF agents failed are associated with rituximab in Rheumatoid Arthritis*. 48(12); 1557-1559

26. Delves H. T. (1980) *Biological Role of Copper*. Ciba Foundation Symposium 79, Excerpta Medica, Amstedam. 5-22
27. Sorenson, J. R. J. (1982) *Metal ions in Biological Systems, inorganic Drugs in Deficiency and desease.* Sigel H.,Mercel decker, Inc., 14;77-113
28. Forestier, J. (1949) *Copper and Gold Salts in Rheumatoid Arthritis*. 1(8); 132-134
29. Stuhlmeler, K. M. (2006) *The anti-rheumatic Gold Salts Aurothiomalate Suppresses Interleukin-1 β-induced Hyaluronan Accumulation by Blocking HAS1 Transcription Repressor*. 4(282); 2250-2258
30. Mercadante, S (1999) *Journal of Pain and Symptom Management*, 5(17); 351-356
31. Charles, A. G and Stern, J. P. (2003) *The Journal of Bone and Joint Surgery (American)* 85;1869-1878
32. Rostom, A. (2007) *Nonsteroidal Anti-inflammatory Drugs and Cyclooxygenase-2 Inhibitors for Primary Prevention of Colorectal Cancer: A Systematic Review Prepared for the U.S. Preventive Services Task Force*. 6(146); 376-389
33. DeMaria, A. N., Weir, M. R. (2003) Coxibs—beyond the GI tract: renal and cardiovascular issues. *Journal of Pain Symptom Manage.* 25(2);41-49
34. Schnitzer, T. J. (2001) *Journal of American Medicine* 110; 46-49.
35. Jackson, M. J. (2002) Molecular *Aspects of Medicine*. 3(23); 209-285
36. de Leeuw, P. W. (1997) *Drugs Aging.* 11:178-185.
37. Brautiga, A. et al (2005) *Journal of Neuroimmunnology.* 166;113-125
38. Chan, F. K. L, et al. (2007). *Combination of a cyclo-oxygenase-2 inhibitor and a proton-pump inhibitor for prevention of recurrent ulcer bleeding in patients at very high risk: A double-blind randomised trial*. 369(9573); 1621–1626.
39. Delves, H.T., (1980) *Biological Role of Copper* Ciba Foundation Symposium. 1(79) Excerpta Medica, Armsterdam 283-299
40. Sorenson, J.R.J. (1976) *Journal of Medicinal Chemistry* 1(19); 135
41. Thordarson D, Aval S, Krieger L (2002) Surgery *for Rheumatoid arthritis*. Foot Ankle Int. 1(23); 486-90
42. Sorenson, J.R.J. (1982) *Metal Ions in Biological Systems*, Sigel(Ed) Marcel Decker, New York

43. Sorenson, J.R.J. (1984) *Chemistry in Britain*. 1(79);1110
44. Schultz, M., Kulis, J., Murison, J., Andrews, G. W. (2008) Australian *Journal of Chemistry* 61(4), ISSN: 0004-9425.
45. Zvimba, J. N. (2005) PhD Dissertation. UCT, Cape Town
46. Berchet, G. J. (1938*) Organic Syntheses* 1(8); 56-8.
47. May, P.M., Williams, D.R., (1977) *Journal of Chemical Society*. Dalton Trans., 588-585
48. Simon, C. H. et al (1998) *Laboratory Screening for Side Effects of Disease Modifying Antirheumatic Drugs in Daily Rheumatological Practice* 1(27); 170-179
49. T Geiger, S. Clarke (1987) *Journal of Biological Chemistry* 2(262); 785-794
50. Sivan, S. S., E Wachtel, E Tsitron, N Sakkee, F van (2008) - *Journal of Biological Chemistry* ASBMB
51. Pillai, A. D.,P. D Rathod, P. X Franklin, H. Padh, K. K. Vasu (2004) *Biochemical and Biophysical Research Communications,* Elsevier
52. Kurosaki, Hirosama et al.(2001) *Journal of Chemical Society* ,Dalton Trans.,443-445
53. Skoog, D. A., Holler, F. J. and Neiman, T. A. (1998) *Principles of Instrumental Analysis*. 5th ed. Brooks/Cole Thomson Learning. 596-599
54. Pregosin, P. S. (1991) *Transition Metal Nuclear Magnetic Resonance Studies in Inorganic Chemistry*. B.V. Amsterdam
55. Rafter, G. W. (1993) *Plasma Thiols, Copper and Rheumatoid Arthritis*. 1(43); 59-61
56. Roberts, N. A. and Cashin, C. H. (1986) *Rheumatology*. 2(25); 230-231

2.DESIGN AND SYNTHESIS OF THE LIGAND

2.1 INTRODUCTION

Previous studies show that high protein diets increase the absorption of Cu(II) [1, 2]. The Cu(II) transport site for albumin protein is one of the most extensively studied binding sites of any protein. Its structure is illustrated in Figure 2.1 [2, 3].

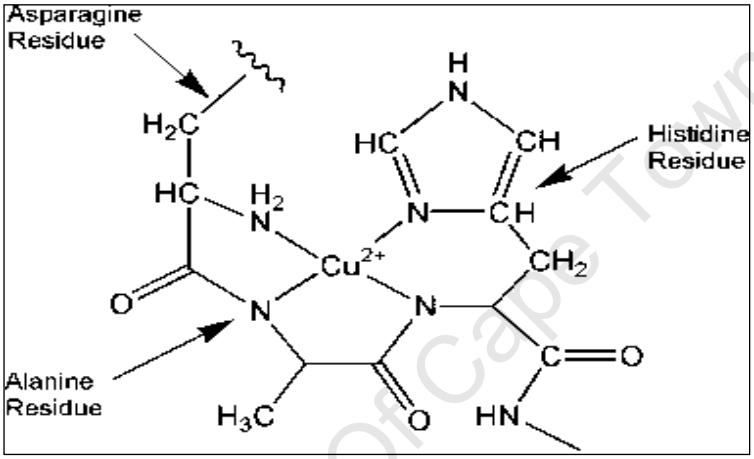

Figure 2.1: Copper binding site in Human Serum Albumin (HSA)

The copper(II) binding site in human serum albumin involves the ∝-NH_2 nitrogen, two peptide nitrogens and an imidazole nitrogen of the N-terminal Asp-Ala-His residue [3]. Human serum albumin is more specific to Cu(II) than most proteins [4. 5]. This makes Cu(II) less bioavailable when complexed with HSA than when complexed with other protein molecules [5]. However, additional histidine encourages uptake of Cu(II) [4, 5]. This is related to the histidine residue of the HSA [4]. Studies suggest the cell recognizes and most probably binds with the Cu(II)-albumin complexes but not satisfactorily recognizes the ternary complex formed by Cu(II), albumin and histidine [5].

2.2 PRINCIPLES OF DESIGN OF THE DRUG (LIGAND)

The designed ligand has donor nitrogen atoms. Nitrogen atoms are said to be more selective for Cu(II) than most bivalent cations [6, 7], especially Ca(II) and Zn(II) which are found in large concentrations in blood plasma [8]. Moreover, the designed ligand has two amide nitrogens. Since coordination to the amide nitrogens results in their deprotonation, the complex of copper(II) and would be formally neutral [9, 10]. The designed ligand is shown in Figure 2.2.

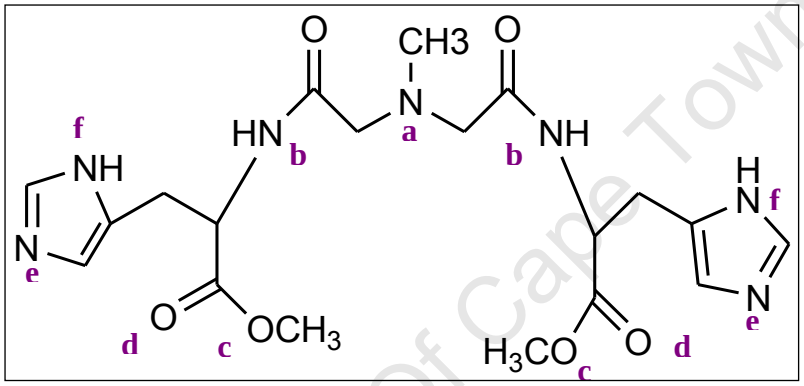

Figure 2.2: The designed ligand (the letters in purple font are used to label the atoms, they are not part of the molecule)

In addition, a ligand that promotes dermal absorption of Cu(II) is desired. For dermal absorption the complex cannot be too lipophilic or it will become trapped in the dermus, however, it cannot be too hydrophilic or it will not penetrate the dermus. The designed ligand has two glycyl residues and two histidine residues. The ligand is therefore believed to be both lipophilic and hydrophilic [9, 10].

Moreover, the ligand that forms stable complexes with Cu(II) is required. The ligand should also form kinetically labile complexes in order to transport and release Cu(II) at the biological sites where it is needed [11]. The stability of the ligand depends on the number of donor atoms, the number of chelate rings, the size of the rings, the number of bonds between the central metal ion and the ligand, and the number of ligands around the central metal ion [11, 12]. An increase in all of these factors, except the latter, increases

the stability of complexes. The designed ligand is expected to form a 5,4,5; 5,5,5 chelating system. Of course not all 5 donor atoms will be in a plane but rather a tetragonally distorted octahedral complex is expected. The vacant site will be occupied by water. An example is shown in Figure 2.3.

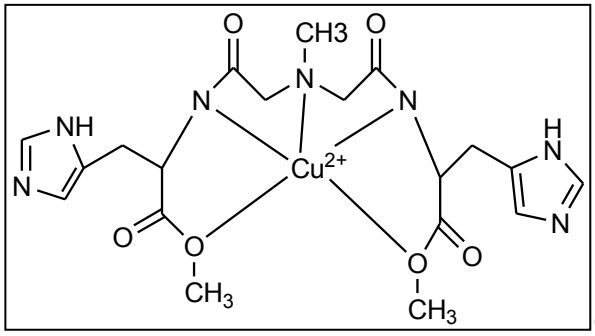

Figure 2.3: Complex formed between Cu(II) and the designed ligand.

The ligand has several binding sites; the N-atom labeled a, the two secondary amide nitrogens labeled b, the two imidazole nitrogens labeled e; f, and the two carboxylate oxygens labeled c. [Figure 2.2]

For comparison of physical properties, measurements were also made on the related ligand, glycyl-L-histidine which represents half of the target ligand.

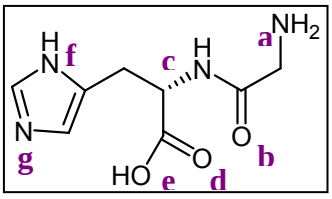

Figure 2.4: Glycyl-L-Histidine (the letters in purple font are used to label the atoms; they are not part of the molecule)

Glycyl-L-histidine was purchased from Sigma-Aldrich and was 99.0% pure Glycyl-L-histidine also has amide nitrogen and histidine moiety as shown in Figure 2.4. This ligand is also expected to be selective to copper since it has several N-atoms, and it is expected to mobilize Cu(II) and make it more bioavailable.

This ligand has several binding sites, from "a" to "g" as shown in purple font in Figure 2.4. Glycyl-L-histidine is expected to form uncharged complexes with Cu(II) since it has an amide nitrogen and a carboxyl group. Coordination to these two groups results in their deprotonation [9, 10].

2.3 SYNTHESIS OF THE LIGAND

The synthesis involves two starting materials; methyliminodiacetic acid and L-histidine methyl ester. This involves three steps; protection of the amino group, activation of the carboxyl group and de-protecting the amino group [12]. The first step of the synthesis was omitted because the nitrogen of the diacid was protected by the methyl group. Polymerization is common where the amino group is not protected [10].

To speed up the reaction and to eliminate side reactions, the carboxyl groups of the methyliminodiacetic acid was activated [13]. There were two main activation groups; carbodiimides and the aromatic oximes [9, 13]. The most common carbodiimides are dicyclohexylcarbodiimide (DCC) and diisopropylcarbodiimide (DIC) [10, 13].
Aromatic oximes are used to solve the problem of racemization [11]. This is the process in which one of the enantiomer of a compound converts to the other enantiomer [11, 12]. The compound alternates between each form while the ratio between laevo and dextro approaches 1:1 at which point it becomes optically inactive. The two common aromatic oximes are 1-hydroxybenzotriazole (HOBt) and 1-hydroxy-7-azabenzotriazole (HOAt) [13, 14].

2.3.1 EXPERIMENTAL

2.3.1.1 Chemicals

All chemicals and reagents were of analytical grade and were used without any further purification**.** Methyliminodiacetic acid and L-Histidine methyl ester were purchased from Sigma-Aldrich and they were both of 99.0% purity.

1-hydroxybenzotriazole (HOBt) was purchased from Sigma-Aldrich and was of 98.0% purity, dicyclohexylcarbodiimide (DCC) was purchased from Merck and it was of 99.0% purity, tetrahydrofuran (THF) and dimethylformamide (DMF) were purchased from Sigma-Aldrich, and triethylamine (Et_3N) was purchased from Sigma-Aldrich and it was of. All solvents were purified with fractional distillation [19].

2.3.1.2 Procedure

In the first reaction vessel, about 0.686mmol methyliminodiacetic acid was dissolved in THF and stirred continuously for 15 minutes and then 1.593 mmol DCC and 0.681 mmol HOBt added. The system was stirred continuously and cooled to 0^oC for 15 minutes. The reaction system was stirred overnight at room temperature under an inert atmosphere of nitrogen. The reaction was monitored and the contents of the reaction system checked using paper chromatography [15-17]. In the second reaction vessel, 1.496 mmol L-histidine was dissolved in EtN_3. When the chromatogram showed that there was no methyliminodiacetic acid left in the reaction vessel, the contents of the second reaction vessel were added into the first reaction vessel. In some cases, a precipitated formed was isolated by evaporating the solvent before addition of L-histidine. The reaction was stirred continuously for 18 to 72 hours at room temperature under an inert atmosphere in nitrogen. The resulting product (oil) was isolated and purified using column chromatography [18-19].

2.3.1.2.1 Reaction Scheme

Step I

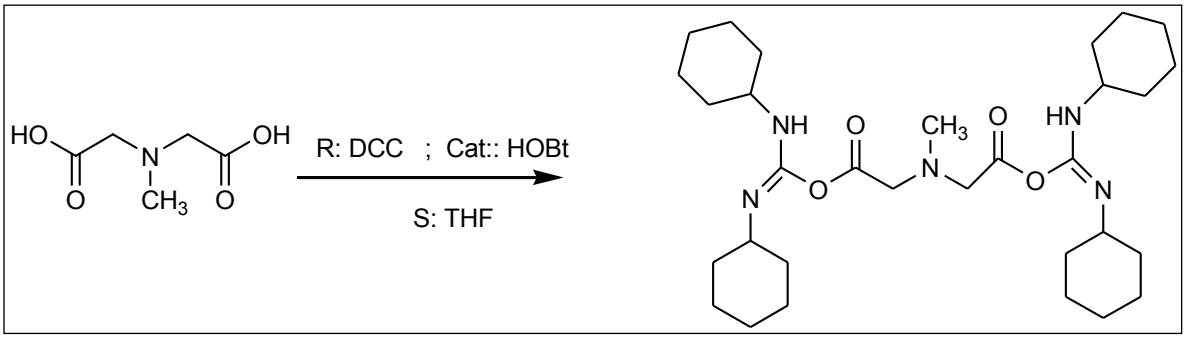

Step II

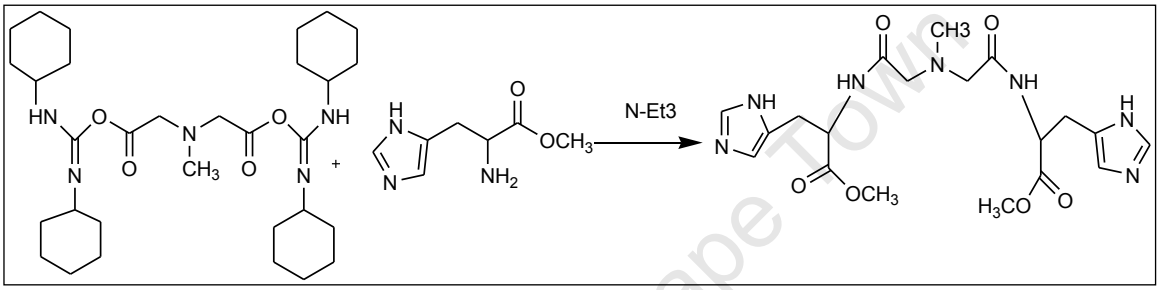

Where R is a reagent, S is a solvent, and Cat is a catalyst

2.3.2 Results and Discussions

When the structure of the product was examined using ^{1}H NMR spectroscopy, there were no peaks showing around 3.22ppm, 3.67ppm and 4.81ppm as was expected. ^{1}H NMR spectroscopy and elemental microanalysis confirmed that the product obtained was not the desired product. The procedure was repeated but DMF was used to activate methyliminodiacetic acid instead of DCC. The physical conditions (temperature and pressure) were also altered. Repeated attempts to synthesize the desired product failed and so this synthetic route was abandoned. Again the expected spectrum was not obtained

REFERENCES

1. Iyer, K.S., Lau, S. Y. J. and Laurie, S.H. (1978) *Journal of Biochemistry* 169;61-69
2. McArdle, H. J., Gross, S. M. Danks, D. M. and Wedd, A. G. (1990) *American Journal of Physiology, Gastrointestinal and Liver Physiology* (6):258
3. Dockal, M., D. C. Carter and F. Ruker (1999) *Journal of Biological Chemistry*. 274; 29303-29310
4. Karakoc, V. et al. (2009) *Selective separation of human serum albumin with copper(II) chelated poly(hydroxyethyl methacrylate) based nanoparticles*. 2(45); 188-193
5. Marx, G., and M Chevion (1986) *Journal of Biochemistry* 236(2): 397–400.
6. Bonomo, R. P. et al. (1995) *Biochemistry* 59(4); 773-784
7. Valko, M., H. Morris, and M. Mazúr (1999) *Journal of Physical Chemistry* 103 (26); 5591–5597
8. Salsabili, N., A. R. Mehrsai and S. Jalaie (2009) *Concentration of blood and seminal plasma elements and their relationships with semen parameters in men with spinal cord injury*. 41;24-28
9. Severini C, Improta G, Falconieri-Erspamer G, Salvadori S, Erspamer V. (2002) *Pharmacology Review*. 54; 285-322.
10. Xuhua, M et al (2009) *Journal of Peptide Science*. 16(2);81-84
11. Hidekazu Katayama (2009) *Pyruvoyl, a novel amino protecting group on the solid phase peptide synthesis and the peptide condensation reaction*. 50(7); 818-821
12. Boesten et al. (1989) *Process for racemizing an optically active N-benzylidene amino-acid amide.* 4847412
13. Mirviss, S. B. (1987) *Racemization of amino acids.* 4713470
14. Chibata et al (1983) *Process for racemizing optically active α-amino acids or a salt thereof.* 4401820
15. Awapara, J. (1948) *Applications of Paper Chromatography to the Estimation of some free Amino acids in Rats*.

16. Davidson, D. I., Sowden, F. J. and Atkinson, H. J. (1951) *Application of Paper Chromatography To Identification and Quantitative Estimation of Amino Acids in Soil Organic Matter Fractions*. 71(5); 347-352
17. Greben, A. E. (1973) *Chemistry and Technology of Fuels and Oils*. *Springer*, New York. 891-893
18. Hamada, J. S. (2002) *Purification of Peptides with Immobilized Enzymes* 120005284
19. Knight, M. et al (1995) *Journal of Chromatography*. 702(2); 207-214

3. GLASS ELECTRODE POTENTIOMETRY

3.1 INTRODUCTION

Glass electrode potentiometry is one of the most reliable methods for studying chemical interactions in solution [1, 2, 3]. In this method, indicators are not used; instead the difference in potentials (emf) is used to predict the end point of a titration reaction. This makes glass electrode potentiometry more reliable over the other since the signals will be created by the analyte only not by the indicator plus the analyte. Moreover, since there are no indicators used, which involve colour changes in most cases, and which only shows colour changes after an end point has been reached, errors due to such conditions are eliminated [2, 3].

However, to use this method, a glass hydronium ion-selective electrode (indicator electrode), a suitable reference electrode and a sensitive potentiometer are needed [4, 5]. To eliminate contamination from the atmosphere, a closed system is preferred. The electrode should be calibrated after every titration, and all solutions used for this kind of titration should be standardized. The composition of at least one of the analytes should be known. Primary chemicals of a known weight are therefore used to standardize the acids/bases which can be used to standardize other solutions like the ligand solutions. Metal ion solutions should also be standardized by described methods [7-9].

The potentiometric titrations are done at a fixed temperature and ionic strength. [4-6] To find the end point from the potentiometric data, a Gran plot is constructed [10, 11]. For this method, an acceptable plot should have two slopes (one slope constructed before end point the other produced after the end point. These two slopes have to meet at one point (end point), and should there be any difference between the two slopes endpoints, this indicates CO_2 contamination which could affect the results since CO_2 forms carbonic acid in aqueous solutions [3-5].

In this study, glass electrode potentiometry was used to study the interactions between the ligand and the protons and the interactions between the three metal ions (Cu(II), Ni(II) and Zn(II)), and the ligand; glycine and glycyl-L-histidine. The potentiometric data was analysed using the Equilibrium Simulations for Titration Analysis (ESTA) software. This data was also used to predict the possible metal/ligand models and to predict the distribution of species in solution.

3.2 THEORY

For the reaction;

$$L + H \leftrightarrow LH$$

Where L is the ligand, H is a proton and LH is a protonated ligand; the thermodynamic protonation constant ${}^{T}K$ of the ligand can be expressed as;

$${}^{T}K_{L1} = \frac{\{LH\}}{\{L\}\{H\}} \qquad (3.1)$$

Where {LH} is the activity of the single protonated ligand, {L} is the activity of the ligand and {H} is the activity of the proton.

Similarly,

$$\{X\} = \Upsilon_X [X] \qquad (3.2)$$

Where {X} is the activity of species X, it can be a ligand, a proton or a metal ion, Υ_X is the activity coefficient of the species X and [X] is the concentration of X.

Therefore,

$${}^{T}K_{L1} = \frac{(\Upsilon_{LH}[LH])}{(\Upsilon_L [L])(\Upsilon_H [H])} \qquad (3.3)$$

Equation (3.3) can be rearranged as;

$$ {}^{T}K_{L1} = \left[\frac{\Upsilon_{LH}}{\Upsilon_{L}\Upsilon_{H}} \right] \left[\frac{[LH]}{[L]\,[H]} \right] \tag{3.4} $$

At constant ionic strength,

$$ \left[\frac{\Upsilon_{LH}}{\Upsilon_{L}\Upsilon_{H}} \right] = \text{constant} \tag{3.5} $$

Since the ionic strength is constant, the equilibrium constant can be expressed as;

$$ K_{L1} = \frac{[LH]}{[L][H]} \tag{3.6} $$

K_{L1}, is the concentration equilibrium constant.

For a ligand that has three protonation constants, ${}^{T}K_{L1,}$ ${}^{T}K_{L2,}$ and ${}^{T}K_{L3}$, the protonation constants can be described in a stepwise manner.

$$ L + H \leftrightarrow LH \qquad K_{L1} = \frac{[LH]}{[L]\,[H]} \tag{3.7} $$

$$ LH + H \leftrightarrow LH_2 \qquad K_{L2} = \frac{[LH_2]}{[LH][H]} \tag{3.8} $$

$$ LH_2 + H \leftrightarrow LH_3 \qquad K_{L3} = \frac{[LH_3]}{[LH_2][H]} \tag{3.9} $$

Likewise, for a ligand with n protonation constants,

$$ LH_{n-1} + H \leftrightarrow LH_n \qquad K_{Ln} = \frac{[LH_n]}{[LH_{n-1}][H]} \tag{3.10} $$

Similarly, for the metal M and the ligand L that react to give a complex ML, the stability constant (K_{ML}) can be described as;

$$M + L \leftrightarrow ML \qquad K_{ML} = \frac{[ML]}{[M][L]} \qquad (3.11)$$

$$ML + L \leftrightarrow ML_2 \qquad K_{ML2} = \frac{[ML_2]}{[ML][L]} \qquad (3.12)$$

Therefore,

$$ML_{n-1} + LH \leftrightarrow ML_n + H \qquad K_{MLn} = \frac{[ML_n][H]}{[ML_{n-1}][LH]} \qquad (3.13)$$

Moreover, the cumulative formation constant (overall formation constant), β can be expressed as;

$$L + H \leftrightarrow LH \qquad \beta_{L1} = K_{L1} = \frac{[LH]}{[L][H]} \qquad (3.14)$$

$$LH + H \leftrightarrow LH_2 \qquad \beta_{L2} = K_{L1}K_{L2} = \frac{[LH_2]}{[L][H]^2} \qquad (3.15)$$

$$LH_2 + H \leftrightarrow LH_3 \qquad \beta_{L3} = K_{L1}K_{L2}K_{L3} = \frac{[LH_3]}{[L][H]^3} \qquad (3.16)$$

$$LH_{n-1} + H \leftrightarrow LH_n \qquad \beta_{Ln} = K_{L1}K_{L2}K_{L3} \ldots K_{Ln} = \frac{[LH_n]}{[LH_{n-1}][H]^n} \qquad (3.17)$$

Similarily,

$$M + L \leftrightarrow ML \qquad \beta_{ML1} = K_{ML1} = \frac{[ML]}{[M][L]} \qquad (3.18)$$

$$ML + L \leftrightarrow ML_2 \qquad \beta_{ML2} = K_{ML1}K_{ML2} = \frac{[ML_2]}{[M][L]^2} \tag{3.19}$$

And

$$ML_{n-1} + L \leftrightarrow ML_n \qquad \beta_{MLn} = K_{ML1}K_{ML2}K_{ML3} \ldots K_{Mn} = \frac{[ML_n]}{[ML_{n-1}][L]^n} \tag{3.20}$$

For the reaction;

$$pM + qL + rH \leftrightarrow MpLqHr$$

Where p is the stoichiometric coefficient of M, q is the stoichiometric coefficient of L and r is the stoichiometric coefficient of H. The formation constant (β) of the reaction can be expressed as;

$$\beta_{pqr} = \frac{[M_pL_qH_r]}{[M]^p[L]^q[H]^r} \tag{3.21}$$

Moreover, the concentrations of $M_pL_qH_r$ from each titration point can be determined and at point k, the concentration of $M_pL_qH_r$ is expressed as;

$$[M_pL_qH_r]_k = \beta_{pqr}[M]_k^p[L]_k^q[H]_k^r \tag{3.22}$$

The total concentration of the free metal ion at point k ($T_{M,k}$) can be expressed as;

$$T_{k,M} = [M]_k + \sum_{i=1}^{N} p\,\beta_{pqr}[M]_p^{\,k}[L]_q^{\,k}[H]_r^{\,k} \tag{3.23}$$

The total concentration of the free ligand at point k ($T_{L,k}$) can be expressed as;

$$T_{k,L} = [L]_k + \sum_{i=1}^{N} q\, \beta_{pqr}\, [M]_p^{\,k}\, [L]_q^{\,k}\, [H]_r^{\,k} \qquad (3.24)$$

The total concentration of the free hydronium ion at point k ($T_{H,k}$) can be expressed as;

$$T_{k,H} = [H]_k + \sum_{i=1}^{N} r\, \beta_{pqr}\, [M]_p^{\,k}\, [L]_q^{\,k}\, [H]_r^{\,k} \qquad (3.25)$$

The coefficient of the proton (r) can be greater or equal to 1 if the complex is protonated. However, the r can have a negative value if the ligand lost all its protons upon complexation with the ligand, or if the hydroxide (OH) has been added to the complex. [10, 11] If r = 0 then the complex is not protonated and there are no hydroxide ions attached to the complex. ML indicates a complex that is not protonated, MLH indicates a complex that has been protonated with one proton, MLH_2 for a complex that has been protonated with two protons and MLH_n means a complex has one central metal ion, one ligand and n protons attached to the complex.

Stability constants depend on temperature as shown by van't Hoff equation;

$$\frac{d\,\mathrm{InK}}{d\mathrm{T}} = \frac{\Delta H^{\ominus}}{RT^2} \qquad \text{OR} \qquad \frac{d\,\mathrm{InK}}{d(1/\mathrm{T})} = -\frac{\Delta H^{\ominus}}{R} \qquad (3.26)$$

Where $\Delta H^{\ominus}$ is the standard enthalpy change of the reaction (expressed in $J.mol^{-1}$), T is the absolute temperature in K and R is the universal gas constant in $J.K^{-1}.mol^{-1}$.

3.3 INSTRUMENTATION

The glass electrode potentiometry instrumentation is in the fashion;

Reference electrode/ salt bridge/ analyte solution/glass electrode
E_{ref} E_j E_g

Each electrode possesses a half reaction. The reference electrode potential, E_{ref}, has a known constant value and it is not affected by the concentration of the analyte solution. Whereas the potential of the glass electrode, E_g, varies with the concentration of the analyte solution [12, 13]. The liquid junction potential, Ej, results due to the difference in concentrations of the analyte solution and the internal reference solution. The observed potential, E_{cell} can therefore be expressed as

$$E_{cell} = E_{ref} + E_j + E_g \quad (3.27)$$

Since E_g varies with the concentration of the analyte solution, the Nernst equation can be written as;

$$E_{cell} = E_{ref} + E_j + E^{\ominus}_g + \frac{RT}{F}\ln\{H\} \quad (3.28)$$

Where $E^{\ominus}_g$ is the standard electrode potential and {H} is the activity of the hydrogen ion. The activity of the proton is expressed as;

$$\{H\} = \Upsilon_H [H] \quad (3.29)$$

Where Υ_H is the activity coefficient of the hydrogen ion and [H] is the concentration of the hydrogen ion.

The ionic strength of the of the solution, I, can be expressed as;

$$I = 1/2\Sigma C_i Z_i^2 \quad (3.30)$$

Where C_i is the concentration of the ionic species, i and Z_i is the charge of the ion.

If the ionic strength and hence the activity coefficient of the H ions are constant then Equation 3.28 can be re-written as;

$$E_{cell} = E_{const.} + \frac{RT}{F} \ln[H^+] \qquad (3.31)$$

However, the potential depends on temperature and the relationship between the two varies with the activity of the hydrogen ion. This can be expressed in terms of the slope factor, s.

$$s = \frac{2.30RT}{F} \qquad (3.32)$$

Putting Equation 3.32 into 3.31 yields;

$$E_{cell} = E_{const.} + s \log[H^+] \qquad (3.33)$$

Calibration of the system requires the calibration of both s and E_{const}.

3.4 EXPERIMENTAL

3.4.1 Preparation of Solutions

All chemicals were of analytical grade and were used without any further purification. All ionic solutions were of 0.15M ionic strength with (Cl^-) Na^+ as the background electrode. Solutions of sodium hydroxide (0.1M) were prepared from Merck ampoules (1.09959-Trisol) in distilled deionised water they were prepared under an inert atmosphere of nitrogen gas. These solutions were standardized with potassium hydrogen phthalate, KHP. The solutions of hydrochloric acid (0.01M) were prepared from Merck ampoules (1.09970-Trisol). These were then standardized with the standard solutions of sodium hydroxide using Gran method methods [11]. The metal solutions were prepared in distilled deionised water and standardized with reported methods for Cu(II), Ni(II) and Zn(II) solutions respectively [8, 9]. The metal ion solutions were in HCl which was 10

times more dilute than the metal itself. This was to prevent the metal ions from hydrolyzing. The ligands were purchased from Sigma-Aldrich and Fluka. They were in powder form and were 99.0% pure.

3.4.2 Potentiometric Measurements

The Ω Metrohm glass electrode was calibrated with a set of Ω Metrohm ion analysis pH buffers from which pH and the Nernstian slope was determined. [11, 12] The slope varied from 58.897 to 59.099. All reactions were performed at 25^{o}C, ionic strength of 0.15M and pH range 2-11 using a Ω Metrohm 848 Titrino plus. Strong acid/strong base titrations were carried out and the potentiometric data used to calculate the electrode response intercept, E^{O}, from the slope and the negative logarithm of the water ion product, pK_w, using the ESTA program.

For the protonation of the ligand, an exact amount of the ligand was weighed into the reaction vessel and known volumes of standard HCl solution were added to it. This was done such that complete protonation was achieved. The solutions were stirred continuously and gently with a Ω Metrohm 801 magnetic stirrer. When a stable temperature of 25±0.1^{o}C was reached the solutions of the ligands were titrated with standards solutions of sodium hydroxide.

For the complexation of the ligands, exact amounts of the ligand was weighed into the reaction vessel and known amounts of the standard solutions of the metal ion solutions were then added. The metal to ligand molar rations varied, between 1:1 and 1:2. The metal ion/ligand system was then titrated with standard solutions of NaOH. .

3.4.3 Data Analysis and Calculations

The potentiometric data was used to calculate the protonation/deprotonation constants of the ligand and the stability constants of the complexes using Equilibrium Simulations for Titration Analysis (ESTA) program. ESTA is a program that was designed to analyse potentiometric data of chemical species in solution [15, 16]. This program has two basic units, namely the simulation unit and the optimization units. The simulation unit (ESTA1) characterises the system on a point by point basis. It does this by using the mass balance equations. This unit is used to calculate complexation functions which help in the interpretation of the data. It can also be used to calculate the speciation of the solution. The plotting unit (ESTA5) is used to put the parameters calculated by ESTA1 in a graphic form.

The optimization units (ESTA2A and ESTA2B) are used to optimize parameters that characterize the titration system as a whole [15]. They give the average values for the titration system. Parameters can be refined using this unit. Other units include the Monte Carlo error propagation unit (ESTA3B) which identifies which parameters need to be refined, and the error imposition unit (ESTA7) which is used to examine the effects of random errors on the values of the refined parameters.

In this study, four tasks from the ESTA program were used. From the potentiometric data, the ZBAR task was used to calculate the formation functions at each titration point. It is from this task that the calculated and the observed formation functions were compared and the residuals were calculated from Equation 3.40 and 3.41 for the proton formation functions and the metal formation functions respectively.

$$\text{Residual pH} = pH^{O} - pH^{C} \tag{3.35}$$

Since the glass electrode is used to study the hydronium ion concentration;

$$E_H = {}^{I}E^{O}_{H} + {}^{S}_{H}\log H \tag{3.36}$$

Similarly;

$$\text{z-bar}_H = \frac{T_H - H + OH}{T_L} \tag{3.37}$$

And;

$$\text{z-bar}_M = \frac{T_L - A + ({}_n\sum \beta_{LHn} H^n)}{T_M} \tag{3.38}$$

Where

$$A = \frac{T_H - H + OH}{({}_n\sum \beta_{LHn} H^n)} \tag{3.39}$$

For proton formation function,

$$\text{Residual formation function} = \text{z-bar}^{O}_{H} - \text{z-bar}^{C}_{H} \tag{3.40}$$

For metal formation function,

$$\text{Residual} = \text{z-bar}^{O}_{M} - \text{z-bar}^{C}_{M} \tag{3.41}$$

Where;

$$\text{z-bar}_H \text{ point residual} = [(pH^{O} - pH^{C})^2 - (\text{z-bar}^{O}_{H} - \text{z-bar}^{C}_{H})^2]^{1/2} \tag{3.42}$$

And;

$$\text{z-bar}_M = [(pA^{O} - pA^{C})^2 - (\text{z-bar}^{O}_{M} - \text{z-bar}^{C}_{M})^2]^{1/2} \tag{3.43}$$

Where pH^O is the observed pH, pH^C is the calculated pH, $z\text{-}bar^O_H$ is the observed proton formation function , $z\text{-}bar^C_H$ the calculated proton formation function, $z\text{-}bar^O_M$ is the observed metal formation function, $z\text{-}bar^C_M$ is the calculated metal formation function, pA^O is the negative logarithm of the observed ligand concentration, pA^C is the calculated ligand concentration, E_H, is the potential of the hydronium ion, $^IE^O_H$ is the standard potential, ^S_H is the slope of the electrode and log H is the logarithm of the proton concentration, T_H is the total concentration of the hydronium ion, H is the concentration of the hydronium ion, OH is the concentration of the hydroxide ion, T_L is the total ligand concentration, A is the ligand concentration, n is the number of protons bind to the ligand, $ß_{LHn}$ is the formation constant of the protonated ligand with n protons, T_M is the total concentration of the metal ion [15].

The second ESTA task is the QBAR. This task is used to calculate the observed and calculated deprotonation functions. Since the deprotonation function is defined as the average number of protons released by the ligand upon complexation with the metal ion then Q-bar is expressed as;

$$\text{Q-bar} = \frac{(T^*_H - T_H)}{T_M} \tag{3.44}$$

Where T^*_H is the calculated total concentration of protons in the system at the observed pH ignoring the presence of all the metal complexes.

When $p = \text{zero}$ and $OH = \frac{K_W}{H}$

The mass balance equations for T^*_H and T_L and be written as;

$$T^*_H = H - OH + \sum_{J=1}^{NJ} r\,(M_pL_qH_r) \tag{3.45}$$

And

$$T_L = L + OH + \sum_{J=1}^{NJ} q\,(M_p L_q H_r) \qquad (3.46)$$

Where $_{NJ}$ is the total number of titration points.

For binary systems, a formation function is defined for the ligand subsystem;

$$\text{n-bar} = \frac{(T^*_H - H + OH)}{T^r_L} \qquad (3.47)$$

For any given M and L stoichiometry (p and q), the average proton stoichiometric coefficient (r-bar) can be calculated.

$$\text{r-bar} = (q \times \text{n-bar}) - (\text{Q-bar} \times p) \qquad (3.48)$$

For ternary systems, the two formation functions, n_L-bar and n_X-bar are defined as;

$$n_L\text{-bar} = \frac{\sum r\,(LH_r)}{T^r_L} \qquad (3.49)$$

$$n_X\text{-bar} = \frac{\sum r\,(XHr)}{T^r_X} \qquad (3.50)$$

If the complex is predominant in solution, the average proton stoichiometric coefficient can be calculated given any M, L and X stoichiometry ($M_pL_qX_sH_r$)

$$\text{r-bar} = (q \times n_L\text{-bar}) + (s \times n_X\text{-bar}) - (\text{Q-bar} \times p) \qquad (3.51)$$

The third task (OBJE) was used for weighting the objective function (U_{obj}) contribution based on the observed emfs and the relative contributions of the most significant errors to the weight at each titration point. This function is expressed as;

$$U_{obj} = (N-n_p)^{-1} \sum_{n=1}^{N} n_e^{-1} \sum_{q=1}^{ne} w_{nq} (y_{nq}^{obs} - y_{nq}^{calc})^2 \quad (3.52)$$

Where;

N is the total number of experimental titration points, n_p is the total number of points being optimized, n_e is the total number of electrodes, w_{nq} is the is the weight of the q^{th} residual at the n^{th} point, y_n^{obs} is the observed variable at the of the q^{th} residual at the n^{th} point and y_n^{calc} calculated variable at the q^{th} residual at the n^{th} point.

Data are optimized by minimizing the objective function. This can be achieved by assuming that the objective function is quadratic with all parameters (Gauss-Newton method)

U_{obj} can therefore be expressed as;

$$U_{obj} = a + p^t b + \frac{(p^t H p)}{2} \quad (3.53)$$

Where a and b are Gauss-Newton quadratic parameter vectors, p is optimization parameter vector, p^t transpose of p and H_{sr} is the Hessian. H_{sr} is expressed as;

$$H_{sr} = \frac{d^2 U_{obj}}{dp_s dp_r} \quad (3.54)$$

The last task of the ESTA program that was used was the OBJT. This works like OBJE except that OBJT the weighting of the objective function is based on the total ion concentration, and OBJT does not allow the Deybe-Hückel liquid junction ion selectivity corrections.

The program also calculates the standard deviations, estimated errors for the parameters being optimized using the method of least squares. The standard deviation σ can be expressed as;

$$\sigma = \left[\frac{U_{obj}\, G_{rr}}{(N - n_p)} \right]^{½} \tag{3.55}$$

The Hamilton R-factor (R^H) can be used to test the agreement between the observed and the calculated values of the refined data. This factor can be expressed as;

$$R^H = \left[\frac{U_{obj}}{\Sigma n_e^{-1} \Sigma w_{nq} (y_{nq}^{obs})^2} \right]^{½} \tag{3.56}$$

The best possible R^H value based on the number of variables and the random errors in the analytical, R^H_{lim} can be expressed as;

$$R_{lim}{}^H = \left[\frac{N}{\Sigma n_e^{-1} \Sigma w_{nq} (y_{nq}^{obs})^2} \right]^{½} \tag{3.57}$$

If R^H is less than R^H_{lim} the model is within the maximum allowed experimental error. [15]

In general, Z-bar was used to estimate the protonation constants of the ligand and the stability constants of the complexes. From the Z_H-bar, the number of protons bound per ligand was estimated, and from the Z_M-bar the number of the ligand bound per metal ion were calculated. From the Q-bar, the number of protons released by the ligand upon complexation with the metal ion was estimated. Q-bar was compared to the n-bar which measures the number of protons that would have bound to the ligand in the absence of the metal ion.

The distribution template of the ESTA programs was used to calculate the distribution of the ligand the metal complexes in solution respectively. The distribution of the ligand depends on the optimised protonation constants and the acid and ligand concentrations, while the distribution of the metal complexes depends on the optimised ligand protonation constants, the optimised stability constants, the ligand concentrations, the acid concentrations and the metal ion concentrations.

3.5 RESULTS

For all the experiments, the slope varied from 58.986 to 59.123; the pKw varied from 13.768 to 13.721; and the E^{o} varied from 399.29 to 414.153 millivolts. The titrations were done in the pH range 2-11 with a glass electrode. All titrations were done at a fixed temperature of 25±1 ^{o}C and a fixed ionic strength of 0.15M with NaCl as the background electrolyte. For the protonation titrations, the ligand was dissolved in standard HCl solution and titrated with the standard NaOH solution. The concentrations of the ligand varied but they were all around 0.001M. The concentrations of the standard solutions of HCl and of NaOH varied but they were around 0.001M and 0.01M respectively.

For the complex formation reactions, the concentrations of the standard metal ions solutions varied and the concentrations of the ligand solutions varied. However, 1:1 metal/ligand systems were made of around 0.001M standard metal ion solutions in 0.0001M HCl and around 0.001M ligand in distilled deionised water. The 1:2 metal/ligand systems were made of around 0.001M standard metal ion solutions in 0.0001M HCl and around 0.002M ligand solutions in distilled deionised water, except for the complexes of glycyl-L-histidine with Ni(II) where around 0.0005M of standard metal ion solutions in 0.00005M HCl and around 0.001M ligand in distilled deionised water were used. The concentrations of the standard solutions of NaOH varied but they were all around 0.01M.

3.5.1 Protonation of Glycine

The glycine system was studied for two reasons. Firstly it is a well known system and hence provided an internal check on the reliability of the experimental system including the operator. Secondly it is part of the molecule of interest and would provide a useful reference. When glycine was titrated with a NaOH the Z-bar levelled off at 1 and the rose up above 1.6 at pH 2.0. As the acid was neutralised, Z-bar levelled off at 1 and then, at pH 8.0 decreased to 0. This gives confidence to our experimental procedure. These final results are summarised in Table 3.1.

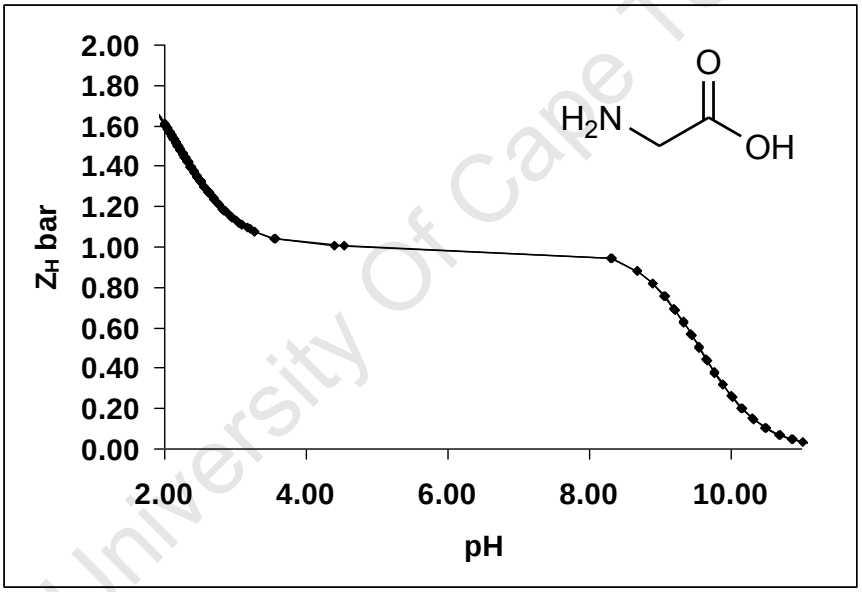

Figure 3.1: Z-bar for the protonation of glycine.

The results were in good agreement with the literature values [16, 17]. The standard deviations were small and the R^H was less than R^H_{lim} thus the model is within the maximum allowed experimental error. (Table 3.1)

Table 3.1: Literature and experimental protonation constants of glycine. Log ß$_{pqr}$ is the logarithm of the sum of overall stability constants, σ is the standard deviation of the Log ß$_{pqr}$, R_H is the Hamiltonian R-factor, R_{lim} is the Hamiltonian R-limit, n_T is the number of titrations, (n_P) is the number of titration points, Log K_{exp} is the logarithm of the experimental stability constants and Log K_{lit} is the logarithm of the stability constants got from literature. [14]

Model p q r	Log ß $_{pqr}$	σ	R^H	R^H_{lim}	$n_T(n_P)$	Log K_{exp}	Log K_{lit}
0 1 1	9.53	0.01	0.003	0.01	4(204)	9.53	9.50(±4)
0 1 2	11.82	0.02				2.29	2.34(±2)

The speciation graph for protonation of glycine is shown in Figure 3.2. The most predominant form of the ligand was LH which formed below pH 2.0. At pH 2.0, 33.68% of the ligand was LH and 66.32% was LH_2. Around 96.70% of LH was formed from pH 3.81 to pH 8.21 where it began to fall gradually. The deprotonated ligand began to form at pH 7.50.

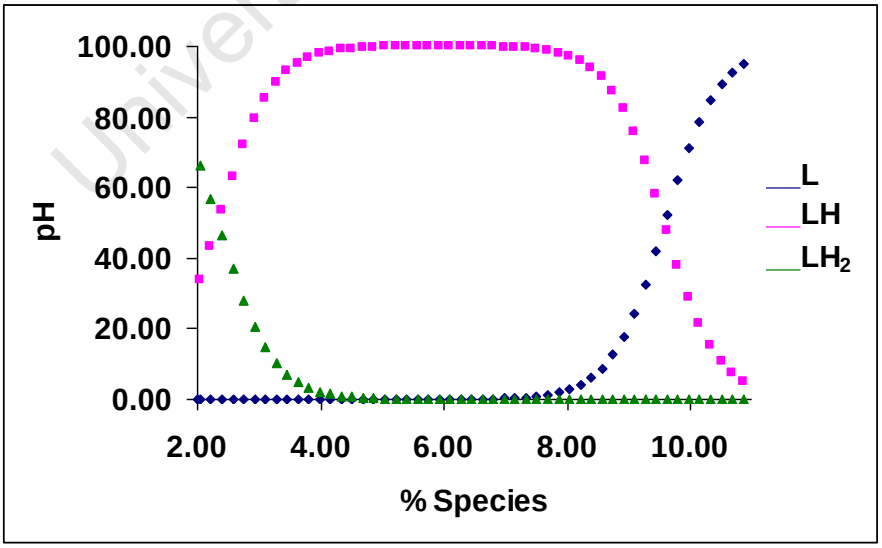

Figure 3.2: Distribution Curve for the protonation of glycine (1:2 metal/ligand system)

3.5.2 Protonation of Glycyl-L-Histidine

Figure 3.3 shows the plot of the formation function, Z-bar as a function of pH for the protonation of glycyl-L-histidine. The Z-bar plot changed direction at pH 7-8, rose up and then levelled off at z-bar = 2 (pH 4-6) and increased slightly above 2.75. This implies that the ligand has three dissociable protons. Full protonation of the ligand occurred at a lower pH, below pH 2 that is why the z-bar plot could only go to 2.75. From the half Z-bar values, it was possible to estimate the three pKa values 8.7, 6.5 and 2.7.

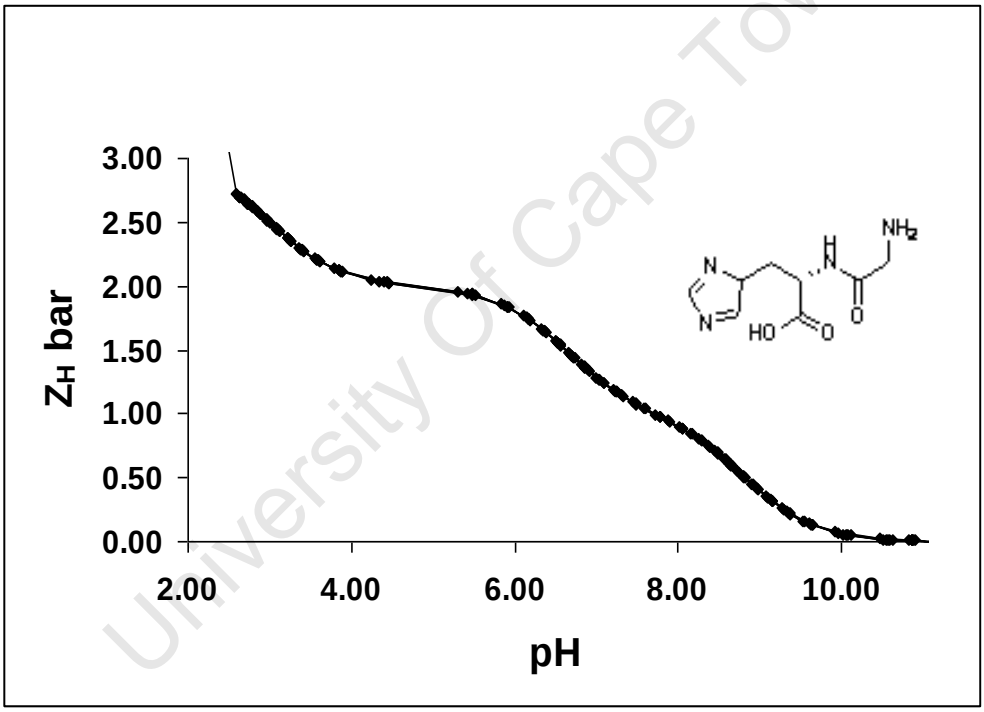

Figure 3.3: Z-bar for the protonation of glycyl-L-histidine

The experimental values of the protonation constants of the ligand estimated using ESTA1 were optimised using ESTA2. The experimental and literature protonation/deprotonation constants of glycyl-L-histidine are presented in Table 3.2. The three protonation constants of glycyl-L-histidine are 8.34, 6.61 and 2.29

respectively. The standard deviations were small and the R^H was less than R^H_{lim} thus the model is within the maximum allowed experimental error. The Log K values did not differ significantly from the literature values. The theoretical plot is represented by a solid line in Figure 3.3. The agreement between the theoretical and the experimental plot gives us confidence in the results.

Table 3.2: Literature and experimental protonation constants of glycyl-L-histidine. Log $ß_{pqr}$ is the logarithm of the sum of overall stability constants, σ is the standard deviation of the Log $ß_{pqr}$, R_H is the Hamiltonian R-factor, R_{lim} is the Hamiltonian R-limit, n_T is the number of titrations, (n_P) is the number of titration points, Log K_{exp} is the logarithm of the experimental stability constants and Log K_{lit} is the logarithm of the stability constants got from literature. [14]

Model p q r	Log $ß_{pqr}$	σ	R^H	R^H_{lim}	$n_T(n_P)$	Log K_{exp}	Log K_{lit}
0 1 1	8.34	0.02	0.004	0.01	4(204)	8.34	8.14(±8)
0 1 2	14.95	0.03				6.61	6.70(±7)
0 1 3	17.24	0.05				2.29	2.52(±2)

Logarithms of the overall protonation constants, log ßs, were used to calculate the distribution of L, LH, LH_2 and LH_3 species in solution. The calculations were performed using ESTA1, and the plot was done using ESTA5. This plot is represented in Figure3.4.

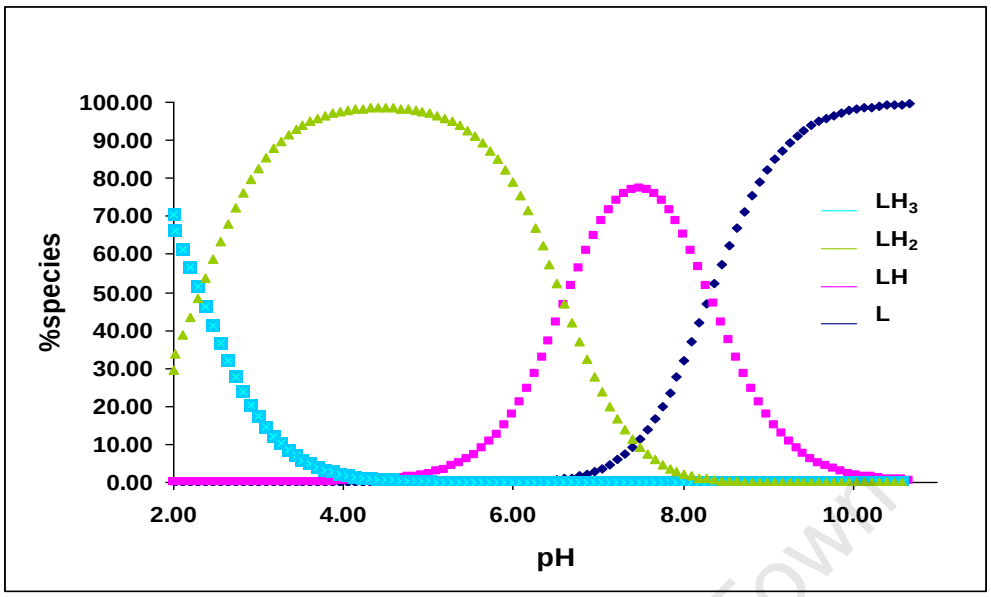

Figure 3.4: Distribution Curve for the protonation of glycyl-L-histidine

Complete protonation of glycly-L-histidine occurred at a very low pH and at pH 2.00 there was about 70.44 percent of the LH_3 species and 29.56 percent of the LH_2 species. This is shown in Figure 3.4. Around pH 2.38, the amount of LH_3 species was equal to the amount LH_2 species. The latter then dominated the system after pH 2.38 to around pH 6.43. The LH species dominated the system from pH 6.52 to about pH 8.25 but a maximum of 77.29 percent of it was formed since three species were present in this pH range, LH_2, LH and L. The neutral form of the ligand began to form at pH 6.60 and 92.68 percent (plus) of it was formed from pH 9.51.

3.5.3 Complex Formation Titrations

3.5.3.1 Cu(II)/Glycine System

When glycine was complexed with Cu(II), 2:1 glycine to Cu(II) molar ratio, the Z_M-bar leveled at Z_M-bar = 2. The ML_2 were therefore the most predominant species in solution. This agrees with literature [14, 16]. The Z_M-bar curve for the Cu(II)/glycine

is shown in Figure 3.5. Moreover, Z_M-bar did not bend backwards because there no hydroxide species formed in the Cu(II)/glycine system.

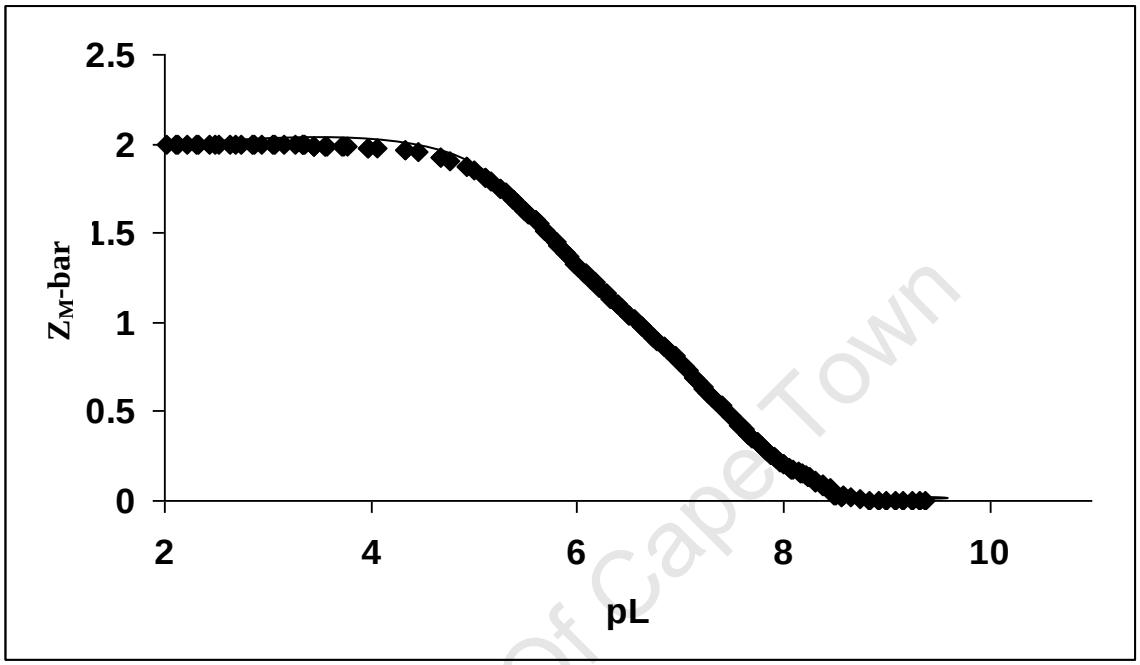

Figure 3.5: Z_M-bar as a function of pL for Cu(II)/Glycine system.

The Q_M-bar for the Cu(II)/glycine system is shown in Figure 3.6. The leveling of n-bar at one means the ligand has one dissociable proton, however, the Q_M-bar rose to a maximum of around 1.86 therefore glycine lost two protons upon complexation with Cu(II). This agrees with the reported data for Cu(II)/glycine [14, 16, 17]. Comparing the Z_M-bar of Cu(II)/glycyl-L-histidine system and the Z_M-bar of Cu(II)/glycine system, the latter rose until a maximum of Z_M-bar = 1.86 was reached, it dropped down gradually and never rose up again. This confirms that there were no hydroxide species formed in the Cu(II)/glycine system.

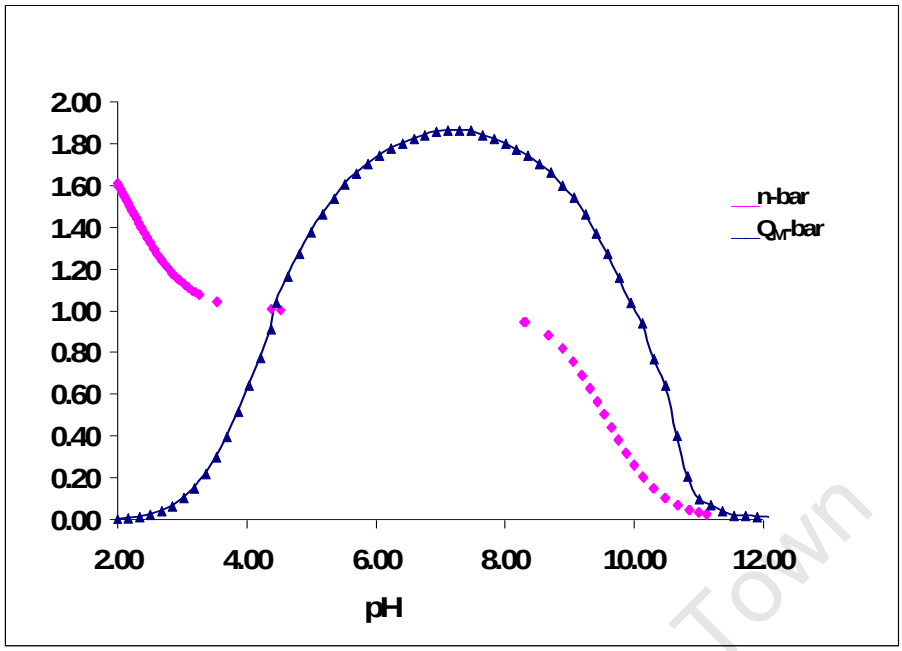

Figure 3.6: Q_M-bar as a function of pH for Cu(II)/glycine system

The stability constants were summarized in Table 3.3. There was no significant difference between the experimental results and the literature values of the log K. The standard deviations and R^H were small, and R^H was less than R^H_{lim} therefore the errors were less than the maximum allowed experimental errors.

Table 3.3: Literature and experimental stability constants of Glycine and Cu(II). Log ß $_{pqr}$ is the logarithm of the sum of overall stability constants, σ is the standard deviation of the Log ß$_{pqr}$, R_H is the Hamiltonian R-factor, R_{lim} is the Hamiltonian R-limit, n_T is the number of titrations, (n_P) is the number of titration points, and Log K_{lit} is the logarithm of the stability constants got from literature. [14]

Model p q r	Log ß $_{pqr}$	σ	R^H	R^H_{lim}	$n_T(n_p)$	Log K_{exp}	Log K_{lit}
1 1 0	8.09	0.004	0.003	0.01	4(216)	8.09	8.15(±9)
1 2 0	15.11	0.006				7.02	6.85 (±1)

The speciation curve for the complexation of glycine with Cu(II) is shown in Figure 3.7. The ML species began to form from pH 2.35. A maximum of 78.60% of the ML species was formed at pH 4.82, and the species began to fall gradually after this pH. At pH 6.22, all the Cu(II) was used up. The ML_2 species formed from pH 3.76, about 93.29 of LM_2 was formed at pH 7.63.

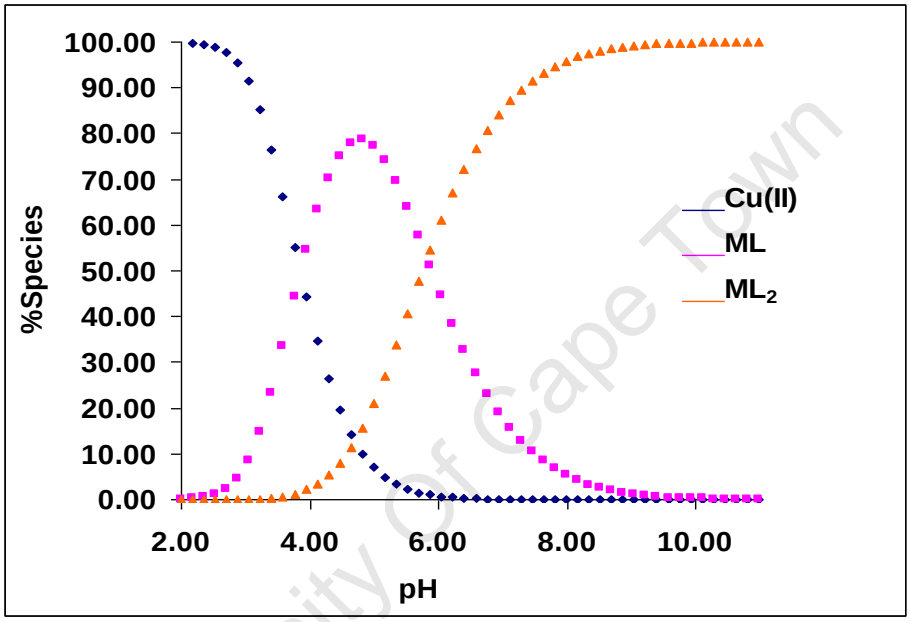

Figure 3.7: The distribution curve for the Cu(II)/Glycine system

3.5.3.2 Cu(II)/Glycyl-L-histidine System

The stability constants of the Cu(II)-ligand solutions were calculated with ESTA program from the potentiometric data. The data was put in the metal/ligand template of ESTA and the protonation constants of the ligand were also put into the template. From the potentials and the protonation constants of the ligand, the stability constants of the ligand complexes were calculated and optimised as mentioned earlier [13]. The ML species were the most predominant species in solution. This is clearly presented in Figure 3.8.

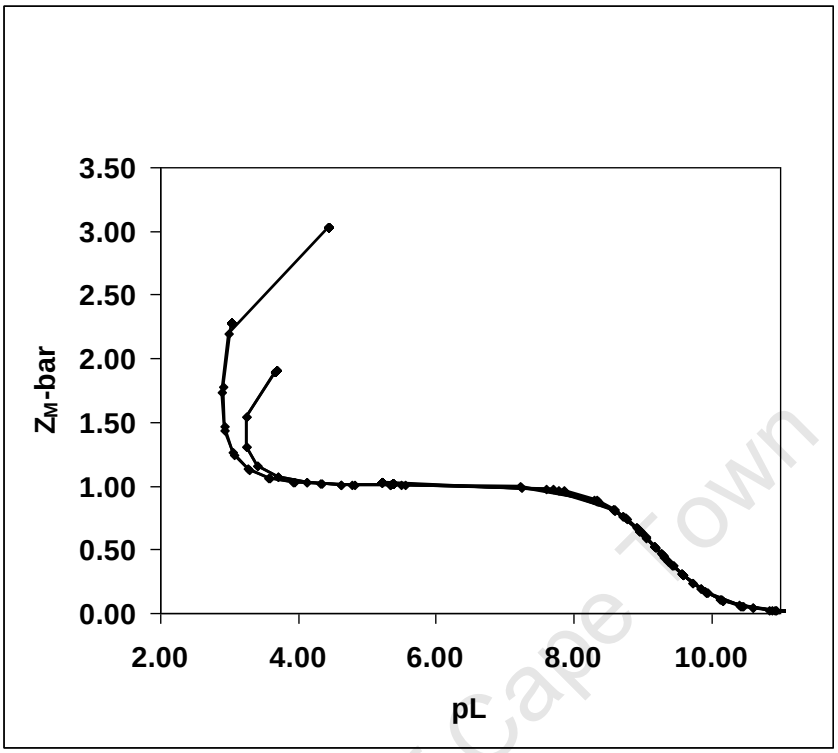

Figure 3.8: Z_M-bar as a function of pL for Cu(II)/Glycyl-L-histidine system.

For clarity, some of the data points are omitted. The solid line is the theoretical curve calculated using results given in Table 3.4. Figure 3.8 shows the Z_M-bar curve for Cu(II)/glycyl-L-histidine system. Z_M-bar levelled off at Z_M-bar = 1 at pH range 3.70 to 7.85. This indicates that the ML species is predominant in this pH range. Figure3.8 was plotted using ESTA5 and the proportion of the metal ion concentration to ligand concentration varied from 1:1 Cu(II)/ligand to 1:2 Cu(II)/ligand ratios. The Z_M-bar for 1:1 Cu(II)/ligand system curved backwards at Z_M-bar = 1 and that of a 1:2 Cu(II)/ligand curved backwards at Z_M-bar = 2. The Z_M-bar function is really only defined for simple, stepwise mononuclear complexation. Hence, when the Z_M-bar function deviates from its normal shape, this indicates that other, more complex species are forming. In this case the Z_M-bar function curves back indicating the formation of deprotonated or hydroxy species. The solid line represents the theoretical plot. The agreement between the two gives us confidence in the model.

Since the Z_M-bar function rapidly becomes undefined when hydroxy species are formed we can use the deprotonation function to depict the data. The deprotonation function for the complexes of Cu(II) and the ligand are plotted in Figure 3.9. The levelling off of the n-bar at n-bar = 2 means the ligand has two dissociable protons. Due to complexation by Cu(II), the ligand began to lose protons from around pH 3.34. At pH 4.8, the n-bar and Q-bar functions intersect and then the Q-bar rises to about Q-bar = 2.2. This indicates that more protons are released from the ligand than were present in the first place. This could happen if one of the amides lost a proton or if a coordinated water molecule lost a proton.

Thermodynamically these two processes are the same. Between pH 6 and 8, the n-bar and Q-bar curves run parallel. This means that in this pH range no change in complexation is taking place (in the analysis of the data, these points would just add to the total experimental error). The ML species formed from pH 3.34 to pH 4.95 where complexation completed and there was no change in speciation until at pH 9.37 where the hydroxide species began to form.

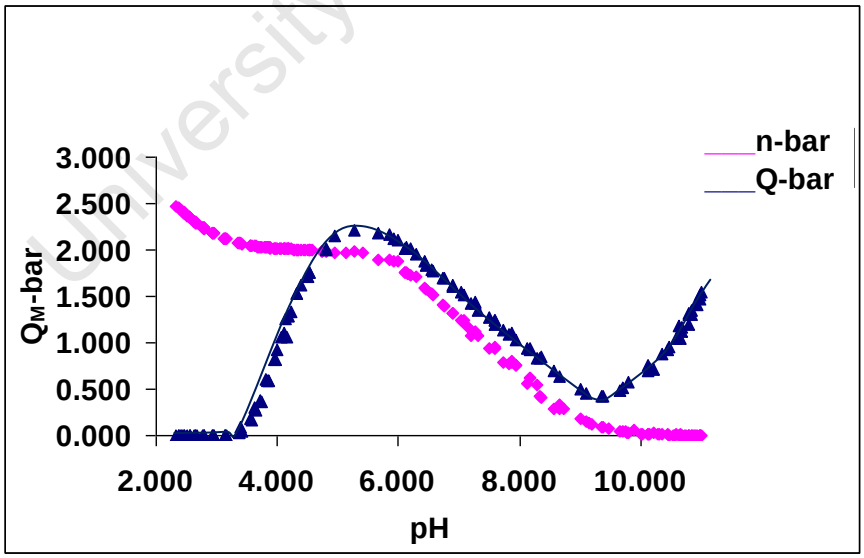

Figure 3.9: Q_M-bar as a function of pH for Cu(II)/Glycyl-L-histidine system

The potentiometric data was analysed using ESTA2 with the results shown in Table 3.4. The experimental model is different from the literature model, but the stability constants for the ML species for both the experimental and the literature data were comparable.

Table 3.4: Literature and experimental stability constants of Glycyl-L-Histidine and Cu(II). Log ß $_{pqr}$ is the logarithm of the sum of overall stability constants, σ is the standard deviation of the Log ß$_{pqr}$, R_H is the Hamiltonian R-factor, R_{lim} is the Hamiltonian R-limit, n_T is the number of titrations, (n_p) is the number of titration points, and Log K_{lit} is the logarithm of the stability constants got from literature. [17]

Model p q r	Logβ_{pqr}	σ	R^H	R^H_{lim}	$n_T(n_p)$	Log K_{exp}	Log K_{lit}
1 1 0	9.162	0.008	0.004	0.009	4(204)	9.162	8.98(±8)
1 2 0	(ML_2 not observed)					-	16.16(±1)
1 1 1	(MLH not observed)					-	3.50 (±2)
1 1 -1	0.387	0.012				4.840	4.09(±6)
1 1 -2	-12.041	0.010				3.214	3.20(±2)
1 1 -3	-22.175	0.017				2.003	-

When the model similar to the literature one was put into ESTA, there were significant differences between the observed and calculated pHs, Z-bars, and some species showed a zero concentration from the first point of the titration to the last. This indicated that the literature model was not appropriate to our experimental conditions. In both Figure 3.8 and 3.9 the solid line was calculated assuming the model and constants given in Table 3.4 were correct. The agreement between the theoretical curves and the experimental data is excellent and lends confidence to our results. The standard deviations were small and the

R^H was less than R^H_{lim} therefore the model is within the maximum allowed experimental error.

The species distribution curve for the complexes of glycyl-L-histidine and Cu(II) is shown in Figure 3.10. At pH 2, there was 100 percent of the free metal ion species. Around pH 2.08, the ML species began to form. At pH 4.90, all the metal ions were used up and 100 percent of the ML species was formed. The ML species began to fall at pH 7.18 where the formation of MLH_{-1} commenced. The MLH_{-1} was formed at the expense of the ML species. About 100 percent of the MLH_{-1} was formed at pH 10.02 even though there was a rapid fall soon after that. A maximum of 3.42 percent of the MLH_{-2} was formed and most of the MLH_{-1} species were converted to MLH_{-3}.

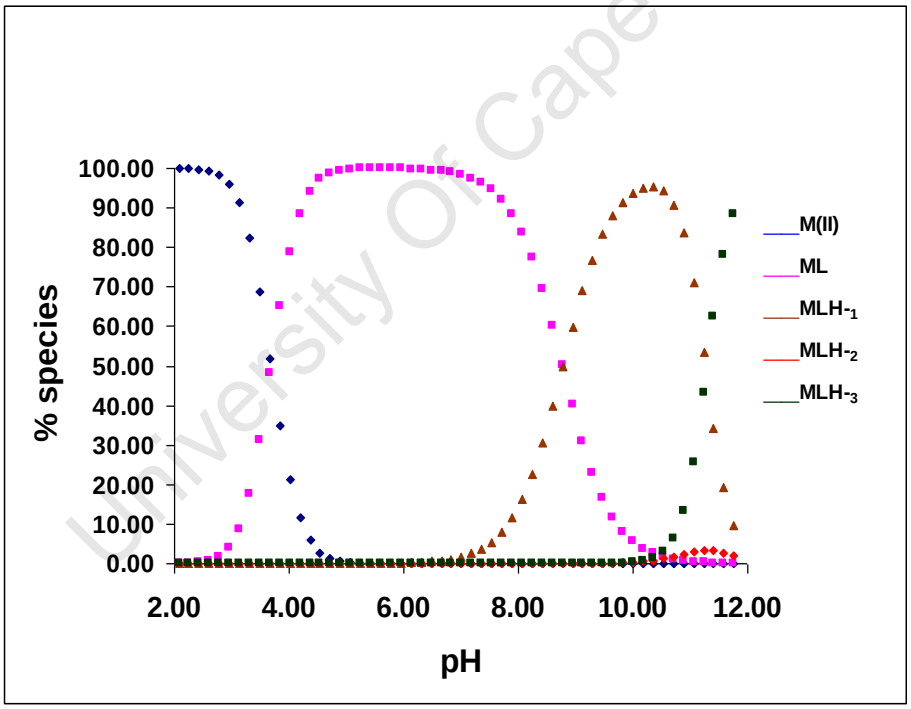

Figure 3.10: The distribution curve for the Cu(II)/Glycyl-L-histidine system (1:2 metal/ligand concentration)

3.5.3.3 Ni(II)/glycyl-L-histidine systems

The stability constants of the complexes of glycyl-L-histidine and Cu(II), were compared with the stability complexes other metal ions, Ni(II) and Zn(II), under the same environmental conditions. The metal to ligand composition ratio varied from 1:1 and 1:2 for all the metal to ligand titrations. The Z_M-bar for the complexation of Ni(II) with glycyl-L-histidine is shown in Figure 3.11. The Z_M-bar curves start to fan back almost immediately indicating that the ML species does not predominant in solution.

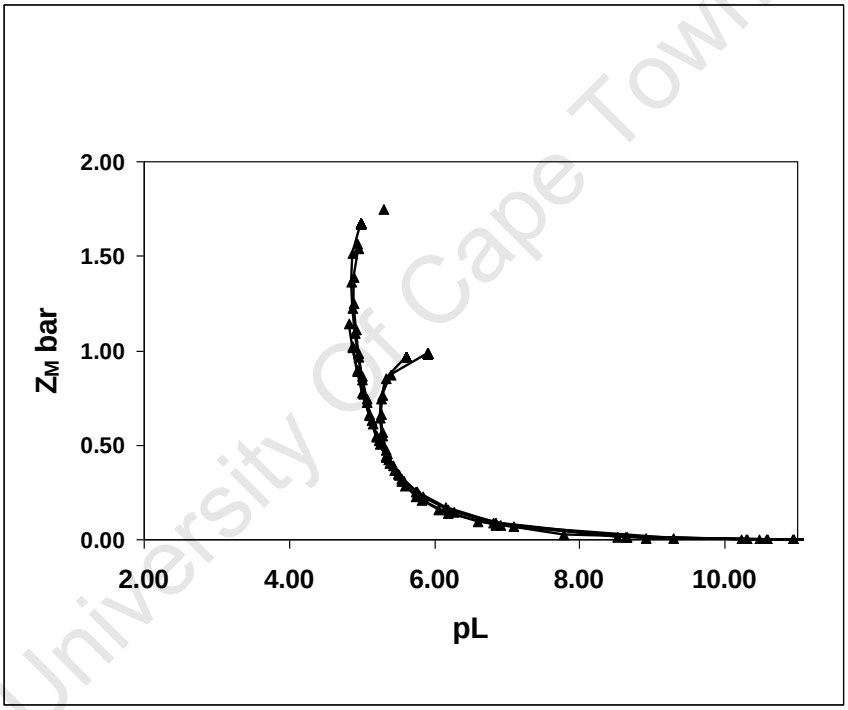

Figure 3.11: Z_M-bar as a function of pL for Ni(II)/Glycyl-L-histidine system.

Figure 3.12 shows the Q-bar for the complexation of Glycyl-L-Histidine with Ni(II). The levelling off of the n-bar at n-bar = 2 means the ligand has two dissociable protons. The ligand began to lose protons from around pH 2.26 upon complexation with Ni(II). There between n-bar and the Q-bar curves intersect at pH 6.47 and at pH 6.61, and the Q-bar rises to a maximum of about Q = 2.26. For both systems, the 1:1 metal/ligand and

1:2 metal/ligand systems, two protons were lost when the ligand was complexed with Ni(II). The graph drops down and runs parallel to the n-bar. The Q-bar rose above n = 2 because hydroxide species were formed. The Q-bar dropped because complexation was complete. The bending of the graphs shows the presence of the hydroxide species in solution. The model is within the maximum allowed experimental error because the standard deviations were small and the R^H was less than R^H_{lim}.

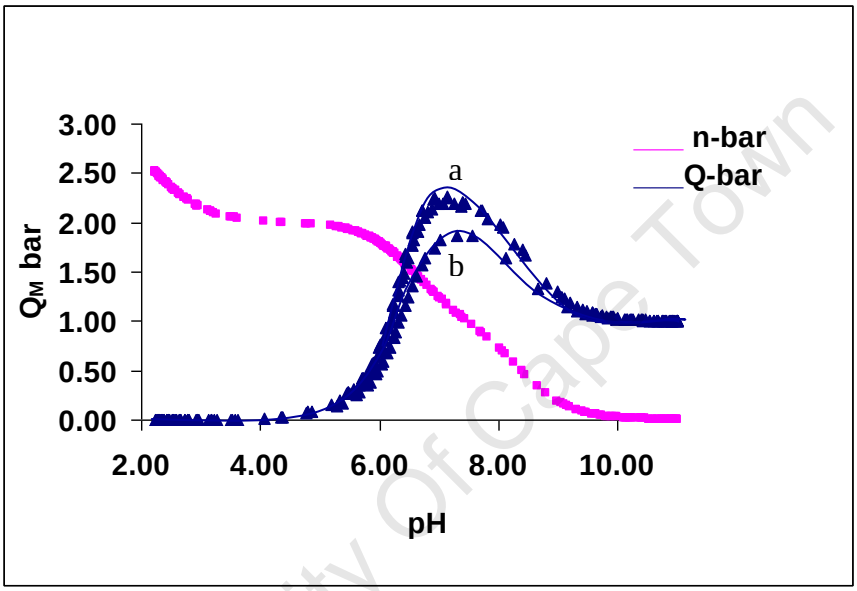

Figure 3.12: Q_M-bar as a function of pH for Ni(II)/Glycyl-L-histidine system

The stability constants of the complexes of Ni(II) and glycyl-L-histidine are presented in Table 3.5. The stability constant of the ML species of the Cu(II)/glycyl-L-histidine system is greater than the stability constant of ML species of the Ni(II)/glycyl-L-histidine system (log K for ML in the Cu(II) = 9.162 and the log K for the Ni(II) = 5.532). The MLH_{-1} from the Cu(II)/glycyl-L-histidine system were less stable than the MLH_{-1} species from the Ni(II)/glycyl-L-histidine system (the log K for the Cu(II) system for MLH_{-1} was 4.840 and log K for MLH_{-1} for the Ni(II) is 6.032). Other species got from the Cu(II) system were not similar to the species got from the Ni(II) system. However, the experimental values of the log Ks were comparable with the log Ks got from literature for

the Ni(II)/glycyl-L-histidine system except for log K of the ML_2 species which was significantly different from the log of the same species from literature.

Table 3.5: Literature and experimental stability constants of Glycyl-L-Histidine and Ni(II). Log ß $_{pqr}$ is the logarithm of the sum of overall stability constants, σ is the standard deviation of the Log ß$_{pqr}$, R_H is the Hamiltonian R-factor, R_{lim} is the Hamiltonian R-limit, n_T is the number of titrations, (n_P) is the number of titration points, and Log K_{lit} is the logarithm of the stability constants got from literature. [14]

Model p q r	Log β_{pqr}	σ	R^H	R^H_{lim}	$n_T(n_p)$	LogK_{exp}	Log K_{lit}
1 1 0	5.532	0.002	0.009	0.011	6(424)	5.532	4.68
1 2 0	14.511	0.034				8.979	9.62(±3)
1 1 1	11.766	0.008				6.562	6.66
1 1 -1	-1.708	0.011				6.032	6.04(±4)
1 2 -1	2.750	0.002				3.53	3.42

Figure 3.13 shows the distribution of species for the Ni(II)/ligand system. At pH 2.29, the MLH species began to form. The splitting of the graph indicates the presence of the MLH species. A maximum of 56.46% of these species was observed at pH 5.81. At pH 4.56, the ML species began to form. Only 14.97% of the ML species were observed in solution and this was observed at pH 6.16. The ML_2 and MLH_{-1} species began to form around the same pH, at pH 5.28. A maximum of 62.02% of ML_2 was observed at pH 6.87, and a maximum of 22.61% of MLH_{-1} species was observed a pH 6.60. The ML_2H_{-1} began to form at pH 6.08. At pH 9.51, there were only two species in solution, the MLH_{-1} and the ML_2H_{-1} species, and only 4.56% of the MLH_{-1} was present at this pH.

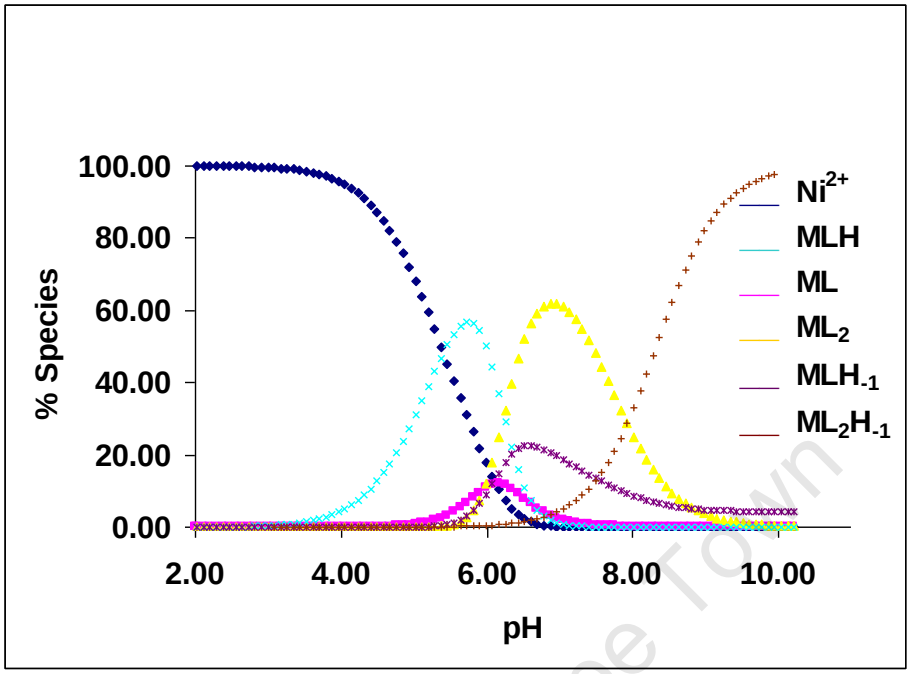

Figure 3.13: The distribution curve for the Ni(II)/Glycyl-L-histidine system. (1:2 metal/ligand concentration)

3.5.3.4 Zn(II)/glycyl-L-histidine systems

Figure 3.14 shows Z-bar for the complexation of the ligand with Zn(II). This was plotted using two sets of data, data from a 1:1 metal/ligand system and data from 1:2 metal ligand systems. The graph levels off around Z-bar = 0.48. The ML species were therefore not predominate species in solution. In fact this levelling off indicates the formation of a protonated species. The bending off of the graph at z-bar = 1 is due to the presence of the hydroxide species from a 1:1 metal/ligand system, and the bending off of the ligand at z-bar = 2 indicates the presence of the hydroxide species from the 1:2 metal/ligand data.

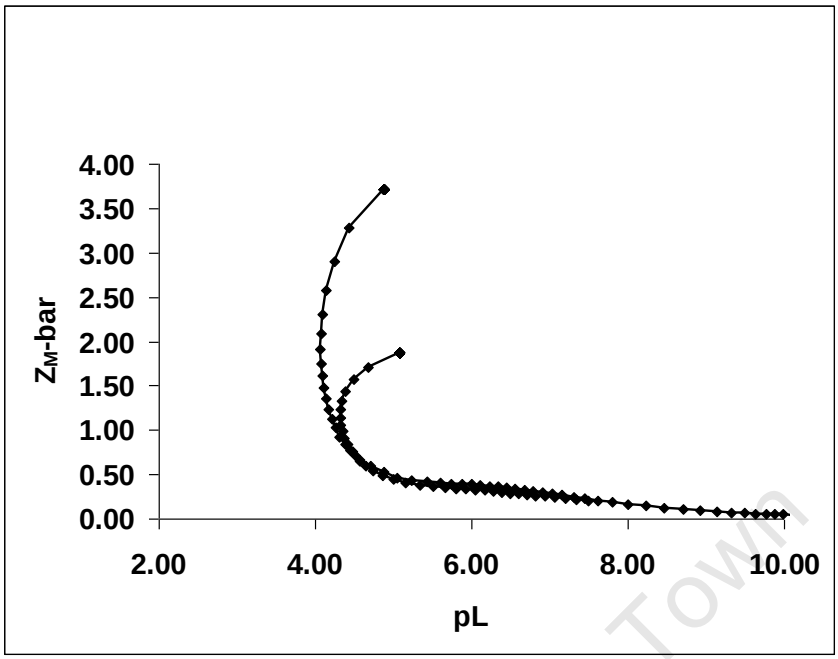

Figure 3.14: Z_M-bar as a function of pL for Zn(II)/Glycyl-L-histidine system.

Figure 3.15 shows the Q-bar for the complexation of Glycyl-L-Histidine with Zn(II). The levelling off of the n-bar at n-bar = 2 means the ligand is capable of losing two protons upon complexation with a metal ion. The ligand began to lose protons from around pH 4.36 upon complexation with Zn(II). The splitting of the graph indicates the presence of the MLH species. There are intersections between n-bar and the Q-bar at pH 6.18 and at pH 6.57, and the Q-bar rises to a maximum of about Q = 2.76 and Q = 1.50 for graph a and graph b respectively. In a 1:2 metal/ligand system, three protons were lost as a result of complexation between the metal ion and the ligand, and in a 1:1 metal/ligand one proton was lost. The graphs drop down and run parallel to the n-bar. The Q-bar rose above n = 2 because the hydroxide species were formed. The Q-bar dropped from pH 7.36 (graph a) and pH 7.40 (graph b). Graph a rose again at pH 9.06 while graph b rose at pH 9.56. These indicate the presence of the hydroxide species.

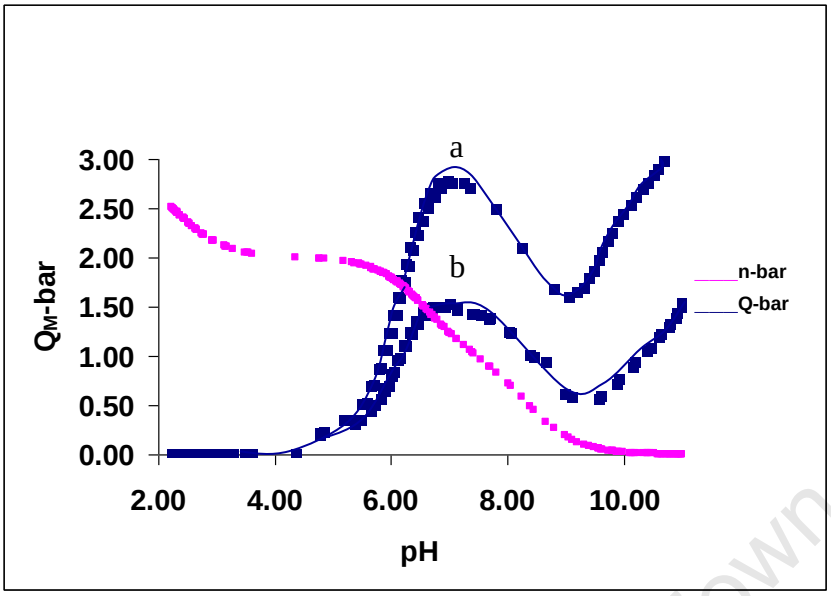

Figure 3.15: Q_M-bar as a function of pH for Zn(II)/Glycyl-L-histidine system

The stability constants for the Zn(II)/glycyl-L-histidine complexes are shown in Table 3.6. Log K for the ML species for the this system is less than the stability constants for the same species of the Ni(II) and the Cu(II) systems. The ligand (glycyl-L-histidine) therefore forms more stable complexes with Cu(II) than it does with Ni(II) and Zn(II). However, the ML were the only common species in the Cu(II) and in the Zn(II) systems. The Ni(II)/glycyl-L-histidine system shared three similar species with Ni(II)/glycyl-L-histidine system; ML, MLH and ML_2 species. The stability constants of all the three complexes (ML, MLH and ML_2) in Ni(II)/glycyl-L-histidine were greater than the stability constants of the same complexes for the Zn(II)/ glycyl-L-histidine system. Glycyl-L-histidine thus forms more stable complexes with Ni(II) than it does with Zn(II). The standard deviations were small compared to the log β values and the R^H was less than R^H_{lim} thus the model is within the maximum allowed experimental error.

Table 3.6: Literature and experimental stability constants of Glycyl-L-Histidine and Zn(II). Log ß $_{pqr}$ is the logarithm of the sum of overall stability constants, σ is the standard deviation of the Log ß$_{pqr}$, R_H is the Hamiltonian R-factor, R_{lim} is the Hamiltonian R-limit, n_T is the number of titrations, (n_p) is the number of titration points, and Log K_{lit} is the logarithm of the stability constants got from literature. [14]

Model p q r	Log β_{pqr}	σ	R^H	R^H_{lim}	$n_T(n_p)$	LogK_{exp}	Log K_{lit}
1 1 0	4.031	0.009	0.008	0.015	6(418)	4.031	3.98
1 2 0	10.209	0.016				6.178	7.9(±2)
1 1 1	10.798	0.013				6.021	6.89
1 1 -1	(MLH_{-1} not observed)					-	6.73
1 1 -2	(MLH_{-2} not observed)					-	9.91
2 2 0	11.689	0.051				10.948	11.11
2 2 -1	4.100	0.023				6.998	7.03

Figure 3.16 shows the distribution curve for the species in Zn(II)/glycyl-L-histidine system. The most predominate species in this system were the ML_2 species which were produced from pH 3.94. This species dominated the system after around pH 5.17 where both the Zn(II) and the ML_2 were at the percentage, 70.27%. MLH started forming from pH 3.24. The production of this species (MLH) increased until a maximum of 32.60% was reached, at 5.32 where after it dropped gradually until it reached zero at pH 6.76. The ML and the M_2L_2 both started to form from pH 5.00. A maximum of 13.60% at pH 5.70 for the ML species and a maximum of 2.60% for the M_2L_2 at pH 5.88 were attained. The small amount of M_2L_2 species both formed is reflected by the high standard deviation of log β for this species. The quantity of ML decreased until all the ML were used up at pH 7.11, and the amount of the M_2L_2 species decreased after the maximum was reached. At pH 6.93 M_2L_2 were used up. The amount of the free Zn(II) ions decreased with pH, at pH 7.11 all the Zn(II) was exhausted, and at the same pH the

MLH_{-1} began to form. The amount of ML_2 in solution decreased gradually with formation of MLH_{-1}.

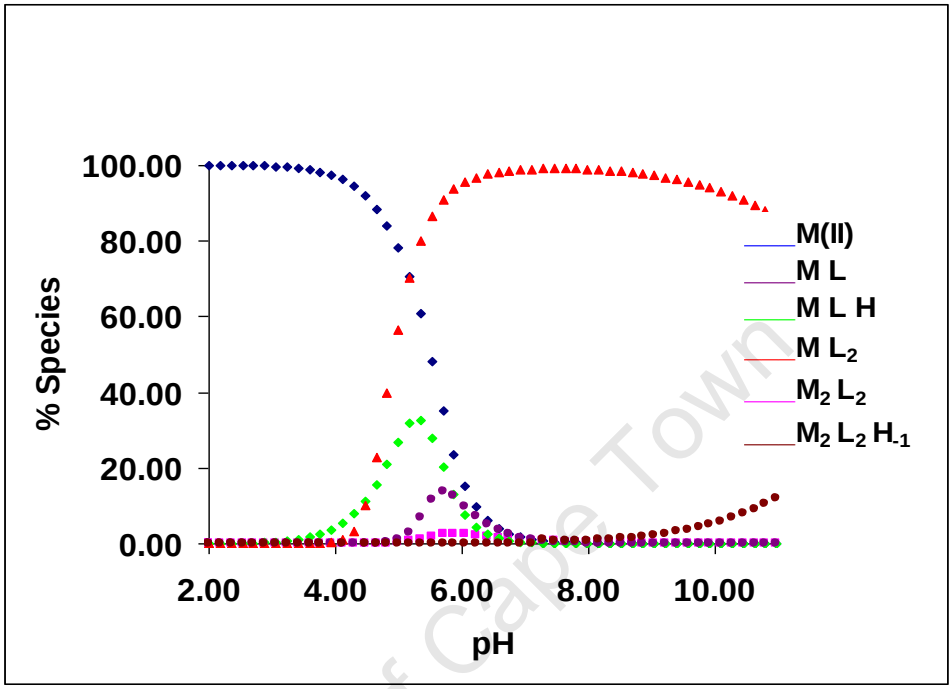

Figure 3.16: The distribution curve for the Zn(II)/Glycyl-L-histidine system. 1:2 (metal/ligand concentration)

3.5.4 Discussion

Comparing the stability constants of the ML species of glycyl-L-histidine with Cu(II), Ni(II) and Zn(II), the stability constant for these species in Cu(II) system were greater than the stability constants in Ni(II) and Zn(II). This is the normal trend one would expect from the Irving Williams stability series.

Moreover, the ML species in the Cu(II) were observed from pH 2.43 to pH 10.71, a maximum peak was reached from pH 4.54 to pH 7.54 (amount of ML at pH 4.54 to pH 7.54 varied from 94.54% to 99.91%). The maximum of 11.94% of the same species in Ni(II) system was observed. ML species in Ni(II)/glycyl-L-histidine system were observed at pH range 4.75 to 7.84. ML in the Zn(II) system were observed from pH 5.00

to pH 6.93, and a maximum of 13.60% of these species in Zn(II)/glycyl-L-histidine system were observed. (Figures 3.5, 3.8 and 3.11)

The ML_2 and the MLH species were not observed for Cu(II). The stability constant (log K = 8.979) for the ML_2 system in the Ni(II) had a larger value than the stability constant (log K = 6.178)in the Zn(II) system by 2.801 log units. In addition, the stability constant (log K = 6.562) for the MLH species in the Ni(II) was 0.541 log units greater than the stability constants (log = 6.021) of the same species in the Zn(II) system. However, literature shows the opposite [17]. From literature [17], the Zn(II) MLH species was 0.23 log units more stable than the Ni(II) complex (Table 3 and Table 4). This contradicts the Irving Williams stability series. Hence we have confidence in our results.

A Zn(II) stability constant greater than that of Ni(II) would also contradict Irving-Williams stability series; [18, 19]

Mn(II) < Fe(II) < Co(II) < Ni(II) < Cu(II) > Zn(II)

The deviations from Irving-Williams stability series may be due to the change of spin or conformation of the central metal ion [18, 20]. In this case, Ni(II) complex may go from octahedral to square planer which would increase the stability of the complex.

However, the stability constant (log = 6.032) of the MLH_{-1} species in the Ni(II) system was greater than the stability constant (log K = 4.840) of the same species in the Cu(II) system by 1.192 log units. This illustrates the difficulty of comparing stepwise stability constants when hydroxyl species are formed. The stability constant includes both the complexation of the ligand and the loss of a proton. Rather than comparing logK, one should, in this case, look at logβ. These are -1.7 and 0.38 for Ni(II) and Cu(II) respectively. The stability constants for MLH_{-1} in both systems were not significantly different from the literature [17] values. These species were not observed in the Zn(II) system.

The MLH_{-2} and MLH_{-3} were not observed in the Ni(II) and in the Zn(II) systems, and there was no data on the stability constants of MLH_{-3} in the Cu(II)/glycyl-L-histidine system from literature. However, the standard deviation of log β_{11-3} was quite small. ML_2H_{-1} species were observed in the Ni(II) system but they were not observed in Cu(II) and in Zn(II) systems. However, the $\sigma_{1\ 2-1}$ was small and the log K for this species was not significantly different from the literature value since the literature values were done at a lower ionic strength (I =0.1M) and the ionic strength for the experimental was 0.15M. The two species M_2L_2 and $M_2L_2H_{-1}$ were observed in the Zn(II) system.

3.5.5 Conclusions

Glycine has two dissociable protons and glycyl-L-histidine has three dissociable protons. The LH form of glycine was more stable than the LH form of glycyl-L-histidine. However, this form (LH) exists at very low pH's for both ligands. The speciation for the protonation of glycine and that of glycyl-L-histidine showed that at pH 4 there was very little LH in solution. The LH_2 form of glycine was less stable than that of glycyl-L-histidine. The second protonation constant of glycine was equal to the third protonation constant of glycyl-L-histidine..

When glycine was complexed with Cu(II), there were only two species formed, ML and ML_2. There were no hydroxide species formed and the Q-bar plot for this system did not show any oscillations as a result. Glycyl-L-histidine formed four different species with Cu(II); ML, MLH_{-1}, MLH_{-2} and MLH_{-3}. The ML species of glycine were less stable than that of Cu(II) and glycyl-L-histidine. However, the ML_2 of Cu(II) and glycine were more stable than the other three species formed between glycyl-L-histidine and Cu(II); MLH_{-1}, MLH_{-2} and MLH_{-3}.

The ML species of Cu(II) and glycyl-L-histidine was more stable than that of Zn(II) with glycyl-L-histidine and of Ni(II) with the same ligand. The Ni(II)-glycyl-L-histidine complex that existed in the form MLH_{-1} was more stable than that of Cu(II)-glycyl-L-histidine. This species was not observed in the Zn(II) system. Unlike Cu(II), both Ni(II) and Zn(II) complexes did not exist in the MLH_{-2} and MLH_{-3} forms. The M_2L_2

species formed between Zn(II) and glycyl-L-histidine was the most stable complex of all the complexes observed in this study. It had a log K value of 10.948.

REFERENCES

1. Meinrath, G., A. Kufelnicki and M. Świątek (2005) *Accreditation and Quality Assurance: Journal for Quality, Comparability and Reliability in Chemical Measurement.* 10(9);
2. Joseph, N.R. (1938) *Heterogeneous Equilibrium of Protein Solutions*. Department of Physical Chemistry, Harvard Medical School, Boston. 389-400
3. Fujinaga, T. and J. D. R. Thomas (1982) *Recent Advances in Analytical potentiometry with Ion-Selective Electrodes*. 305; 631-633
4. Takuhiro, N. (1998) *Biophysical Chemistry*. 71(3); 173-184
5. Golovnev, N. N., O. S. Romanova and N. V. Busygina (1999) *Journal of Analytical Chemistry*. 55(5); 508-511
6. Sharmaa, G. and J.P. Tandona (1970) *Journal of Inorganic and Nuclear Chemistry.* 32(4);1273-1278
7. Datta, P. K., Madhup Chandra and Arun K. Dey (2005) *Ternary complexes of copper(II), nickel(II) and zinc(II) with nitrilotriacetic acid as a primary ligand and some phenolic acids as secondary ligands*. 5(1); 340-380
8. Motekaitis, R. J. et al (1982) *Journal of Inorganic Chemistry* 21(12); 4253–4257
9. Molochnikov, L. S. et al. (2003) *Coordination of Cu(II) and Ni(II) in polymers imprinted so as to optimize amine chelate formation*. 44(17); 4805-4815
10. Schwartz, L. M. (1987) *Journal of Chemical Education.* 64(11); 947
11. Lee, Y-H. (1978) *Water, air and soil pollution:* The slope of Gran's plot: A useful function in the examination of precipitation, the water-soluble part of airborne particles, and lake water. 10(4); 457-469
12. Guilbault, G. G., D. N. Kramer, P. Goldberg (1963) *Journal of Physical Chemistry.* 67(9); 1747–1749
13. Gaikwad, P. D. et al. (2007) *International Journal of Electrochemical Science.* 2; 488-497
14. Pettit, L. D. and Powell, H. K. J. (1993) *Stability Constant Database*. Academic Software, Timble, Otley, Yorks LS21 2PW, UK.
15. Murray, K and Newman, C. T. (1989) *Equilibrium Simulations for Titration analysis; Manual Version 3.0.* Processing and Chemical Manufacturing

Technology Division Council for Scientific and Industrial Research, Pretoria, South Africa.

16. Brookes, G. and Pettit, L. D. (1975) *Journal of Chemical Society* Dalton. 2112
17. Martin, R. B. and Edsall, J. T. J. (1960) *Journal of American Socociety* 82;1107
18. Solomon,L. R., A. M. Bond, J. W. Bixler, D. E. Hallenbeck, K. M. Logsdon. (1983) *Inorganic Chemistry.* 22(11);1644–1648
19. Lippard, S. J. and J. M. Berg.(1994) *Principles of Bioinorganic Chemistry*. University Science Books, CA, USA. 24
20. Carl, W. F. and Rogers, L. B. (1966) *Inorganic Chemistry* 5 (4); 616-621

4. ISOTHERMAL TITRATION CALORIMETRY

4.1 INTRODUCTION

Calorimetry is a technique used to study thermodynamic properties of chemical interactions [1-3]. There are three different methods in which calorimetric measurements can be made, and there are three different calorimetric instruments for each method; adiabatic or isoperibol system, the heat conduction calorimetry and the isothermal titration calorimetry.

A calorimeter that has a temperature controlled jacket can be operated in two modes, the adiabatic mode and the isoperibol mode [2]. In an adiabatic system, the temperature of the reference cell is adjusted throughout the experiment to keep it equal to the temperature of the sample cell [1]. Therefore there is no heat transfer between the sample cell and the reference cell. The heat of the reaction is then given by Equation 4.1 [1, 2]. The signal for this technique is in ^{o}C/sec (temperature units per unit time). The heat change, Δq, can be calculated from the energy equivalent of the calorimeter equivalent, ε_c [1, 5, 6].

$$\Delta q = \varepsilon_c \Delta T \tag{4.1}$$

For the calorimeter that is in an isoperibol mode the temperature of the reference cell is kept constant throughout the experiment while the temperature of the reference cell is changing [2]. In this case, there is heat transfer between the two cells and it needs to be corrected to account for the heat loss between the sample cell and the reference cell [2]. The raw signal is the same as the one for adiabatic calorimetry and the heat change is also calculated using Equation 4.1.

The heat conduction calorimeter has a heat flow sensors coupled with the heat sink that is kept at a constant temperature. These sensors are connected to the reference cell. The sensors are used to monitor the temperature change (ΔT) of the sample cell. The raw signal for this method is the voltage; this voltage varies with ΔT that is created by the chemical reaction [1, 7, 8].

In isothermal titration calorimetry (ITC), the temperature of the sample cell is kept constant. The sample cell is connected to the temperature controllers. During a chemical change, the heat gained (or lost) is detected and the power applied to the heat controllers changes accordingly to keep the temperature of the sample cell constant. The raw signal for this method is in the units of power (μCal/sec or μJ/sec) [1, 7]. The raw signal is converted to ΔH by integrating it (the raw power) over the time it took the heat controllers to reach the baseline value [1].

In this study, ITC was used to determine equilibrium constants (K) of the complexes at different pH. It was also used to determine the heats of binding (ΔH) of the complexes, the entropy (ΔS) and the number of ligands (N) bound to the Cu(II) ions. ITC was chosen over the other calorific methods because all four variables; K, ΔH, ΔS and N can be obtained from a single ITC experiment at a fixed pH with a corresponding buffer, and since the functions of the instrument are operated with a software the results conversions of the raw signal to the final ITC results are faster and accurate [7, 8]. With modern ITC calorimeters, direct measurements of the binding constants (equilibrium constants) can be made from $K = 10^2\ M^{-1}$ to $K = 10^9\ M^{-1}$. With competitive binding technique, a range of $10^9\ M^{-1}$ to $10^{12}\ M^{-1}$ can be covered [1].

In addition, ITC can be used to analyse coloured solutions, all complexes of Cu(II) used in this study were coloured. More over, the ITC calorimeter can be operated in the temperature range 10^oC to 40^oC, pressure range of 700 Pa to 1060Pa in humid environments (humidity of 0 to 70%). ΔG was calculated from K, ΔH, ΔS and N using thermodynamic equations (Equations 4.6-4.9) [8, 9].

However, the technique has limitations. The method only gives the conditional binding constants since the system consists of the metal ions, the ligand, the buffer and the complexes. Also equilibrium constants are not as precisely determined as with glass electrode potentiometry.

Isothermal titration calorimetry is often used for biological applications where the interaction of the buffer and metal ion are ignored. Since the concentration of the buffer is normally much higher than that of the metal ion and since it is known, that in the absence of a buffer, at biological pH's, the metal ion would precipitate as the hydroxide, this assumption is very strange. What is actually being measured is:

$MBH_n + L \leftrightarrow ML + BH_n$

Where MBH_n is the protonated metal ion-buffer complex, BH_n is the buffer with n number of protons and ML is the metal-ligand complex. Moreover, since both the sample (metal ion solution) and the burette contents (ligand) are buffered the final ITC measurements is the summation of the heats of ionization of the buffer, heats of dilution of the buffer and the heats of binding of the ligand to the metal ion.

The protonation/deprotonation constants of the ligand could not be studied with this method since the ITC measurements were done at a fixed pH with corresponding buffers. The sequential analysis of the complexation of the ligand with the metal ions, which could help characterize the individual species in solution and to observe how the speciation varies with pH change was also not possible for the same reason. If the buffers are not used, the titration system will produce heats of neutralization which are very exothermic and can mask the actual heats of binding.

$H^+ + OH^- \leftrightarrow H_2O$; ΔH_{neu} is very large

Moreover, the analysis could not be done at lower pH since acidic solutions may corrode the ITC sample cell. The analysis at pH above 8 were also not possible since copper(II) ions precipitated with buffers at higher pH.

4.2 THEORY

In this study, there are n number of species in solution, the free ligand, free copper(II) ions and the complexes formed. A basic understanding of this system would require the knowledge of two primary thermodynamic parameters, the equilibrium constants for the binding process, K, and the binding stoichiometry , N [1, 3]. A more advanced way of understanding this interaction can be established if the enthalpy change (ΔH) and the entropy change (ΔS) for the formation of the complex are known [1, 2, 4]. The thermodynamic relationship of the three species, the free ligand, copper(II) ions and the complexes can be established by the Equations 4.2 to 4.9 [1, 3, 5].

For the reaction;

$M + L \leftrightarrow ML$

The binding constant, *K* can be expressed as;

$$K = \frac{[ML]}{[M][L]} \qquad (4.2)$$

Where [ML] is the concentration of the complex, [L] is the concentration of the free ligand and [M] is the concentration of the free metal ion. The dissociation constant, K_d can be expressed as;

$$K_d = \frac{[M][L]}{[ML]} \qquad (4.3)$$

Therefore,

$$\frac{1}{K_d} = \frac{[M][L]}{[ML]} \quad (4.4)$$

Putting Equation 4.4 into Equation 4.2 yields;

$$\frac{1}{K_d} = K \quad (4.5)$$

The relationship between the three species M, L and ML can be represented in Figure 4.1.

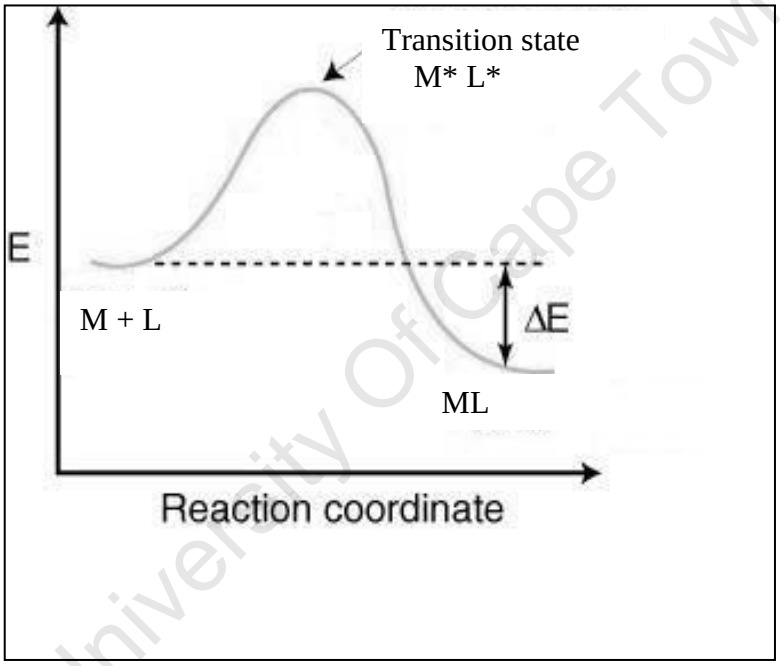

Figure 4.1: A typical free energy diagram for a free metal ion M and a free ligand L going into ML (complex). M* and L* are the species M and L at transition state.

From Figure 4.1, M and L gain energy to get to the transition state, and the product (ML) has a lower overall energy compared to the energy of M and the energy of L at their ground state. The Gibbs free energy change depends on the temperature. For any reaction, the Gibbs free energy change can be expressed as;

$$\Delta G^{\ominus} = -RT\ln K_{(eq)} \quad (4.6)$$

The actual ΔG of the reaction can be expressed as;

$$\Delta G = \Delta G^{\ominus} + RT\ln K \qquad (4.7)$$

Putting Equation 4.2 into Equation 4.7 yields;

$$\Delta G = \Delta G^{\ominus} + RT\ln \left[\frac{[ML]}{[M][L]} \right]_{actual} \qquad (4.8)$$

The relationship between ΔG, ΔH, T and ΔS is expressed as;

$$\Delta G = \Delta H - T\Delta S \qquad (4.9)$$

Where $K_{(eq)}$ is the equilibrium constant, [M], [L] and [ML] are the concentrations of the free metal ion, free ligand and the complex respectively, ΔG^{O} is the standard Gibbs free energy change, R is the universal gas constant, T is the temperature in Kelvin, ΔG is the actual Gibbs free energy change, ΔH is the enthalpy change and ΔS is the entropy change for the complex formation.

The unique advantage of ITC is that it is possible to get all these parameters from a single experiment if it is done under optimum conditions.

Optimum conditions for ITC are as follows:

1. The ITC experiments must be done under conditions where the heat change is altered from successive injections producing curved thermograms.
2. The curve in the thermogram is plotted as a function of the macromolecule [M], and the equilibrium constant K.

Titrations with reactions having very large equilibrium constants ($K > 10^{8} M^{-1}$) need to be performed at low macromolecule concentrations to produce reasonable curve in the

thermogram, but at high enough concentrations to produce measurable heats. The reverse should be done for weak complexes ($K < 10^4\ M^{-1}$) [1, 5, 6].

It is exceptionally important that the Cu(II) solutions and the ligand solutions be matched with regard to the pH and the concentrations of the buffer [1]. If the two solutions are not properly matched, there may be heats of dilution that may accompany the heats of formation of the complexes [1, 7-9].

However, raw data for ITC can be corrected by running three blank experiments [1]. The first blank experiment can be done by titrating the ligand into the buffer in the sample cell. This will take care of the heats of dilution of the ligand since the ligand will be diluted upon titration with Cu(II). In the second blank titration, Cu(II) solution can be titrated into the buffer in the sample cell. This will take care of the heats of dilution that were produced upon titration of the ligand with Cu(II). The third blank titration can be a buffer to buffer titration. This will be used to zero the ITC instrument [1].

The corrected heat can be calculated using equation 4.10 and 4.11.

$$Q_{corr} = Q_{mear} - Q_{dul,lig} - Q_{dil,Cu(II)} - Q_{blank} \qquad (4.10)$$

Sometimes the ligand may release a proton when titrated with the metal ion. This proton will bind with the buffer and this will be accompanied with the heats of ionization of the buffer. [1, 5]

$$Q_{corr} = Q_{mear} - (n_p \Delta H_{ion}) \qquad (4.11)$$

Where Q_{corr} is the corrected heat, Q_{mear} is the measured heat, $Q_{dul,lig}$ is the heat of dilution of the ligand solutiion, $Q_{dil,Cu(II)}$, is the heat of dilution of the copper(II) solution, Q_{blank} is the heat of dilution of the blank, n_p is the number of protons released by 1mol of the ligand upon complexation and ΔH_{ion} is the enthalpy change of protonation of the buffer.

4.3 EXPERIMENTAL

4.3.1 Preparation of Solutions and Data Handling

The ligand, $CuCl_2.2H_2O$ and the buffers were purchased from Sigma-Aldrich. They were of analytical grade and were used without any further purification. The Cu(II) solutions were prepared from a standard solution of $CuCl_2$. The ionic strength of the Cu(II) was adjusted to 0.15M with NaCl. The ligand solutions were prepared by dissolving a weighed amount of the ligand in distilled deionised water. Both the ligand and Cu(II) solutions were buffered with 20μM buffer (Buffer solutions were prepared by Dave Woolley, Division of Chemical Pathology, Clinical Laboratory Sciences, Faculty of Health Sciences, University of Cape Town). The buffers used were NH_4 Ac/Acetic acid (ammonium acetate/acetic acid buffer) for pH 5.0, MES.TMAH (2-[N-morpholino] ethanesulfonic acid) for pH 6.0, MPOS.TMAH (3-[N-morpholinino] propanesulfonic acid) for pH 7.0 and EPPS.TMAH (3-[4,(2-hydroxyethyl)-1-piperazinyl] propanesulfonic acid) for pH 8.0.

4.3.2 ITC Measurements

The ITC cell was washed with distilled deionised water and rinsed with Cu(II) solution. The ITC syringe was rinsed off with the ligand solution before the experiment was run. Both the cell and the syringe contents were degassed to get rid of the bubbles before each and every titration. All experiments were done at 25±1^{o}C and 700rpm. The experiments were run such that the baseline does not shift and such that the curves do not oscillate. This was achieved by adjusting the reference power. All titrations were run such that a 1:2 Cu(II)/ligand ratio was achieved, except for the titrations at pH 8 where a 1:3 Cu(II)/ligand ration was used. The titrations were done in the pH range 5-8, Cu(II) precipitated at higher pH.

4.3.3 Experimental Details

A known volume of standard Cu(II) solutions was injected into the sample cell that was cleaned and rinsed thoroughly prior to loading. The sample cell contents were stirred continuously until a constant temperature was reached. The syringe was loaded with the ligand solutions. The syringe was purged twice to remove contaminants and any air bubbles that could have been trapped in. When the sample cell had reached a steady temperature of 25^{o}C, the ligand was sequentially titrated into the sample cell until the set number of injections was reached.

4.4 RESULTS

The calibration of the instrument was checked with sodium/EDTA titrations before and after every titration. The pH was measured with a CRISONmicro pH meter equipped with a Metrohm electrode. The results of the sodium/EDTA titrations are as shown in Figure 4.2. Similar results were obtained for the same system under the same conditions and molar ratio.

When Ca(II) was titrated with EDTA at pH 6.0 with MOPS buffer at 25^{o}C, the most predominant species in the Ca(II)/EDTA system were the ML species since N was about one. From literature, the most predominant species in solution at pH 6 are the ML species [10-12]. The experimental results therefore match with the literature results. However, the experimental value for the equilibrium constant was significantly different from the literature value. This is because ITC can only measure the conditional equilibrium constants, and the ITC measurements were done at 0.15M ionic strength with NaCl, while the literature values were in 0.1M ionic strength.

Log K_{exp} = 5.562, the literature values of the log Ks for Ca(II)/EDTA at 0.1M ionic strength were 10.65 (±8) log units [14] and 10.97 log units [13]. This illustrates the difference between potentiometry and ITC. The literature results refer to the formation of the complex from the bare ligand and metal ion. The ITC results are conditional

constants and refer to the average binding constant of the species present under the conditions of the experiment. In this case the reaction would be (ignoring the presence of the buffer):

$$Ca(II) + EDTA.H_2 \rightarrow CaEDTA + 2H^+$$

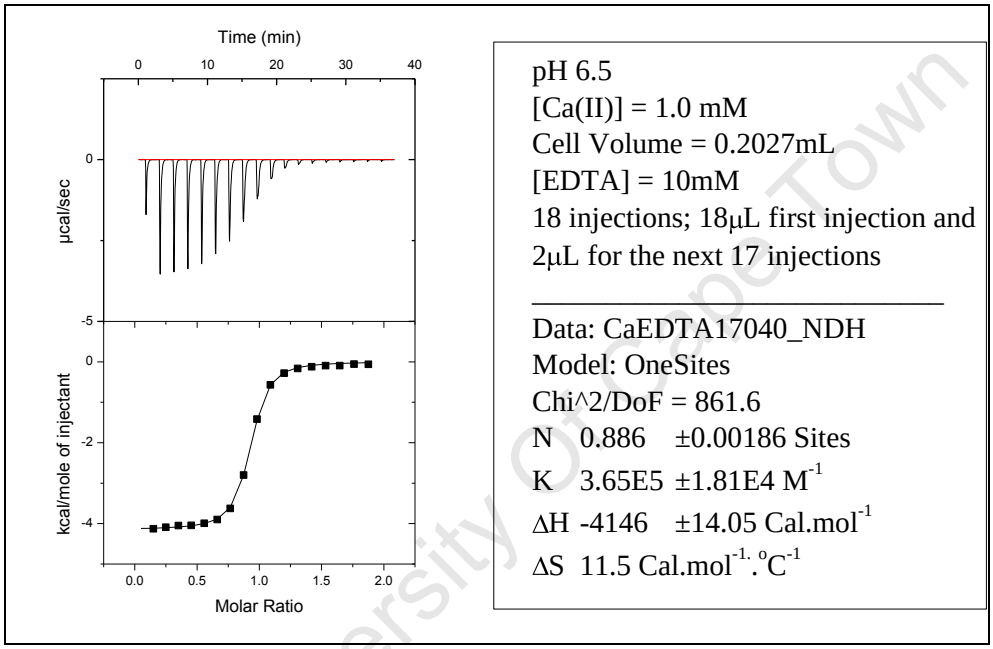

Figure 4.2: ITC results for Ca(II)/EDTA at pH6.5

4.4.1 Determination of Heats of Dilution of Buffers

Titrations of Cu(II) with the buffers were done to check how strongly the buffers bind to the Cu(II) ions. Buffers that can bind weakly with the metal ion are needed to reduce competition with the ligand

At pH 5, Cu(II) was titrated with ammonium acetate/acetic acid buffer and the results are presented in Figure 4.3. The log K for Cu(II)/buffer system at pH 5 was very small thus the complex formed between the buffer and Cu(II) at this pH was a weak complex. A

horizontal thermogram (y=0) was observed, this shows that there were very poor interactions between the buffer and Cu(II) even though the N value was ~1 (with an error of 523). The heats of dilution were too little and the change in entropy was undefined. This makes the buffer useful at this pH because it will not compete with the ligand.

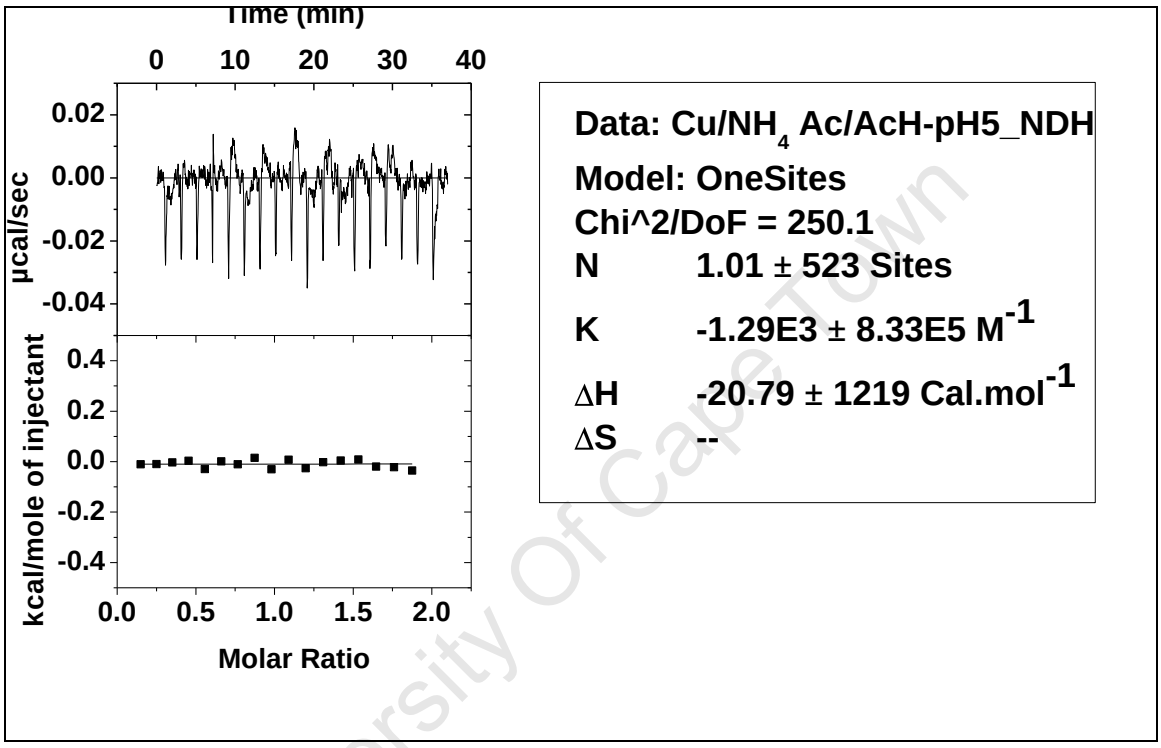

Figure 4.3: ITC for Cu(II)/Ammonium acetate-Acetic acid buffer at pH5.0

The titrations of Cu(II) with the buffer at pH6 also gave a horizontal thermogram (y=0). (Figure 4.4) The value for ΔG was undefined, the reaction was exothermic and the heats of dilution at this pH were too little, close to zero. The interaction between Cu(II) ions and this buffer at this pH is very weak, which makes the buffer useful at this pH because it will not compete with the ligand.

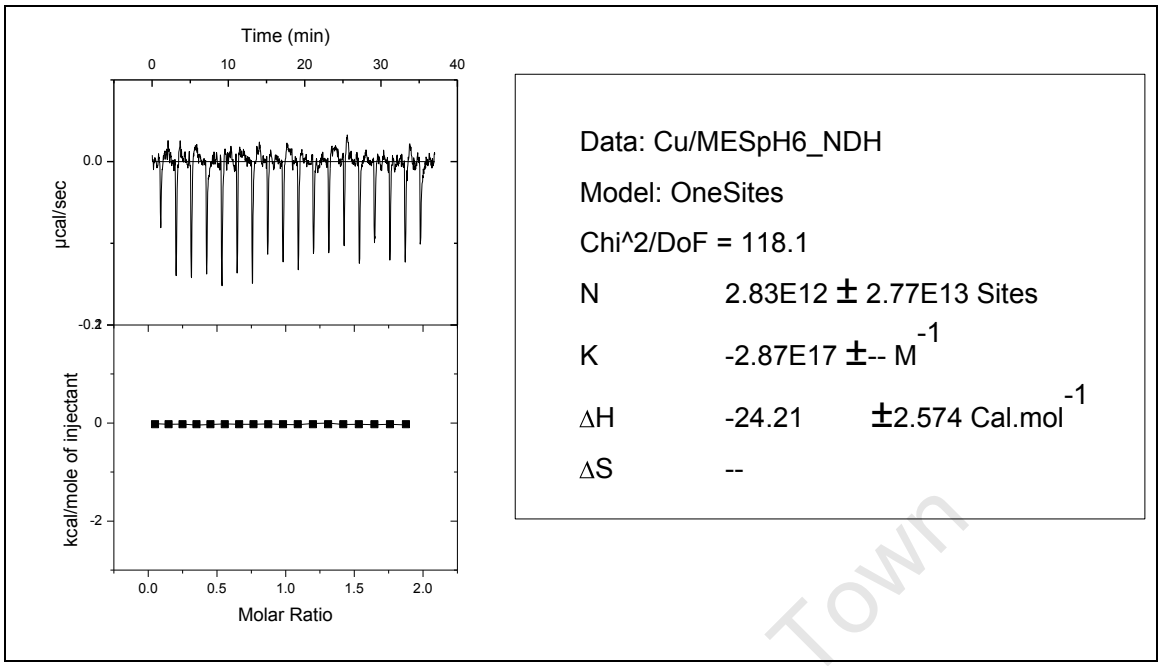

Figure 4.4: ITC results for Cu(II)/2-[N-morpholino] ethanesulfonic acid buffer at

Figure 4.5 shows the thermogram that characterizes the Cu(II)/MOPS system. When Cu(II) was titrated with 3-[N-morpholinino] propanesulfonic acid buffer at pH 7.0, heat was evolved, unlike the ammonium acetate/acetic acid buffer and the 2-[N-morpholino] ethanesulfonic acid buffer. The equilibrium constant reported by the software is meaningless because the heat change is not altered between successive additions (see above). This is also shown by the standard error in the reported K which is 10^5 larger than the K itself. However, since a significant amount of heat is evolved the data must be corrected for this. The buffer can therefore be used in Cu/glycyl-L-histidine and in Cu(II)/glycine titrations, but the stability of the complex relative to the buffer complex will be obtained

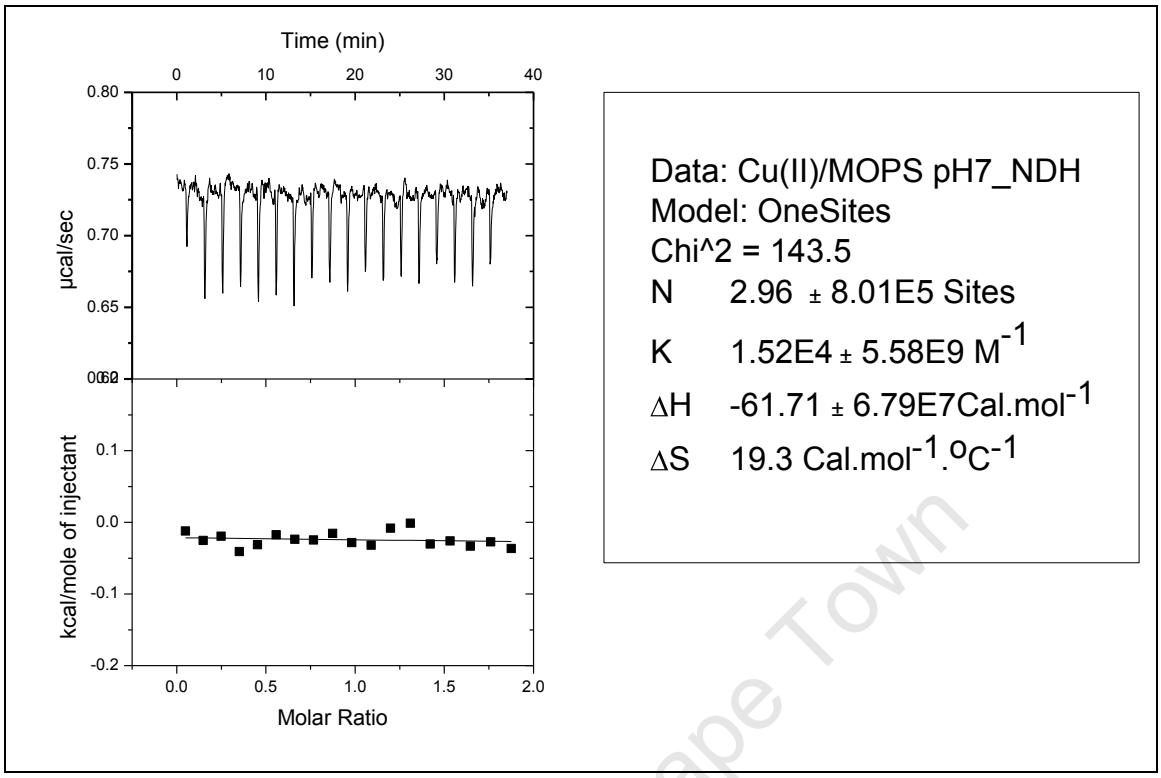

Figure 4.5: ITC results for Cu(II)/3-[N-morpholinino] propanesulfonic acid buffer at pH 7.0

Figure 4.6 shows the thermogram that characterizes the Cu(II)/EPPS system. When Cu(II) was titrated with 3-[4,(2-hydroxyethyl)-1-piperazinyl] propanesulfonic acid buffer at pH 8.0, heat was evolved, unlike the ammonium acetate/acetic acid buffer and the 2-[N-morpholino] ethanesulfonic acid buffer. The equilibrium constant reported by the software is meaningless because the heat change is not altered between successive additions. This is also shown by the standard error in the reported K which is 10^4 larger than the K itself. However, since a significant amount of heat is evolved the data must be corrected for this. The buffer can therefore be used in Cu/glycyl-L-histidine and in Cu(II)/glycine titrations, but the stability of the complex relative to the buffer complex will be obtained

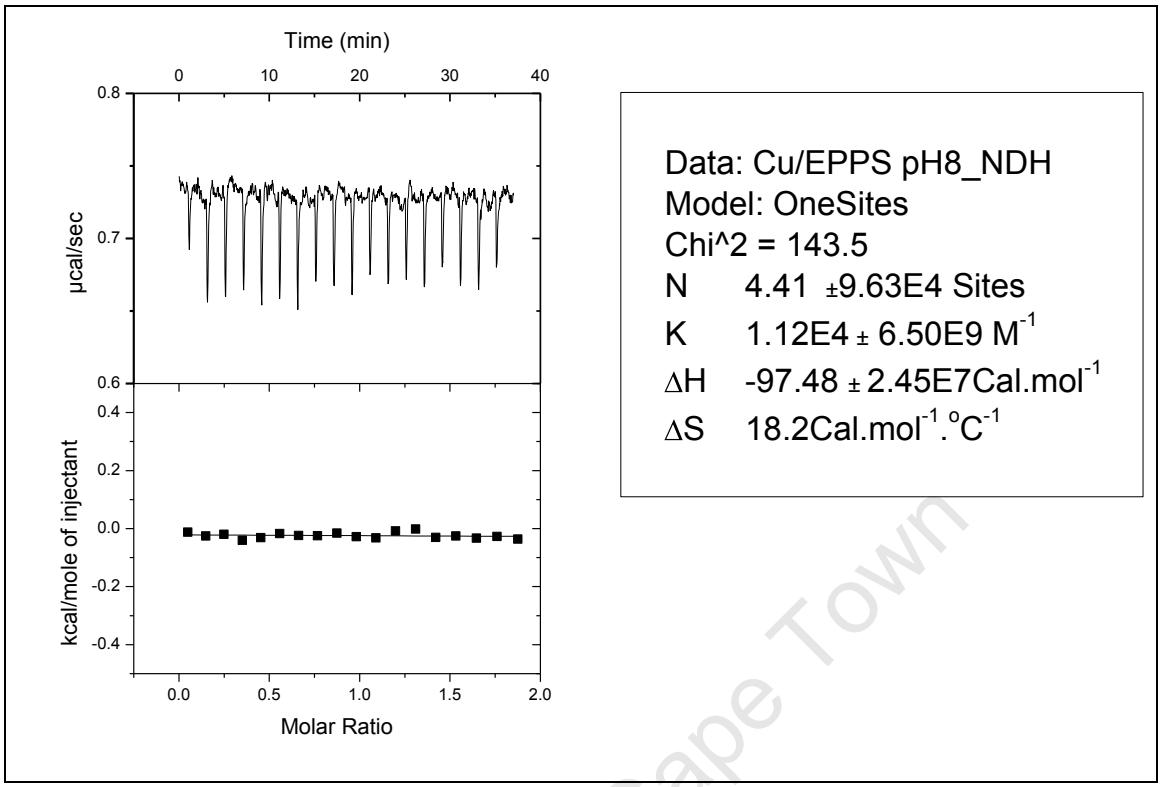

Figure 4.6: ITC results for Cu(II)/ 3-[4,(2-hydroxyethyl)-1-piperazinyl] propanesulfonic acid) for

4.4.2 Glycine Complexes

The corrected thermodynamic data for Glycine-Cu(II) system at pH 5 is shown in Figure 4.7. At this pH, the reaction was endothermic. The integrated heat data was fit with one site binding model using a package of software that came with the instrument, Origin70. This was done for all Cu(II)/glycine and Cu(II)/glycyl-L-histidine systems from pH5-pH8.

The values for N, K, ΔH and ΔS were calculated using Origin70, and are presented in Figure 4.7. A one site model was used and the value for N is approximately one, thus the ML species were predominant at this pH. This model corresponds with the one got with potentiometry at the same pH. However, the ML species gave a small value of log K (Log K = 3.045). According to published data on Cu(II)/glycine complexes, ML species were predominant in solution at pH 5 but at this pH the ML species were

gradually being converted to ML_2 [12]. The speciation graph for potentiometric titrations of Cu(II) with glycine have been reported in Section 3.5.3.1, Figure 3.7. For this endothermic reaction (positive ΔH) the formation of ML was non spontaneous since ΔS was also positive (products were more disordered than reactants), ΔG is therefore positive and was calculated as 3.97 Kcal.mol^{-1}. ΔG was calculated using equation 4.9.

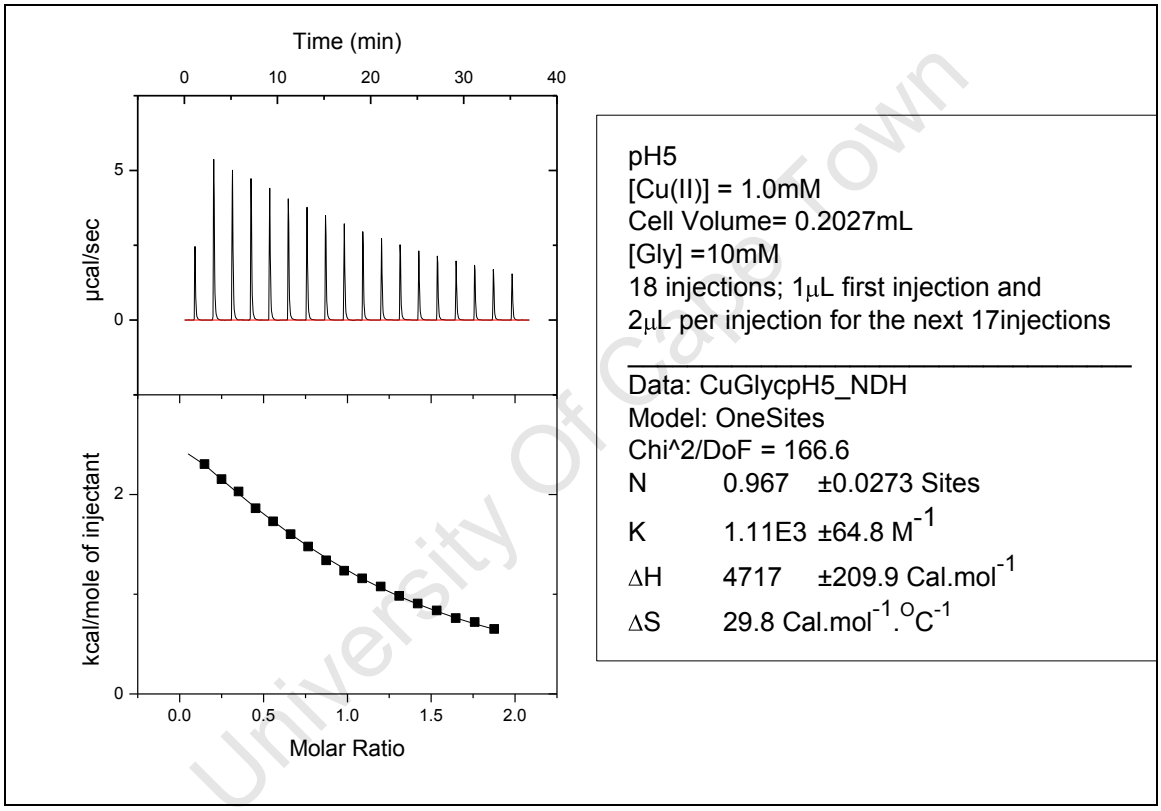

Figure 4.7: ITC results for Cu(II)/ Glycine at pH5.0

Results for Glycine-Cu(II) system at pH 6 are represented in Figure 4.8. Since ΔS was positive the products were more disordered than the reactants. The copper(II) complexes at this pH showed a log K value of 4.009. The species formed at pH 6 were therefore more stable than the species formed at pH 5. The ML species the value for N is around one. However, glass electrode potentiometry data gave ML_2 as the most predominant species at this pH [12].

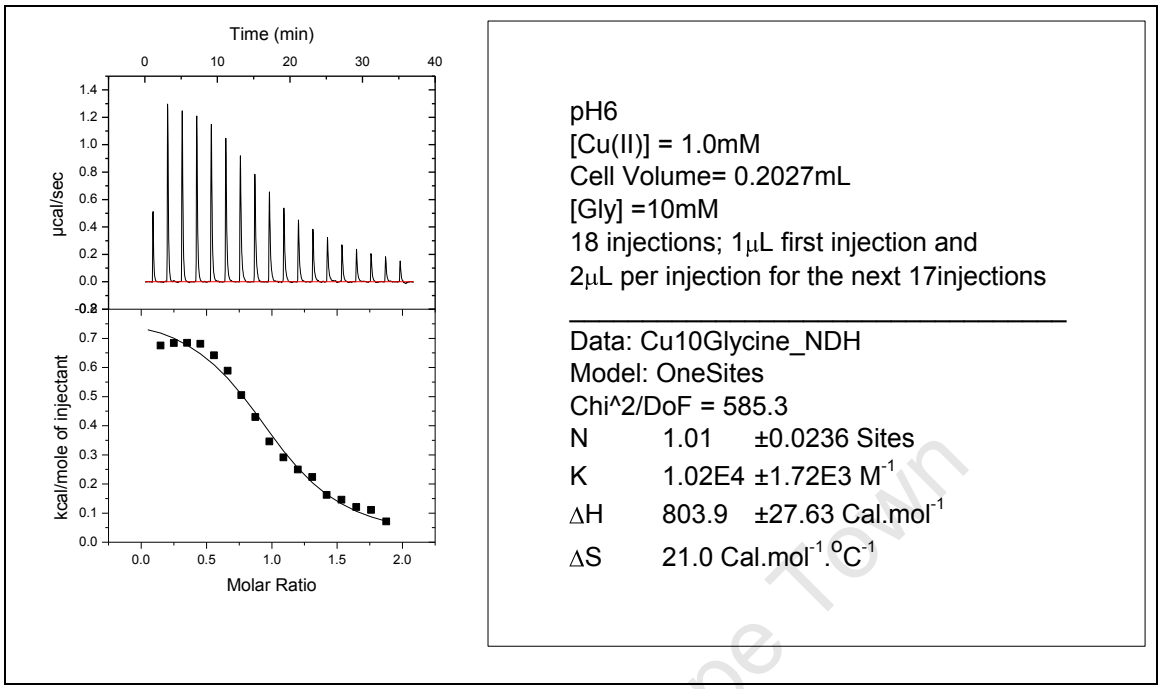

Figure 4.8: ITC results for Cu(II)/ Glycine at pH6.0

At pH 7, the glycine-Cu(II) system gave a very small value of N, N=0.467. However, the standard deviation for N was very little. Log K at this pH was calculated to be 3.804 log units. This was an exothermic reaction, the value for ΔS was positive. ΔG was calculated as -3.32Kcal.mol^{-1}. The thermogram for Cu(II)/Glycine system is shown in Figure 4.9.

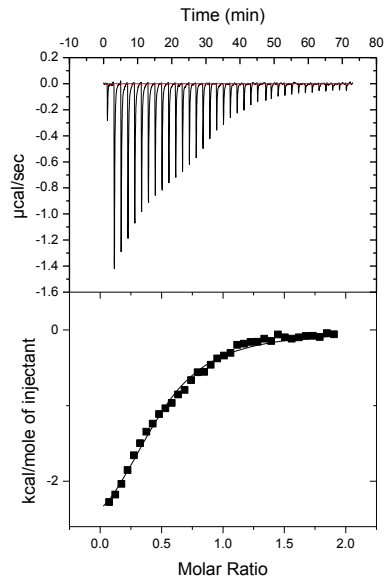

pH7
[Cu(II)] = 1.0mM
Cell Volume= 0.2027mL
[Gly] =10mM
36 injections; 1µL first injection and
2µL per injection for the next 35injections

Data: Cu1Gly10pH7_NDH
Model: OneSites
Chi^2/DoF = 2781

N	0.467	±0.0162 Sites
K	6.37E3	±628 M^{-1}
ΔH	-3145	±144.4 $Cal.mol^{-1}$
ΔS	6.85 $Cal.mol^{-1}.{}^{o}C^{-1}$	

Figure 4.8: ITC results for Cu(II)/ Glycine at pH7

At pH8, the ML_2 species were predominant since the value of N was about 2. This agrees with potentiometric data at pH8. Moreover the reaction favours the product side since ΔH was negative and ΔS was positive. ΔG was calculated as -3.07$Kcal.mol^{-1}$ using equation 4. The reactants are therefore more disordered than the products. At this pH, log K = 4.238. This is summarized in Figure 4.9. The equilibrium constant measured at the different pH's are different because they are conditional constants that are affected by competition with H^+ which changes with pH. Also the buffers were different at the different pH's.

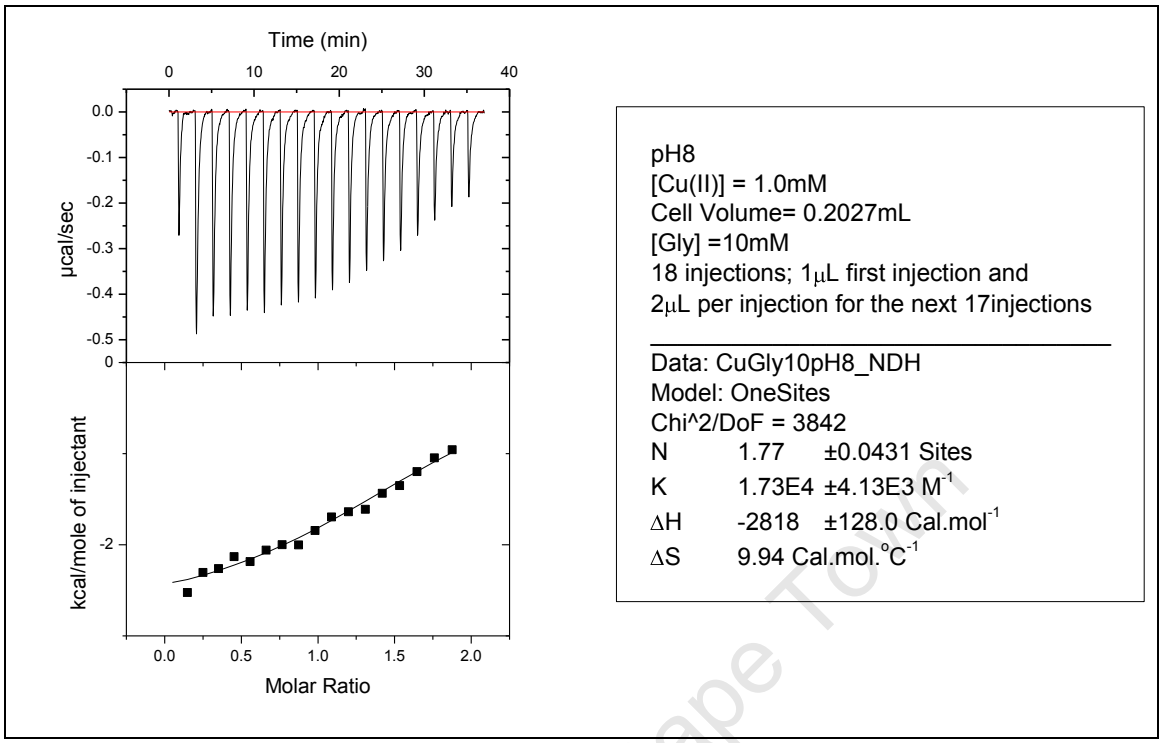

Figure 4.9: ITC results for Cu(II)/ Glycine at pH8.0

4.4.2 Glycyl-L-Histidine Complexes

At pH 5, N is ≈1 therefore the ML species were predominant in the Cu(II)/Glycyl-L-Histidine system. This agrees with the results got from potentiometry. [Section 3.5.3.2] log K = 6.083. The reaction is fairly exothermic with ΔH 9Kcal/mol. The thermogram is shown in Figure 4.10.

From potentiometry, at pH 5, 99.72% of the metal ion was as the ML. This percentage was maintained until the system was at pH 7.01 where the amount started decreasing. At this pH, all the Cu(II) was used up and ML species were the only species found in solution.

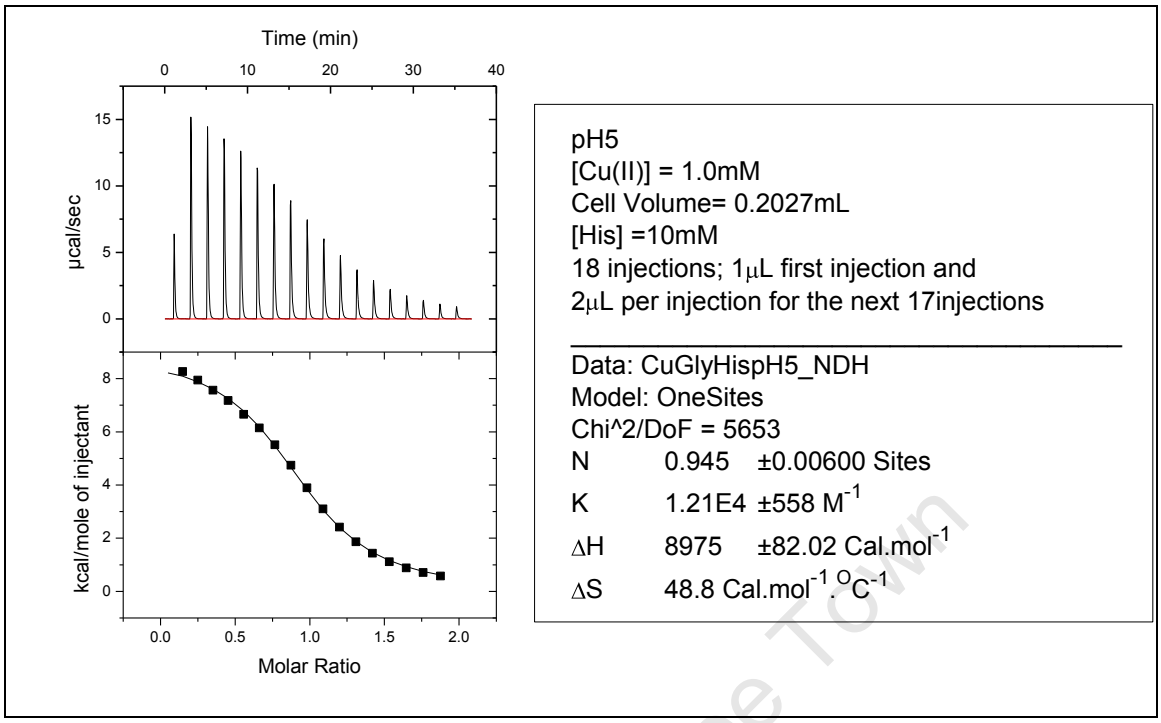

Figure 4.10: ITC results for Cu(II)/ Glycyl-L-histidine at pH5.0

At pH 6, N was around one thus the ML species were predominant in solution. (Figure 4.11) However, log K = 5.719 at this pH. Both ΔH and ΔS are negative. The reactants were therefore more disordered than the products. ΔG was calculated as -12.3.Kcal.mol^{-1} using Equation 4.

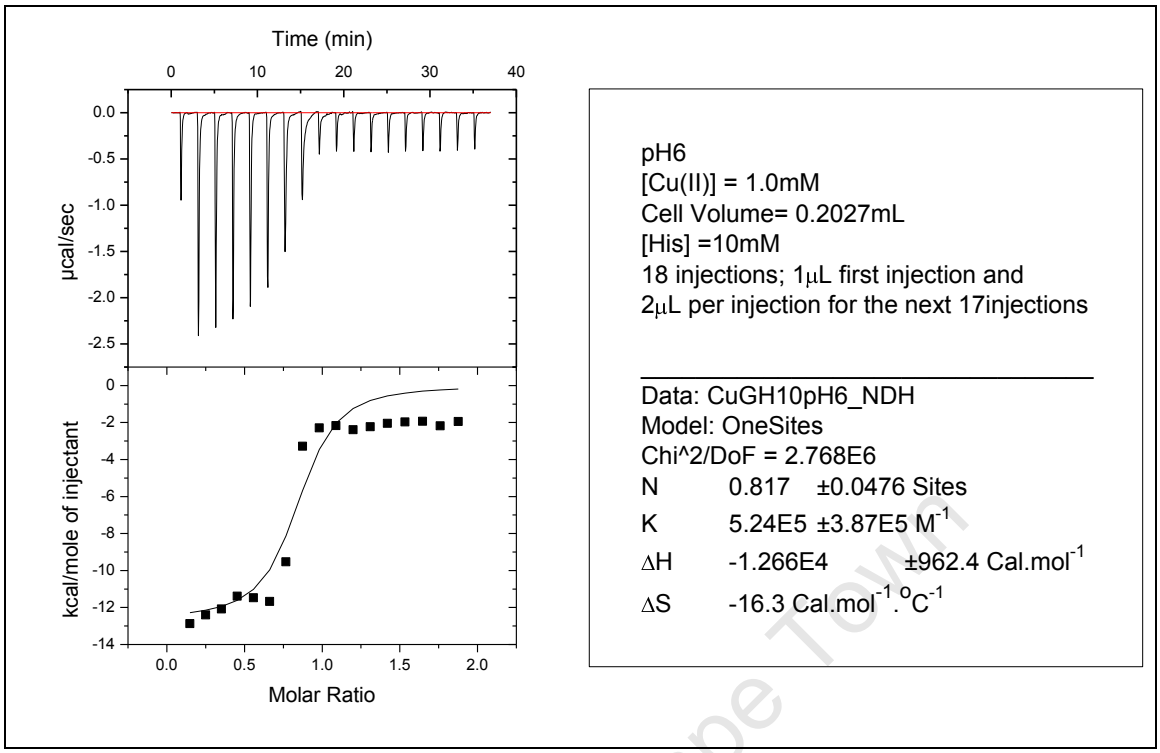

Figure 4.11: ITC results for Cu(II)/ Glycyl-L-histidine at pH6.0

At pH7, the value of N is less than 1, therefore at this pH the interaction between the ligand and Cu(II) was very poor. A small N value also indicates the change of speciation. The reaction was spontaneous since ΔH is negative and ΔS is positive. ΔG was calculated as -6.85KCal.mol^{-1}. Results are illustrated in Figure 4.12. At pH 7 the concentration of the ML species was decreasing and the MLH_{-1} began to form.

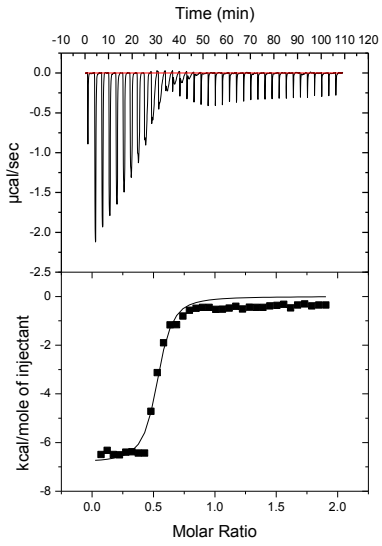

pH7
[Cu(II)] = 1.0mM
Cell Volume= 0.2027mL
[His] =10mM
36 injections; 1µL first injection and
2µL per injection for the next 35injections

Data: Cu1GlyHis10pH7a_NDH
Model: OneSites
Chi^2/DoF = 1.316E5

N	0.517	±0.00925 Sites
K	1.37E5	±3.92E4 M^{-1}
ΔH	-6833	±181.8 $Cal.mol^{-1}$
ΔS	0.576	$Cal.mol^{-1}.{}^{o}C^{-1}$

Figure 4.12: ITC results for Cu(II)/ Glycyl-L-histidine at pH7.0

At pH 8, the ML species were predominant in solution since $N \approx 1\ M^{-1}$. This agrees with the potentiometric data. Log K = 3.914 at this pH. This was a spontaneous reaction since ΔH is negative and ΔS is positive. ΔG was calculated as $-3.17 Kcal.mol^{-1}$. The thermogram for Cu(II)/glycyl-L-histidine system at pH 8 is shown in Figure 4.13.

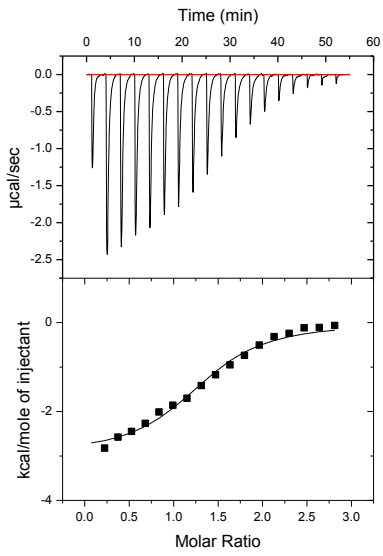

pH8
[Cu(II)] = 1.0mM
Cell Volume= 0.2027mL
[His] =15.0mM
18 injections; 1µL first injection and
2µL per injection for the next 17injections

Data: Cu1GlyHis15pH8_NDH
Model: OneSites
Chi^2/DoF = 9465

N	1.32	±0.0351 Sites
K	8.21E3	±1.51E3 M^{-1}
ΔH	-2968	±112.8 $Cal.mol^{-1}$
ΔS	$7.96 Cal.mol^{-1}.{}^{o}C^{-1}$	

Figure 4.13: ITC results for Cu(II)/ Glycyl-L-histidine at pH8.0

4.5 DISCUSSION

The complexes of glycine and copper(II) showed a larger equilibrium constant value at pH8 where the ML_2 species were predominant in solution. Therefore the ML_2 species were more thermodynamically stable than other complexes formed at pH 5-7. However, the reaction gave a large negative value of the conditional ΔG at pH 7. The spontaneity decreased from pH 5-7, at it increased from pH 7-8, therefore the Cu(II)/glycine complexes in acidic solutions are not thermodynamically stable but the stability increases in basic solutions.

The complexes of Cu(II) and glycyl-L-histidine were more stable, thermodynamically at pH 5 log K = 6.083. However, the production of ML was more spontaneous at pH 6 where a large negative value of ΔG was observed. ΔG decreased from pH 5 to pH 6 and it increased from pH 6 to pH 8. However, according to the ITC data, the ML species were predominant throughout the study, from pH 5-8. According to the speciation

graph, the ML species were predominant from pH 3.84 to pH 8.59 and there was no significant change in the amount of ML in solution from pH 4.54 where a percentage of 97.21 was observed to pH 7.36 where a percentage of 96.29 was observed. The speciation from ITC agrees with the speciation from potentiometry. The thermodynamic properties of the complex solutions are summarized in Table 4.1.

Table 4.1: Thermodynamic properties of Cu(II)/glycine and Cu(II)/glycyl-L-histidine complexes.

pH	Cu(II) titrated with	Buffer	N (Sites)	Log K (M^{-1})	ΔH ($KCal.mol^{-1}$)	ΔS ($Cal.mol^{-1}.^oC^{-1}$)	ΔG ($Kcal.mol^{-1}$)
5	Glycine	NH_4Ac/ acetic acid	0.967	3.045	4.717	29.8	- 3.972
5	Gylcyl-L-histidine	NH_4Ac/ acetic acid	0.945	6.083	8.975	48.8	- 7.755
6	Glycine	MES	1.01	4.009	0.8039	21.0	- 0.2789
6	Glycyl-L-histidine	MES	0.817	5.719	-12.66	-16.3	-12.25
7	Glycine	MOPS	0.467	3.804	-3.145	6.85	-3.316
7	Glycyl-L-histidine	MOPS	0.517	5.137	-6.833	0.576	-6.847
8	Glycine	EPPS	1.77	4.238	-2.818	9.94	-3.067
8	Glycyl-L-histidine	EPPS	1.32	3.914	-2.968	7.96	-22.87

At pH 5 to pH 7, complexes of glycyl-L-histidine and Cu(II) were more stable than the complexes of glycine and Cu(II) by 3.038 log units at pH 5, by 1.710 log units at pH 6 and by 1.333 log units at pH 7. At pH 8, the complexes of glycine and Cu(II) were more stable than the complexes of glycyl-L-histidine by 0.324 log units. The ML species in a glycyl-L-histidine system were therefore more stable than the ML species of

glycine, and the ML_2 species of glycine (dominant in solution at pH 8) were more stable than the ML species (dominant in solution from pH 5 to pH 6) at pH 8.

For the first three titrations, Cu(II)/glycine pH 5; Cu(II)/glycyl-L-histidine pH 5 and Cu(II)/glycine pH 6, the total heats of binding were positive (endothermic reaction). Glycyl-L-histidine system (pH 5) being the most endothermic followed by the glycine system at pH 5 then followed by the glycine system at pH 6. Titrations of Cu(II) with glycyl-L-histidine at pH 6 to pH 8 were exothermic with the titrations at pH 6 being the most exothermic, followed by pH 7, followed by pH 8. Titrations of Cu(II) with glycine from pH 7 to pH 8 were exothermic, with titrations at pH 7 producing more heat than the other.

The entropy for the titrations of Cu(II) with glycyl-L-histidine decreased from 48.8 $Cal.mol^{-1}.{}^{o}C^{-1}$ (pH5) to -16.3 $Cal.mol^{-1}.{}^{o}C^{-1}$ (pH6) and it increased to 0.576 $Cal.mol^{-1}.{}^{o}C^{-1}$ at pH 7 and it increased again to 7.96 $Cal.mol^{-1}.{}^{o}C^{-1}$ at pH 8. ΔS for the titrations of Cu(II) with glycine decreased from pH 5 to pH 7 and then it increased at pH 8.

4.6 CONCLUSIONS

Ammonium acetate/acetic acid buffer was suitable for the ITC measurements at pH 5.0, 2-[N-morpholino] ethanesulfonic acid buffer was suitable to be used at pH 6.0, 3-[N-morpholinino] propanesulfonic acid buffer was suitable to be used at pH 7.0 and it was convenient to use 3-[4,(2-hydroxyethyl)-1-piperazinyl] propanesulfonic acid buffer at pH 8.0.

The speciation from ITC the results agreed with that of potentiometry. The ML species of Cu(II) and glycine formed at lower pH's, and the ML_2 formed at higher pH's. From pH 5 to pH 8 the most predominant species of the Cu(II)-glycyl-L-histidine system was ML, however different species began to form at pH 7 where N dropped to 0.517. In the glycine system, ML was the most predominate species in solution at pH 5 and at pH 6.

New species began to form at pH 7 where N dropped to 4.67. At pH 8, ML_2 was the most predominant species in solution.

ITC results also showed that ML_2 of Cu(II) and glycyl-L-histidine were more stable than ML of the same system. The interaction between Cu(II) and glycine at pH 5 and pH 6 was endothermic, and the interaction at pH 7 and pH 8 gave out heat. The interaction between Cu(II) and glycyl-L-histidine at pH 5 was endothermic and it was exothermic at pH 6-7. Reactions of Cu(II) and glycyl-L-histidine were more spontaneous than the reactions of Cu(II) and glycine at the same pH, the formation of ML at pH 8 being the most spontaneous reaction of all the complex formation reaction of Cu(II) and the two ligands, glycine and glycyl-L-histidine.

REFERENCES

1. Freyer, W. F and Lewis, E. A. (2008) *Methods in Cell Biology*. 84;79-99
2. Jessup, R. S. (1970) *Precise Measurement of Heat Combustion with a bomb Calorimeter*. 7; 20-22
3. Good, D. W., D. M. Fairbrother, Guy Waddington (1958) *Journal of Physical Chemistry*. 62 (7);853–856
4. Abraham, T. et al (2005) *Journal of Biochemistry* 44 (33); 11279–11285
5. Horn, J. R. et al. (2001) *Journal of Biochemistry*. 40 (6);1774–1778
6. Weber, G. (1995) *Journal of Physical Chemistry* 99; 1052−1059
7. Ladbury, J. E. and Babur Z. Chowdhry (1996) *Journal* of *Chemistry & Biology*. 3(10);791-801
8. Jelesarov, I and Bosshard, H. R. (1999) *Journal of Molecular Recognition* 12; 3-18
9. Chaires, J. B. (1997) *Biophysical Chemistry* 64; 15−23.
10. Griko, Y. V (1999) *Biophysical Chemistry*. 79(2) 117-127
11. Stephan, C. H. (2007) *Evaluation of three Beryllium sequestering Agents by Isothermal Titration Calorimetry*. Department of Chemistry, Montréal, Canada.
12. Nielsena, A. D., Claus C. Fuglsang and Peter Westh (2003) *Analytical Biochemistry*. 314(2); 227-234
13. Keefer, R. M. (1946) *Journal of American Chemical Society* 68; 2329
14. Keefer, R. M. (1948) *Journal of American Chemical Society* 70; 476
15. Griko, Y. V., Hendrix, T. and Peter, L. P. (2000) *Journal of Biophysical Chemistry* 1(14);27-34
16. Jokl, V. J. (1964) *Chromatography*. 14;71

5. SPECTROSCOPY AND ANCILLARY STUDIES

5.1 ULTRAVIOLET-VISIBLE (UV-Vis) SPECTROPHOTOMETRY

5.1.1 Introduction

Coloured species absorb light in the UV-Vis region [1, 2]. The amount of radiation absorbed can be measured in several ways;

i. The absorbance (A),
ii. The transmittance (T) and
iii. The percentage transmittance (% T)

The absorbance of the solution depends on the concentration of the species solution, the path length of the sample cell and the absorbtivity of the species [2, 3]. This can be expressed by Beer's Law;

$$A = \varepsilon bc \qquad (5.1)$$

Where;

A is the absorbance of the species, ε is the absorbtivity (molar extinction coefficient), b is the path length of the sample cell and c is the concentration of the absorbing species. When a beam of monochromatic radiation is directed into a coloured sample solution, some of the light is absorbed by the solution and some of it is radiated as shown in Figure 5.1.

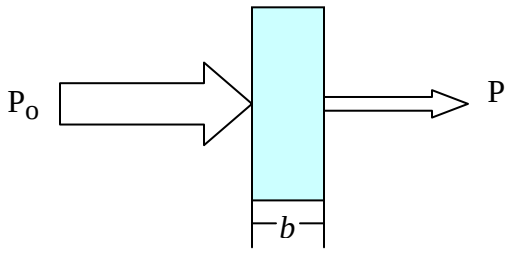

Figure 5.1 shows a single beam of light of radiation power P_O going through the sample cell of path length *b* and the single beam of light of radiation power P leaving the sample cell

The absorbance can be expressed in terms of P_o and P as in Equation 5.2.

$$A = \text{Log} \left(\frac{P_o}{P} \right) \tag{5.2}$$

Transmittance (T), which is described as the fraction of incident light that passes through a sample at a specified wavelength can be expressed in terms of P_o and P as;

$$T = \left(\frac{P}{P_o} \right) \tag{5.3}$$

$$T^{-1} = \left(\frac{P_o}{P} \right) \tag{5.4}$$

Putting Equation 5.4 into equation 5.2 yields;

$$A = \text{Log } T^{-1} \tag{5.5}$$

The absorption of radiation in the UV-Vis region corresponds with the excitation of electrons [3, 4]. In coordination chemistry, electrons that engage in bonding are mainly the *d* electrons. Most transition metal (of which Cu(II) is one) complexes have colour and they absorb light in the UV-Vis region because of the energy gained when electrons are transformed from a lower energy level to the higher energy level. The difference between energy levels corresponds with the wavelength of the absorbed light and is often within in the UV-Vis range [4, 5]. These are the so called *d- d* transitions [5].

In this study, UV-Vis spectrophotometry was used to examine the structure of complexes in solution.

From spectrophotometric data, the models that were observed with potentiometry were compared with the UV-Vis spectra obtained at difference pH's. However, the stability constants were not re-calculated with UV-Vis spectrophotometry since most complexes contain broad overlapping absorption bands which make the evaluation of the stability constants not as precise as in potentiometry. Instead the data were used to infer something about the structure of the species in solution.

5.1.2 Experimental

5.1.2.1 Preparation of Solutions

1:2 Cu(II)/glycyl-L-histidine solutions were prepared in distilled deionized water. These solutions were of known volume and known concentration. The complex solutions were titrated with standard NaOH solution and standard HCl solution to adjust the pH from 3.71-11.55 in about 1.0 increments. The pH was measured with a CRISONmicro pH meter equipped with a Metrohn electrode. The volume of acid/base added was noted and the concentrations of the Cu(II)/ligand recalculated.

5.1.2.2 UV-Vis Measurements

A clean sample cell (curvet) was rinsed with distilled water. The UV-Vis machine was zeroed with distilled deionized water. The UV-Vis machine (Hewlett Packard 8452A Diode Array Spectrophotometer) was set at 350nm-820nm. Absorbances of the samples were measured from pH 3.71 to pH 11.55. The curvet was rinsed with the sample solutions before every measurement.

5.1.2.3 Data Handling

Since the speciation of the solution changes with pH it is always not possible to measure the spectrum of an individual species directly. Instead the spectra at different pH values need to be deconvoluted to yield spectra for individual species. This was done using a

home written computer program. This program requires the concentration of each and every species in each solution and then calculates the molar extinction coefficients at different wavelengths. This is then the spectra of each species. UV_SPECTRA.EXE was used to calculate the molar extinction coefficients of Cu(II) and the complexes ML, MLH_{-1}, MLH_{-2} and MLH_{-3} respectively. The agreement between the calculated and the observed absorbances (the residual absorbance) was calculated. The residual absorbance was calculated using Equation 5.6

$$\text{Residual absorbance} = A^o - A^c \qquad (5.6)$$

Where A^o is the observed absorbance and A^c is the calculated absorbance.

5.1.3 Results

When the pH of the Cu(II)/glycyl-L-histidine system was increased from pH 3.71 to pH 8.91, the color of the complexes changed gradually from blue to a faint purple colour. This shows that there was a different species formed at pH 8.17. When the pH was changed from 8.17 to pH 11.55, the colour of the solution changed from a faint purple colour to a deep purple colour. This indicates the formation of the new species at pH 11.55.

Figure 5.2 shows a plot of absorbance as a function of wavelength for the Cu(II)/glycyl-L-histidine systems from pH 3.71 to pH 11.55. From Figure 5.2, as the pH increased, the maximum wavelength shifted towards shorter wavelength. This indicates the presence of different species in solution at different pH's. There is no isobestic point as several species are in equilibrium at the same time.

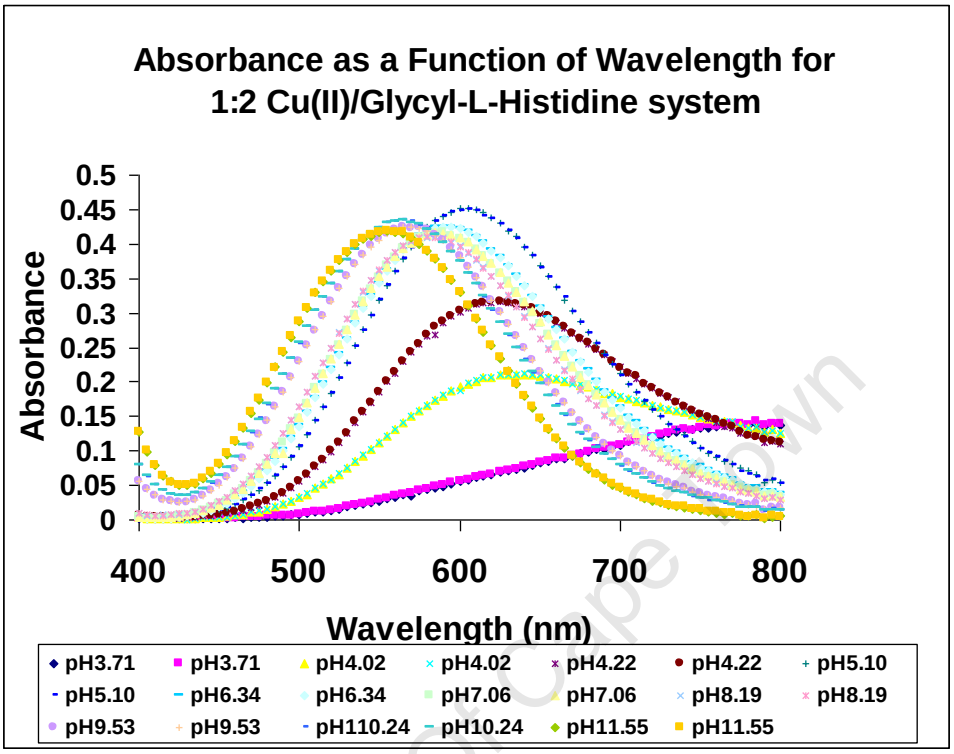

Figure 5.2: Raw UV-Vis data; absorbance of Cu(II)/glycyl-L-histidine as a function of wavelength from 400nm to 800nm UV-Vis region.

Figure 5.3 shows the molar extinction coefficients as a function of wavelength for the species Cu(II), ML, MLH_{-1}, MLH_{-2} and MLH_{-3} respectively. Since the program calculates the extinction coefficients at each wavelength independently, the fact that smooth curves are obtained for each species lends confidence to the model and equilibrium constants obtained from potentiometric study. From the spectra, the wavelengths of maximum wavelength (λ_{max}) can be estimated. These results are given in Table 5.2. The ε for $[Cu(H_2O)_4]^{2+}$ was 1.485$dm^3.mol^{-1}.cm^{-1}$ which compares well with the literature value of 1.5$dm^3.mol^{-1}.cm^{-1}$.

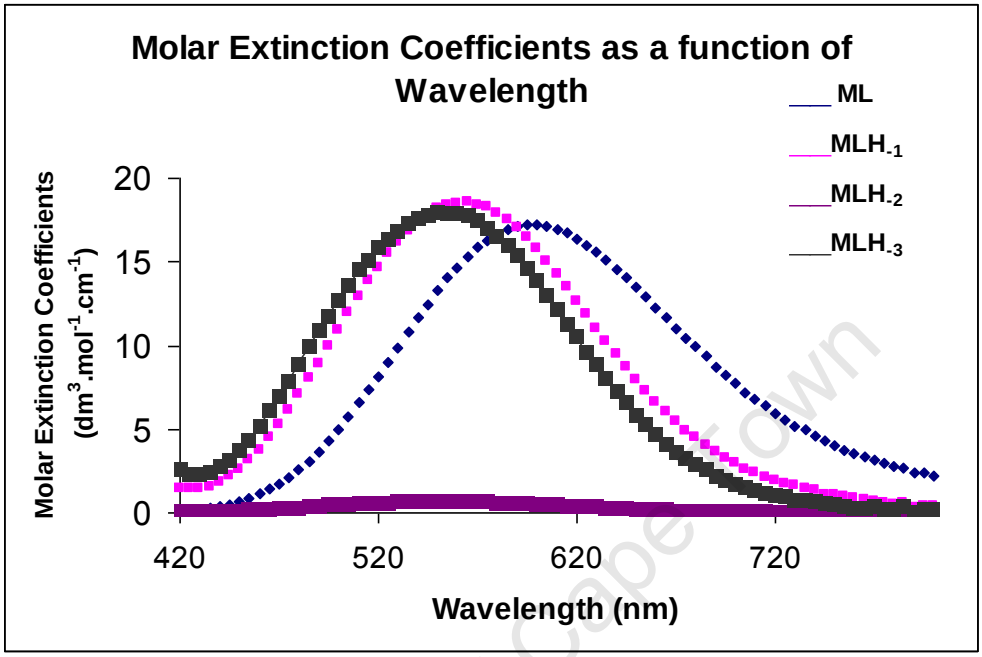

Figure 5.3: ; Molar extinction coefficients a function of λ_{max} for Cu(II)/glycyl-L-histidine systems at varying pHs

Table 5.2; Molar extinction coefficients and λ_{max} for Cu(II)/glycyl-L-histidine systems a varying pHs

SPECIES	ε ($dm^3.mol^{-1}.cm^{-1}$)	λ_{max} (nm)
ML	17.22	600
MLH_{-1}	18.56	565
MLH_{-2}	0.67	554
MLH_{-3}	18.01	550
$[Cu(H_2O)_4]^{2+}$	1.48	800+

The interpretation of the spectra was made using Billo's method (updated by Presenti and co-workers) [6]. The λ_{max} of species can be estimated using Equation 5.7

$$\lambda_{max} = 10^3/\sum n_i \nu_i \qquad (5.7)$$

Where n_i is the number of equatorial donor group and ν_i is the ligand field of the complex. The ν_i values for corresponding donor groups are shown in Table 5.1.

Table 5.1; ν_i values for corresponding electron donor groups.[9, 10]

Electron Donor Group	ν_i (μm^{-1})
Carboxylate oxygen	0.353±0.008
Water oxygen	0.296±0.006
Hydroxide oxygen	0.39±0.03
Alcoholate oxygen	0.39±0.03

5.1.4 Discussion

None of the species absorbed UV-Vis light in the range 240-300nm therefore Cu(II) did not bind on the carboxylate oxygen of the ligand because none of the λ_{max}'s corresponded to ν_i of 0.353μm^{-1} . Glycyl-L-histidine thus has three possible binding sites, the amide nitrogen, one of the two imidazole nitrogens and the terminal NH_2 group. The possible structures of the complexes are shown below with regard to Billo's method;

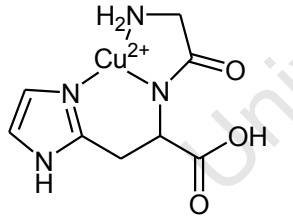

a

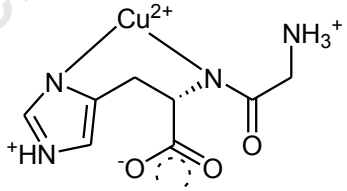

b

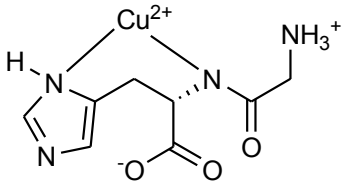

c

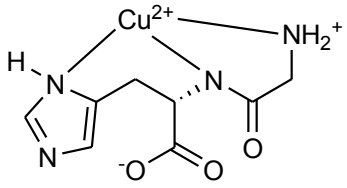

d

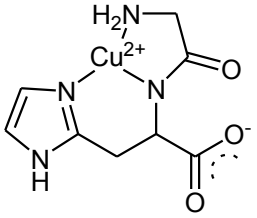

e

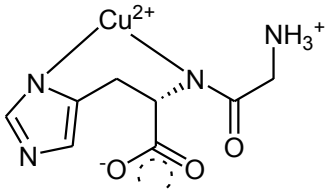

f

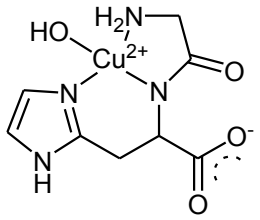

g

5.1.5 Conclusion

The structures “a”, “b” “c” and “d” are possible structures for ML. However, the complex is highly unlikely to have existed in the “a” form since the pKa of the COOH for this ligand was 2.29. Structures “b” is more appropriate than “c” because there is more electron cloud on the protonated imidazole N-atom of Structure “b” than there is in the imidazole N-atom of Structure “c”. The terminal NH_2 was deprotonated at high pH (pKa 8.34) therefore ML is highly unlikely to exist in “d” form. The most possible structure of ML is therefore structure “b”.

The most possible structures for MHL_{-1} are “e” and “f”. MHL_{-1} forms at high pH (beyond 8.34 which is the pKa of the terminal NH_2 group thus MHL_{-1} is highly likely to exist in “e” form than in “f” form. Structure “g” is highly likely to be MLH_{-3}.

5.2 NMR SPECTROSCOPY

5.2.1 Introduction

Unlike in ultraviolet-visible spectroscopy, in nuclear magnetic resonance spectroscopy (NMR) the absorption of radiation is not by the *d* electrons but it is by the nuclei that are exposed to a magnetic field [5, 6, 7].

In this study, ^{1}H NMR spectroscopy was used to investigate the sequence of protonation of the ligand; and to examine the sequence of complexation of glycyl-L-histidine with Cu(II). Upon protonation, the NMR signals of the ligand close to the basic site are expected to shift. The signals are expected to shift to low to high field as the amount of acid is decreased [8, 9].

Moreover, since Cu(II) has an electronic configuration of [Ar] $3d^9$, Cu(II) compounds are paramagnetic [10, 11]. The NMR signals of the ligand are expected to broaden when Cu(II) binds to the ligand. The broadness of the resonance is dependent on the concentration of the metal ion and the internuclear distance between the nucleus and the metal ion. By monitoring the differential broadening, it is possible to obtain information about the site of coordination.

5.2.2 Experimental

5.2.2.1 Preparation of Solutions

All solutions were prepared in D_2O. The pD of the solutions was adjusted sequentially from pD 2 to pD 11 using 0.01M NaOD and 0.001M DCl solutions. The pH was measured with CRISONmicro pH meter equipped with Metrohm electrode. The ^{1}H NMR measurements were done on a VXR 300 MHz spectrometer. Tertiary butyl alcohol was used as a reference as it gave a single, intense signal which was independent of pH.

5.2.2.2 NMR Measurements

For the protonation of the ligand, the pH of the ligand solution was adjusted to pH 3.85, pH 5.77, pH 6.96, pH 7.46, pH 8.08, pH 9.29, and pH 10.95 with DCl/NaOD. The spectra at each of these pH's was measured. For the complex formation titrations, Cu(II) solutions were titrated into the ligand solution. For some titrations, the pH was kept constant and the amount of Cu(II) was varied, while others, the amount of Cu(II) was kept constant and the pH was varied as shown in Table 5.3. The solutions were put in the order that they appear in the spectra on Figure 5.7.

Table 5.3; A table showing the pH and amount (in mM) of Cu(II) titrated into the ligand solutions for the ^{1}H NMR measurements

Solutions	pH	[Cu(II)] / mM
1	7.42	10
2	7.42	20
3	7.42	30
4	7.42	60
5	7.42	110
6	8.05	110
7	10.09	110

Since DCl was used to adjust the pH instead of HCl, the pH measurements were therefore in pD units. pD was converted to pH by Equation 5.8.

$$pH = pD - 0.4 \quad (5.8)$$

The t-butyl alcohol was used as an internal reference. The change in chemical shift was plotted as a function of pH as in Figure 5.6.

5.2.3 RESULTS

5.2.3.1 Protonation of the Ligand

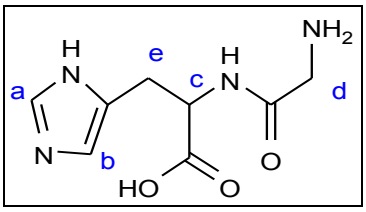

Figure 5.4: The structure of the ligand showing the protons that can be observed by ^{1}H NMR spectroscopy. The letters "a" to "e" correspond with the ones on Figure 5.5 and Figure 5.7.

The results for the ligand titration are shown in Figure 5.5. The assignments for the spectra are indicated and follow the numbering in Figure 5.4. The signals "a" and "b" were the first to shift from low to high field. The shifting of signals "a" and "b" was due to the deprotonation of one of the N-atoms of the imidazole group. These signals started shifting at a very low pH and were still shifting at pH 9.

Signal "d" started to shift from pH 8.08. A significant change in the position of the "d" signal was observed at a higher pH. This was due to the deprotonation of the peripheral amine nitrogen. The sequence of protonation of glycyl-L-histidine was in this manner; the pKa of 2.29 corresponded to the protonation of the carboxylic group, the protonation of the imidazole nitrogens was at pKa = 6.61 and the terminal NH_2 corresponded to pKa = 8.34.

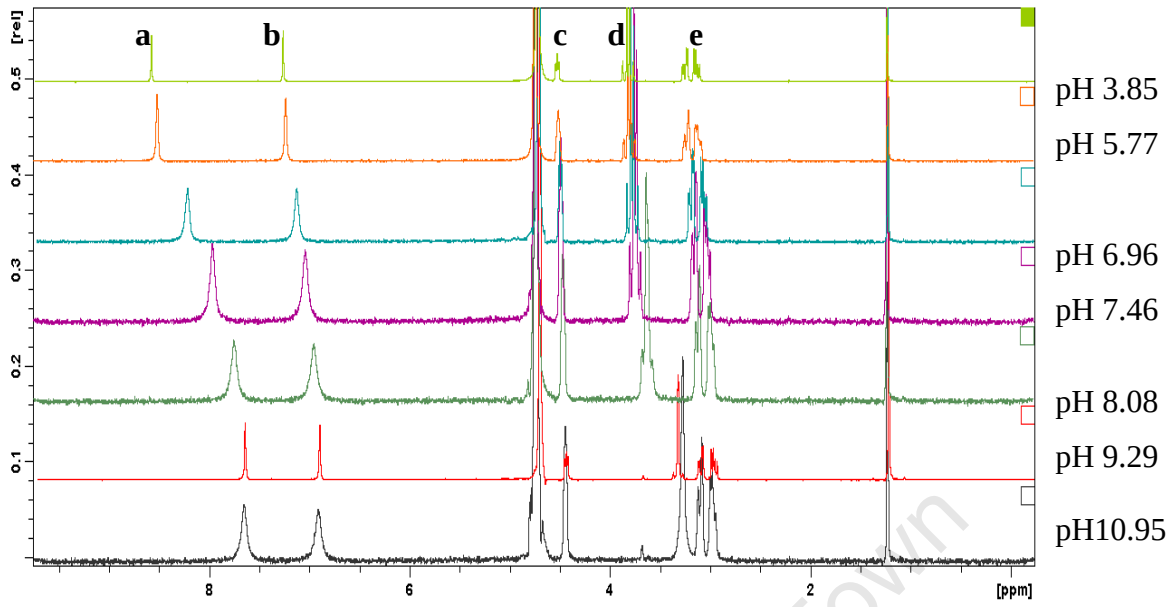

Figure 5.5: ^{1}H NMR for the protonation of glycyl-L-histidine

The change in the position of the signals was plotted as a function of pH as shown in Figure 5.6. The graphs a, b, c and e in Figure 5.6 show the pKa of around 6.6 and graph e shows a pKa of around 8.3. These were in good agreement with the pKas of the imidazole nitrogen (pKa = 6.61) and pKa of the terminal NH_2 group (pKa = 8.34) calculated from glass electrode potentiometry. [Section 3.5.2; Table 3.2] the other pKa could not be observed, potentiometrically, since it occurred at a very low pH (pKa = 2.29).

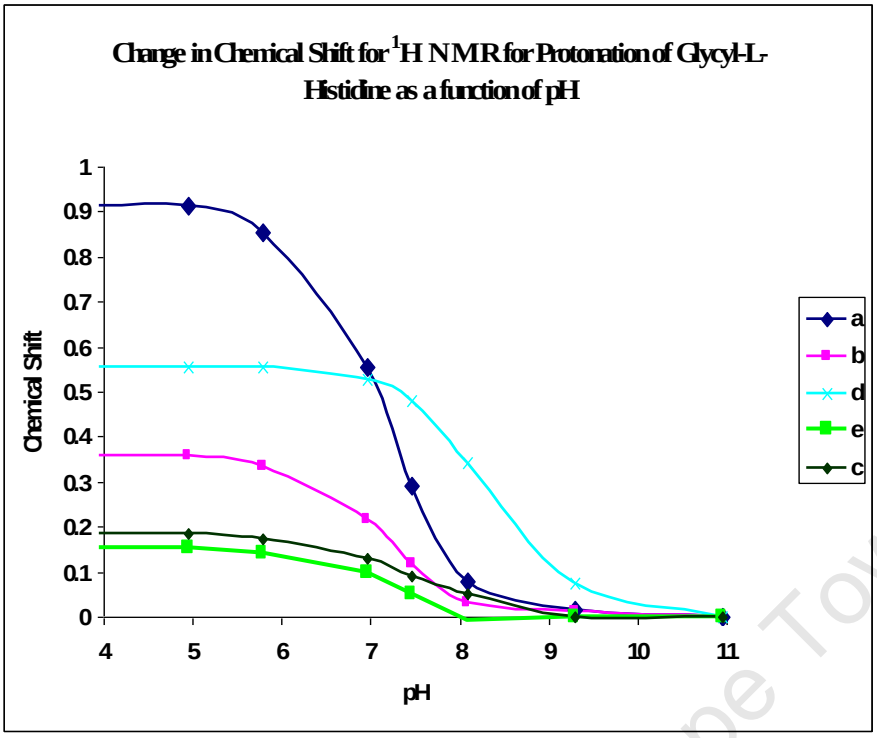

Figure 5.6: Change in chemical shift for the protonation of glycyl-L-histidine

5.2.3.2 Complexation of the Ligand with Cu(II)

The spectrum for the complexation of the ligand with Cu(II) is shown in Figure 5.7. When the pH (pH 7.42) was kept constant and the amount of Cu(II) titrated into the ligand solution, the signals did not shift significantly but they broadened extensively, with signals "a" and "b" showing the most observable changes. The most predominant species at pH 7.42 is the ML species and this indicates that the imidazole must be coordinating to the Cu(II). Since "d" is not broadened, the Cu(II) is not coordinated to the terminal amine.

The signals broadened and shifted significantly when the pH was varied and the amount of Cu(II) was kept constant. The shifting is due to the pH change and the broadening is due to the Cu(II). At pH 8.05, there are two species in solution, the ML and the MLH_{-1}.

At pH 10.09, the most predominant species is the MLH_{-1}. The most affected signals were signal "a", signal "b" and signal "d". The copper ion was therefore bonded to one of the imidazole nitrogens and to the primary amine.

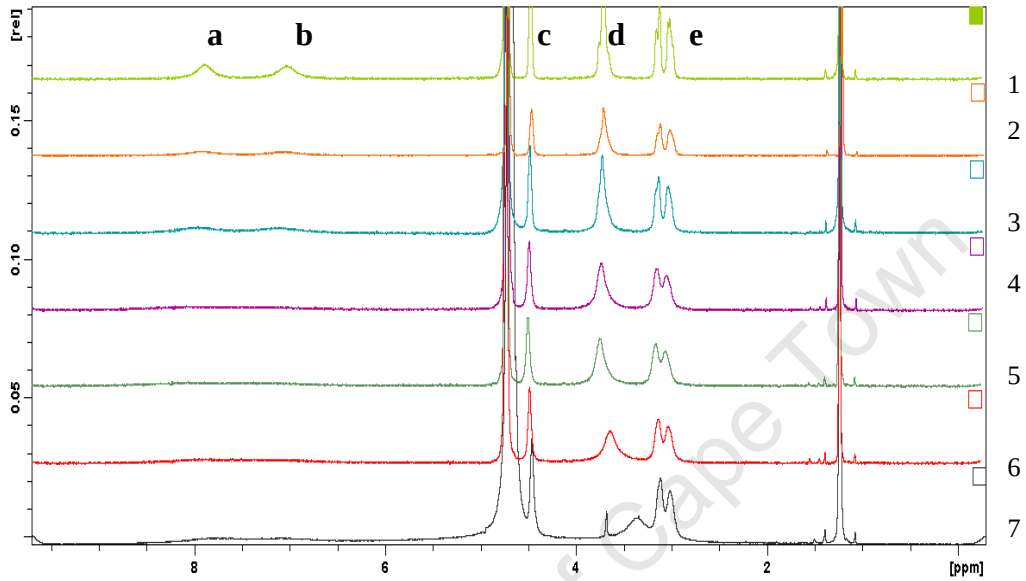

Figure 5.7: ^{1}H NMR for the complexation of glycyl-L-histidine with Cu(II).
Spectrum 1 (pH=7.42; [Cu(II)] = 10mM)
Spectrum 2 (pH=7.42; [Cu(II)] = 20mM)
Spectrum 3 (pH=7.42; [Cu(II)] = 30mM)
Spectrum 4 (pH=7.42; [Cu(II)] = 60mM)
Spectrum 5 (pH=7.42; [Cu(II)] = 110mM)
Spectrum 6 (pH=8.05; [Cu(II)] = 110mM)
Spectrum 7 (pH=10.09; [Cu(II)] = 110mM)

The pH for the complex formation titrations was not varied much therefore a similar graph as in Figure 5.7 could not be constructed.

5.2.4 Conclusions

The three protonation constants of glycyl-L-histidine were assigned to the carboxyl group, the imidazole nitrogens and the terminal NH_2 group respectively. The carboxyl group was protonated at very low pH, followed by the imidazole nitrogens. The terminal NH_2 group was protonated in very basic solutions.

Glycyl-L-histidine had three binding sites for Cu(II); one of the imidazole nitrogens, the amide nitrogen and the nitrogen of the terminal NH_2 group. Complexation began on the imidazole nitrogen and the amide nitrogen, at pH 7.42. Cu(II) bonded to the nitrogen of the terminal NH_2 group at higher pH.

5.3 BLOOD PLASMA MODEL

5.3.1 Introduction

The speciation of glycyl-L-histidine and Cu(II) in blood plasma was studied with ECCLES (Evaluation of Constituent Concentrations in Large Equilibrium Systems) [12]. ECCLES is a database that uses cumulative stability constants to predict clinical properties of species in blood plasma. The program has a preprocessor, MIX, which estimates the stability constants (log βs) of mixed complexes that are predominant in blood plasma [13].

In addition, ECCLES also gives the plasma mobilizing indices (p.m.i). By definition p.m.i is the ratio of the total concentration of low molecular weight metal complex species in the presence of the drug to that of normal plasma. The plasma mobilizing index gives extend to which the ligand (drug) can move the metal ion in blood plasma from a protein bound form to the low molecular weight form. The greater the value the better the mobilizing capacity [12, 13].

5.3.2 RESULTS

Table 5.4 gives the speciation of glycyl-L-histidine in blood plasma. The LH species was the most predominant species in blood plasma followed by LH_2. About 79.4 % of the glycyl-L-histidine species was in LH form, and about 11.5 % was in LH_2 form. The remaining 9.1% was shared within the metal ion/glycyl-L-histidine complexes.

Table 5.4: A table showing the distribution of protonated and the complex form glycyl-L-histidine species in blood plasma. The concentration were put in descending order. The initial concentration of the ligand was 1.00E-10

Species.	Where M is;	Species Concentration (M)	Species Distribution (%)
LH	-	7.94E+00	79.4
LH_2	-	1.15E+00	11.5
ML	Zn(II)	9.76E-06	-
LH_3	-	9.20E-06	-
MLH	Zn(II)	2.28E-06	-
M_2L_2	Zn(II)	4.02E-07	-
$M_2L_2H_{-1}$	Zn(II)	2.59E-07	-
ML_2	Zn(II)	1.47E-08	-
ML	Cu(II)	1.31E-11	-
MLH_{-1}	Cu(II)	5.53E-13	-
MLH_{-1}	Ni(II)	4.44E-13	-
ML	Ni(II)	3.09E-13	-
MLH	Ni(II)	2.12E-14	-
MLH_{-2}	Cu(II)	5.16E-18	-
MLH_{-3}	Cu(II)	9.47E-21	-
ML_2	Ni(II)	2.94E-22	-
ML_2H_{-1}	Ni(II)	1.28E-26	-

This means that even though, the Cu(II) complex is more stable than the Zn(II) complex, Cu(II) is not able to compete with Zn(II) *in vivo*. This is because the Zn(II) concentration is so much higher than the Cu(II) concentration. Also glycyl-L-histidine is not able to significantly mobilize Cu(II). It requires a ligand concentration of 0.1M in order to increase the low molecular mass fraction of Cu(II) 10 fold. This concentration is unreasonably high. For these two reasons glycyl-L-histidine is unlikely to be of value as a copper mobilizing agent. It may however be able to increase the dermal absorption of copper.

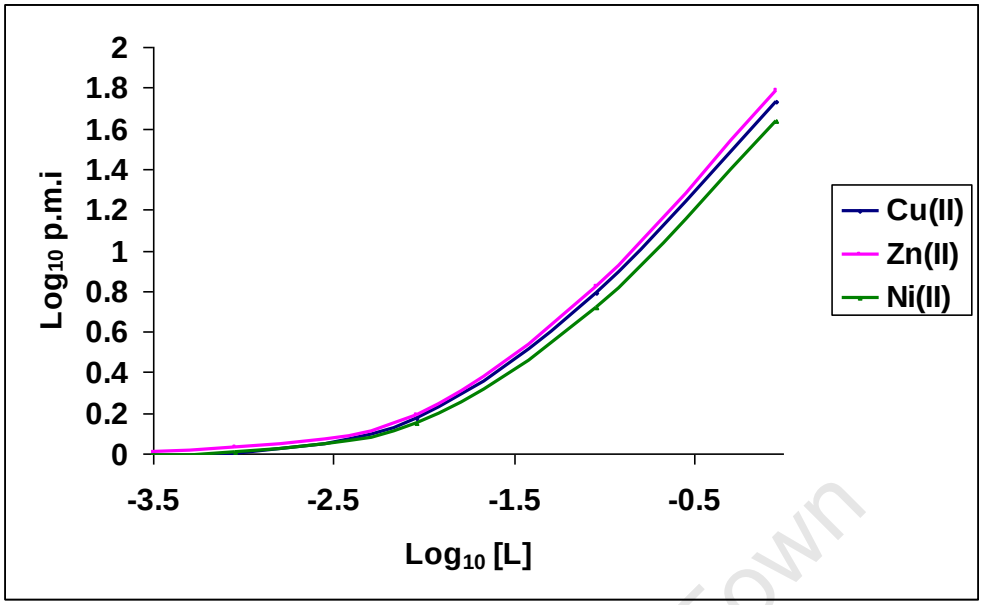

Figure 5.8: Log_{10} p.m.i as a function of log [L] for the complexes of glycyl-L-histidine and the three metal ions; Cu(II), Zn(II) and Ni(II)

The results were compared to data that was reported earlier [14, 15]. PrDPr which was reported to mobilize Cu(II) more than Zn(II); TRIEN which was reported to mobilize Cu(II) more than other ligands: DTPA, EDDA, TTDA and DTDA (structures Appendix 2). The mobilizing abilities of PrDPr and TRIEN were better than the mobilizing index of glycyl-L-histidine as shown in Figure 5.9. The gap between Cu(II)/glycyl-L-histidine and Cu(II)/PrDPr was huge. The ability of TRIEN to mobilize Cu(II) in blood plasma was better than that of PrDPr.

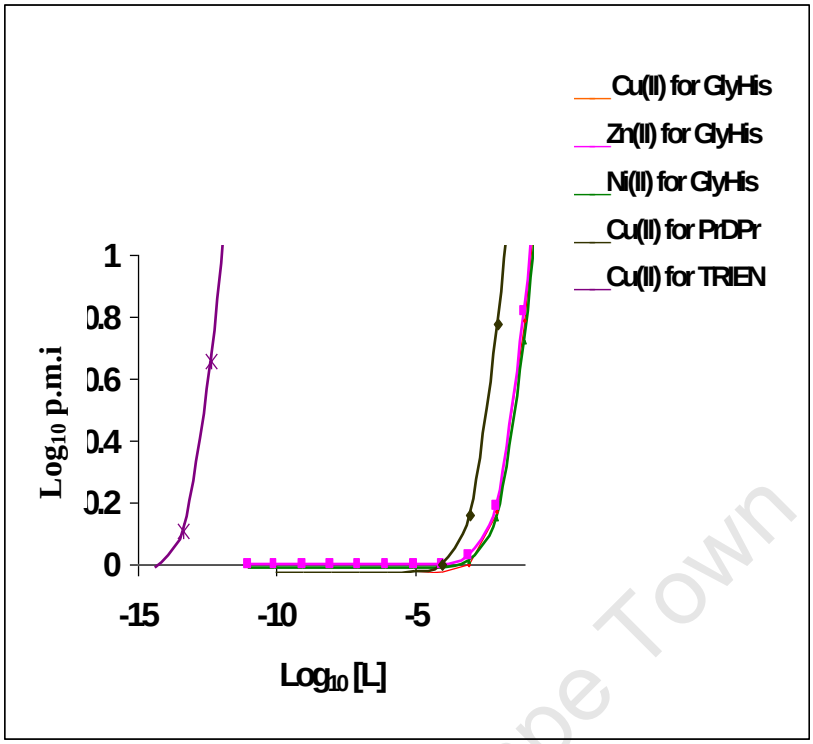

Figure 5.9: Log_{10} p.m.i for a glycyl-L-histidine system compared to Cu(II)/PrDPr system and Cu(II)/TRIEN system..

5.3.3 Conclusions

Glycyl-L-histidine existed mainly existed as LH in blood plasma. Under physiological conditions, very little metal complexes of glycyl-L-histidine were found. This means that glycyl-L-histidine would mobilize Ni(II) in blood plasma before if mobilizes Cu(II) This is not desirable. The p.m.i of Cu(II), Ni(II) and Zn(II) complexes with glycyl-L-histidine was in the sequence;

$$Ni(II) < Cu(II) < Zn(II)$$

Moreover, when the glycyl-L-histidine was compared to DTPA, EDDA, TTDA and DTDA it had very low p.m.i therefore it is not the suitable to be used as an anti-inflammatory agent.

REFERENCES

1. Uihlein, M., Schwab, E. (1982) *Chromatographia*. 15; 140.
2. Birks, J. W., Frei R. W. (1982) *Trends in Analytical Chemistry*, 1(15); 361.
3. Kawaoka, K., Khan, A. U., Kearns, D. R.(1967) *Journal of Chemical Physics* 46: 1842.
4. Andersen, K. B. and Spange-Larsen, J. (1997) *Spectrochimica Acta Part A: Molecular and Biomolecular Spectroscopy*. 53(14): 2615-2625
5. Bird,M., G. Gaudiano and T.D. Koch.(1991) *Journal of American Chemical Society* 113; 308
6. Eriksson, M., B. Nordén and S. Eriksson.(1988) *Biochemistry*. 27; 8144
7. Thoem, J. V., Jan C. A. Boeyens, Gloria J. McDougall, Robert D. Hancock (1984) *Journal of American Chemical Society*106 (11); 3198–3207
8. Lammers, H et al (1998) *Inorganica Chimica Acta*; 277(3); 193-201
9. Wang, X. and Yi Lu (1999) *Biochemistry*; 38(28); 9146–9157
10. Murthy, N. N., Kenneth D. Karlin, Ivano Bertini, and Claudio Luchinat (1997) *Journal of American Chemical Society*119 (9); 2156–2162
11. Zelentsov, V. V. (2004) *Journal of molecular and Structural Chemistry* 7(4); 513-51
12. Jackson, G. E., Peter M. May and David R. Williams (1978) *Journal of Inorganic and Nuclear Chemistry* 40(6); 1227-1234
13. Filella, M. and Enric Casassas (1987) *Inorganica Chimica Acta* 136(3) 177-183
14. Odisitse, S. (2003) PhD Dissertation. UCT, Cape Town.
15. Kelly, M. (1998) PhD Dissertation. UCT, CAPE TOWN. 114-117

6. GENERAL DISCUSSIONS AND CONCLUSIONS

The stability constants of the ligand, glycyl-L-histidine, were compared to the stability constants of glycine since glycyl-L-histidine has a glycine terminal. The stability constants of the ligand with Cu(II) were also compared to the stability constants of Ni(II)/glycyl-L-histidine and Zn(II)/glycyl-L-histidine complexes.

The values of the stability constants for all these systems were in agreement with the literature values [1-7].

The equilibrium constant for the copper(II) complexes of glycine and copper(II) complexes of glycyl-L-histidine were also investigated with isothermal titration calorimetry. This method was not as accurate as glass electrode potentiometry since the latter did not involve buffers; the change in potential described the interaction between the metal ion and the ligand, while the signal in isothermal titration calorimetry described the interaction between the metal ion, the buffer and the ligand.

Moreover, since ITC could not be used for sequential titrations of the metal ion solution with the ligand solution, the speciation graph for the metal/ligand system could not be constructed from pH 2 to pH 11 as in glass electrode potentiometry. ITC measurements could not be done at very low pHs and high pHs. Very acidic solutions could corrode the ITC sample cell and Cu(II) precipitated out in basic solutions ($pH \geq 9$).

The method was used from pH 5 to pH 8, and in this pH range, the buffers used were NH_4 Ac/Acetic acid (ammonium acetate/acetic acid buffer) for pH 5.0, MES.TMAH (2-[N-morpholino] ethanesulfonic acid) for pH 6.0, MPOS.TMAH (3-[N-morpholinino] propanesulfonic acid) for pH 7.0 and EPPS.TMAH (3-[4,(2-hydroxyethyl)-1-piperazinyl] propanesulfonic acid) for pH 8.0.

The heats of dilution of these buffers were measured before the metal ion/ligand titrations could be made. This was done to check if the heats of dilution are too high to mask the real heats of binding of the ligand and the metal ion. The heats of dilution for all the four buffers were negligible.

The ITC machine was calibrated with a simple system of Ca(II)/EDTA. The ITC results for this system were in good agreement with the ITC measurements for same system that have been reported before [8].

According to the potentiometric studies ML species of Cu(II)/glycyl-L-histidine and Cu(II)/glycine were predominant at pH 5, and from pH 6-8 the ML_2 species of Cu(II)/glycine system was predominant in solution. When Cu(II) was titrated with glycyl-L-histidine at pH 5 in ammonium acetate/acetic acid buffer, the most predominant species were ML. This was an endothermic reaction and conditional equilibrium constant was 4.083. When Cu(II) was titrated with glycine at the same pH, the conditional equilibrium constant was 3.045. This was an endothermic reaction and ML species were predominant in solution. The Cu(II)/glycine complexes at this pH were less stable than the Cu(II)/glycyl-L-histidine complexes at the same pH.

When Cu(II) was titrated with glycyl-L-histidine at pH 6 in MES buffer, the most predominant species was ML. The conditional equilibrium constant for this system at pH 6 was 5.719. The ML species was predominant is solution since $N \approx 1$. This was a spontaneous exothermic reaction since ΔH is negative and ΔS is positive. When Cu(II) was titrated with glycine at the same pH, the conditional equilibrium constant was 4.009. This was an endothermic reaction and ML species was predominant in solution. The Cu(II)/glycine complexes at this pH was less stable than the Cu(II)/glycyl-L-histidine complexes at the same pH.

At pH 7, in Cu(II)/glycyl-L-histidine system N was less than 1. This shows that there was a different species formed at this pH. At pH 8, the N value was 1.32. The reaction at pH 7 and pH8 for the same system was exothermic. The change in entropy was

positive for both reactions, thus the forward reaction at this pHs was favoured. Log K for the pH 7 titration was 5.137 and log K for the pH 8 titration was 3,914.

At pH 7, in Cu(II)/glycine system N = 0.467. This shows that there was a different species formed at this pH. At pH 8, N ≈ 2. ML_2 species were predominant at this pH. The reaction at pH 7 and pH 8 for the same system was exothermic. The change in entropy was positive for both reactions, thus the forward reaction at this pHs was favoured. Log K for the pH 7 titration was 3.804 and log K for the pH 8 titration was 4.238.

UV-Vis spectrophotometry and 1H NMR were used to predict the structure of complexes of glycyl-L-histidine with Cu(II). The visible spectra obtained for the different Cu(II)/Glycyl-L-histidine in solution are typical of Cu(II) complexes in a tetragonally distorted, octahedral environment. Only one broad band is observed for each species and this can be assigned to the *d-d* transition. The molar extinction coefficients are also typical of Cu(II) complexes and reflect the distortion of the metal-ion environment.

The energy of the transition is dependent on the metal-ion environment. Billo, Presenti and co-workers [9, 10] have devised an empirical method of estimating λ_{max} for different coordination spheres. These are shown in Figure 5.3. These values were compared to the values calculated using Equation 6.1.

$$\lambda_{max} = 10^3/\sum n_i \nu_i \qquad (6.1)$$

Where λ_{max} is the maximum wavelength, n_i is the number of equatorial donor group and ν_i is the ligand field of the complex. The measured values agree with the values calculated in Section 5.1.3.

From ^{1}H NMR, deprotonation of the ligand commenced on the carboxylate group, followed by the imidazole nitrogen followed by the N-atom of the NH_2 terminal. However, only two protonation constants (log K = 6.6 and log K = 8.3) of the ligand

were observed with ^{1}H NMR because deprotonation of the carboxylate group occurred at very low pH's. The possible structure of the ligand are shown as LH_3 for the ligand that has three dissociable protons, LH_2 for the ligand that has two dissociable protons, LH for the ligand that has one dissociable proton and L for the neutral form of the ligand. However, the LH_3 form of the ligand was not observed with ^{1}H NMR since deprotonation of the carboxylate H-atom occurs at very low pH's.

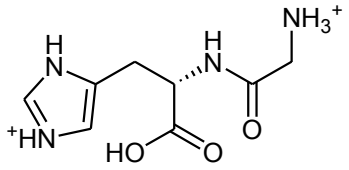

LH_3

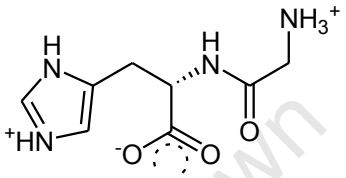

LH_2

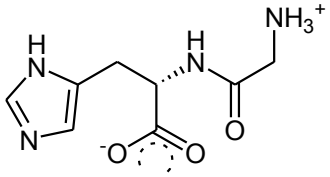

LH

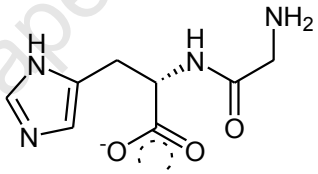

L

At pH 3.85 and pH 5.77, the ligand was in LH_2 form; at pH 6.96, pH 7.48 and pH8.08, the ligand was in LH form and at pH 9.29 and pH 10.95, the ligand was in its neutral form, L. The structures of glycine are show below.

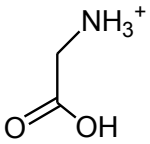

LH_2

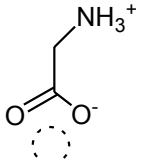

LH

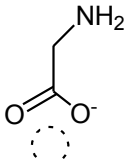

L

At pH < 2 to pH 4.20, glycine exists as LH_2, at 2 < pH < 11, the ligand there was LH in solution, the neutral form of glycine formed at pH 7.50.

For complex formation titrations, Cu(II) bonded to the imidazole nitrogens and on the N-atom of the terminal NH_2 group since the affected signals were "a", "b" and "d". When the pH was kept constant (pH 7.42), the signals did not shift significantly but they broadened as the amount of Cu(II) ions was increased in solution. When the amount of Cu(II) ions in solution was kept constant ([Cu(II)] = 110mM]), the ^{1}H NMR signals did not broaden significantly but they shifted significantly. This shows that different species were formed at different pH's.

At pH 7.42, the most predominant species were the ML species. The most possible structures of the complex at this pH are structures "a" and "b". From potentiometry (Q-bar plot), the ligand lost two protons upon complexation with the ligand. This makes Structure "b" more suitable for ML than Structure "a". Moreover, from the ^{1}H NMR, the signal for the "d" protons (Figure 5.4) was not shifting at pH 7.42 where the ML species were predominant.

At pH 8.05, the "d" signal shifted from high field to low field. At this pH, the central metal ion was bonded to the electron donor atom of the terminal NH_2 group.

The structures of ML and ML_2 for Cu(II)/glycine complexes is labeled "a^1" and "b^1" respectively. ML2 exists in two forms, the *cis* and the *trans* form.

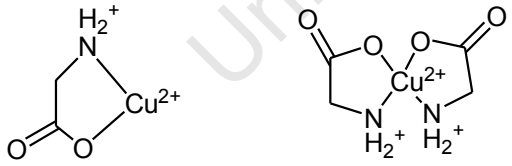

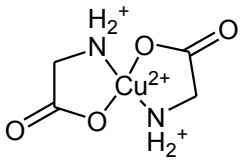

a^1 cis-b^1 trans-b^1

Combining UV-Vis and ^{1}H NMR results gave the structures of Cu(II)/glycyl-L-histidine as;

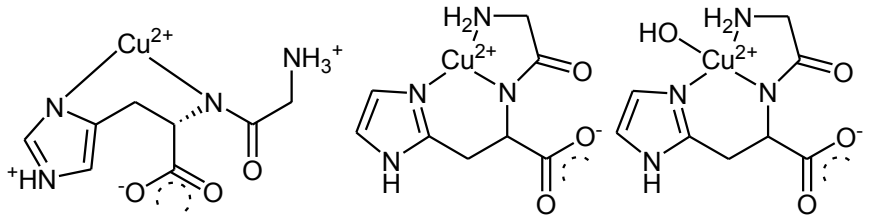

To test whether the ligand can increase the low molecular weight copper(II) complexes in blood plasma, the cumulative equilibrium constant of the ligand and of the Cu(II)/glycy-L-histidine complexes were put in a computer blood plasma model. ECCLES was used to evaluate the capacity to which the ligand can increase concentration low molecular weight Cu(II) complexes in blood plasma. From ECCLES output, most of the ligand in blood plasma existed in LH and LH_2 form. The ligand was not able o compete with endogenous blood plasma ligands. Moreover, the complex form of the ligand was mostly Zn(II) not Cu(II). The ligand therefore has a higher capacity of mobilizing Zn(II) than it does for Cu(II). This is because *in vivo* concentration of Zn(II) is much higher than does it for Cu(II). However, the ligand mobilized Cu(II) in blood plasma than it mobilized Ni(II), and the difference between the two mobilizing capacities was not negligible. PrDPr has been reported to mobilize Cu(II) than Zn(II) [11].

When data for this ligand with Cu(II) was compared to that of Cu(II) with glycyl-L-histidine, PrDPr had a higher mobilizing capacity the latter. Moreover, when Cu(II) complexes of glycyl-L-histidine were compared to Cu(II) of TRIEN, which has been reported to have a higher mobilizing capacity for Cu(II) in blood plasma [12]. Glycyl-L-histidine had a lower mobilizing capacity than TRIEN. The stability constants of the three ligands; glycyl-L-histidine, PrDPr and TRIEN are shown in Table 5. 5.

Table 5.5: Stability constants of Cu(II) with glycyl-L-histidine, PrDPr and TRIEN

Ligand	Species	Log β
Glycyl-L-histidine	**ML**	**9.162**
	MLH_{-1}	**0.387**
	MLH_{-2}	**-12.041**
	MLH_{-3}	**-22.175**
PrDPr [14]	**ML**	**4.344**
	MLH	**8.421**
	MLH_{-1}	**0.575**
	MLH_{-2}	**-4.679**
TRIEN [14]	**ML**	**20.323**
	MLH	**23.437**
	MLH_{-1}	**8.61**

From potentiometric data, TRIEN formed very stable complexes with Cu(II) compared to glycine and PrDPr. However, the ML species of Cu(II) complexes with glycyl-L-histidine were more stable than the ML species of PrDPr with Cu(II). However, the MLH_{-1} and MLH_{-2} of PrDPr were more stable than the MLH_{-1} and MLH_{-2} of glycyl-L-histidine and it is these species which are formed at physiological pH. In addition the specificity of both TRIEN and PrDPr for Cu(II) over Zn(II) was much greater.

CONCLUSION

The thermodynamic stability of glycyl-L-histidine with H^+, Cu^{2+}, Zn^{2+} and Ni^{2+} have been successfully measured using glass electrode potentiometry. These results were compared to the stability of the glycine complexes. *In silica* modeling of blood plasma speciation, using the determined stability constants showed that the ligand was not able to effectively mobilize Cu(II) *in vivo*. This is both because the complexes are not stable enough to compete against endogenous ligands and also because it is not sufficiently selective for C(II) over Zn(II). Since Zn(II) is present in blood plasma at a much higher concentration than Cu(II), the Zn(II) complex preferential forms.

Spectroscopy was used to study the structure of the different species in solution. From these results it was postulated that in the ML species the metal coordinates to one of the imidazole N-atoms nitrogens and the amide nitrogen.

The final conclusion is that glycyl-L-histidine is not suitable as a Cu(II) based anti-inflammatory drug. The inability of the ligand to mobilize Cu(II) *in vivo* is perhaps surprising since it is so similar to HSA, the endogenous copper transport protein. These results need to be compared with the terminal amino acid sequence of HSA.

6.1 FUTURE WORK

Ligands with two acetylhistidine moieties will be used, one with a cage and the other without a cage. The structures of the proposed ligands are shown below.

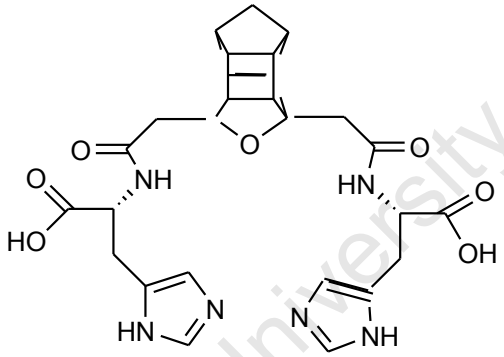

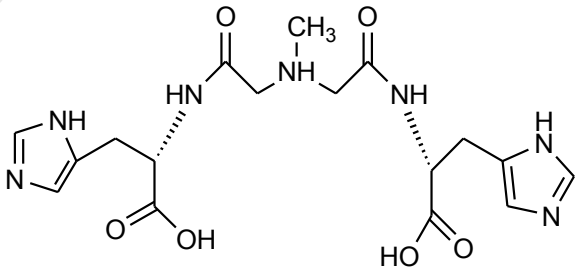

R EFERENCES

1. Brookes, G. and Pettit, L. D. (1975) *Journal of Chemical Society.* Dalton. 2112
2. Martin, R. B. and Edsall, J. T. J. (1960) *Journal of American Society* 82;1107
3. Charles, R. G. (1954) *Journal of American Society* 76;5854
4. Koltun, L. (1963) *Journal of Biological Chemistry* 238;1367
5. Flood, H. V., Lorzs, V. Tidskr. Kjemi. Berg. (1945) *Journal of Inorganic Biochemistry*. 5; 83
6. Rabenstein, D. L. et al (1985) *Journal of American Society* 107; 6435
7. King, J. (1951). *Journal of American Society*. 75; 155
8. Griko, Y. V., Hendrix, T. and Peter, L. P. (2000) *Journal of Biophysical Chemistry* 1(14);27-34
9. Billo, E. J. (1974) *Inorganic and Nuclear Chemistry Letters* 10; 613.
10. Sigel, H. and R.B. Martin (1982) *Chemical Reviews* 82;385.
11. Odisitse, S. PhD Dissertation. (2003) UCT, Cape Town.
12. Kelly, M. (1998) *Metal Ion Equilibrium in biofluids-Copper and Rheumatoid Arthritis.* PhD Thesis. Department of Chemistry, University of Cape Town, Cape Town, South Africa. 114-117

Appendix 1 (COMPUTER MODEL OF BLOOD PLASMA)

BDP0

GLYH

PLED	Glycyl-L-histidine(Ligand under study)
EHP4	
EDD5	glycine,N,N'-1,2-ethanediylbis-N-(2-hydroxyphenyl0)
HYD1	ethylene dinitrilo-N,N'-dinitrilo-N,N'-diacethylhdroxamic-N,N'-diacetic acid
HBD4	ACETYL-HYDROXAMIC ACID
CAT2	HBED
TRN2	CATECHOL
TTH6	TIRON-1,2-DIHYDROXYBENZENE-3,5-DISULFONIC ACID
PMG3	TRIEN-HEXA-ACETIC ACID
DDD1	N-PHOSPHONOMETHYLGLYCINE
DTD2	DUMMY LIGAND
ALA1	DTDA
ABA1	ALANATE
ARG0	AMINOBUTYRATE
ASN1	ARGININE
ASP2	ASPARAGINATE
CIT1	ASPARTATE
CYS2	CITRULLINATE
CIS2	CYSTEINATE
GLU2	CYSTINATE
GLN1	GLUTAMATE
GLY1	GLUTAMINATE
HIS1	GLYCINATE
HYP1	HISTIDINATE
ILE1	HYDROXYPROLINATE
LEU1	ISOLEUCINATE
LYS1	LEUCINATE
MET1	LYSINE
ORN1	METHIONATE
PHE1	ORNITHINATE
PRO1	PHENYLALANATE
SER1	PROLINATE
TAU1	SERINATE
THR1	TAURINE
TRP1	THREONINATE
TYR2	TRYPTOPHANATE
VAL1	TYROSINATE
HSN0	VALINATE
CO32	HISTAMINE
PO43	CARBONATE
SIL2	PHOSPHATE
SO42	SILICATE
SCN1	SULPHATE
NH30	THIOCYANATE
ACA2	AMMONIA
CTA3	ASCORBATE
LTA1	CITRATE
MLA2	LACTATE

OXA2	MALATE
PVA1	OXALATE
SLA2	PYRUVATE
SCA2	SALICYLATE
TRA2	SUCCINATE
OPN2	TARTRATE
GSH3	OX-PENICILLAMINATE
GSS4	RED-GLUTATHIONATE
PEN2	OX-GLUTATHIONATE
TET0	RED-PENICILLAMINATE
EDT4	TRIETHYLTETRAMINE
GH	EDTA
GGH1	1-GLYCYLHISTIDINATE
PMA0	DIGLYCYLHISTIDINATE
BAL2	PEPTIDE MIMICKING ALBUMIN (N-METHYL-DIGLYCYLHISTIDINE
DFO2	2,3 DIMERCAPTOPPROPANOL (BAL)
DTP5	DESFERRIOXAMINE
CDT4	DTPA
ACT1	CDTA
ANT1	ACETATE
ASA1	ANTHRANILATE
CIQ1	ACETYLSALICYLIC ACID
FEN0	CARBOXY-ISOQUINOLINE
ATH1	FENAMOLE
SGL2	BENZOYLATED THIAPROLINE (D12267)
THP1	D12408
DPA1	5,5-DIMETHYLTHIAZOLIDINE-4-CARBOXYLIC
EDD2	2,3-DIAMINOPROPIONATE
NTA3	EDDA (ETHYLENEDIAMINEDIACETIC ACID)
EGT4	NTA
EHP4	EGTA
HDT3	EHPG
ODT4	HOEDTA
DHG1	EEDTA
DAB1	DIHYDROXYETHYLGLYCINATE
AEE0	2,4-DIAMINOBUTANOATE
EDM1	2(2-AMINOETHYLAMINO)ETHANOL
DMP3	ETHYLENEDIAMINEMONOACETATE
DMS4	2,3-DIMERCAPTOPROPANE SULPHONIC ACID
CAP2	2,3-DIMERCAPTOSUCCINIC ACID
TTD2	CAPTOPRIL
DTD2	TTDA (3,6,9,12-TETRAAZATETRADECANEDIOIC ACID)
MLT1	DTDA (3,6,9=TRIAZAUNDECANEDIOIC ACID))
OXME	MALTOL
EDT8	OXAMIDEDIOXIME
APD0	ETHYLENEDIAMINETETRAMETHYLPHOSPHONATE
HED3	PAMIDRONIC ACID
HID2	HEDTA
H +1	HIDA
OH-1	
AL+3	
CD+2	
CA+2	

CO+2	
CU+1	
CU+2	
FE+2	
FE+3	
PB+2	
MG+2	
MN+2	
NI+2	
PU+4	
SR+2	
ZN+2	
GD+3	
SM+3	
HO+3	
GA+3	
UO+2	
F -1	
CARB	
TFRN	PROTEIN SIMULATOR-CARBOXYLATE FUNCTIONS
ALBM	PROTEIN SIMULATOR-TRASNSFERRIN
	PROTEIN SIMULATOR-ALBUMIN

Appendix 2 (STRUCTURES OF DTPA, DTDA and TTDA)

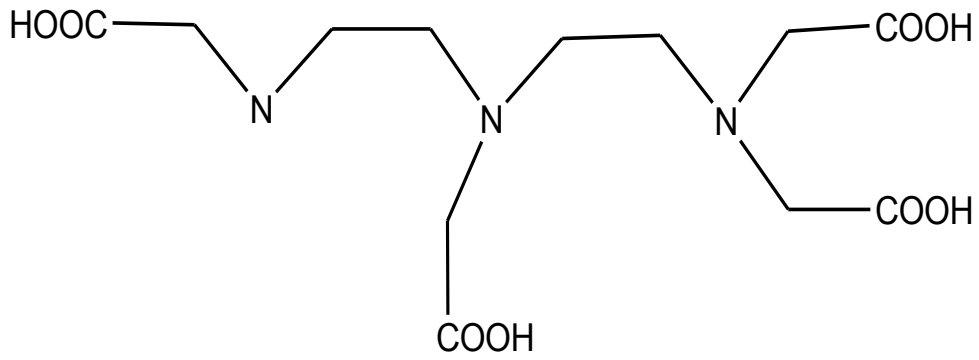

DTPA:

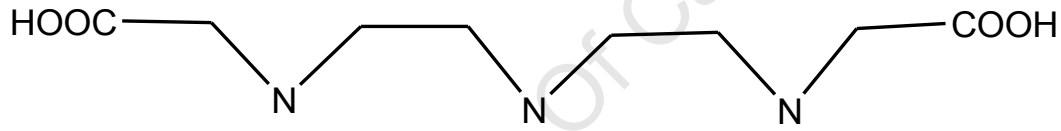

DTDA: 3,6,9,-TRIAZAUNDECANEDIOC ACID

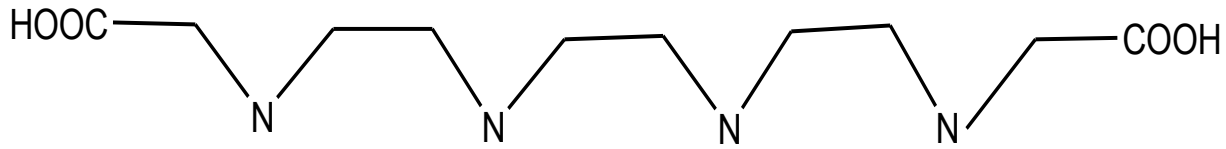

TTDA: 3,6,9,12-TETRA-AZATETRADECANEDIONIC ACID